REPORT DOCUMENTATION PAGE

AFRL-SR-BL-TR-98-

0813

Public reporting burden for this collection of information is estimated to average 1 hour per response, including and maintaining the data needed, and completing and reviewing the collection of information. Send comme information, including suggestions for reducing this burden, to Washington Headquarters Services, Directorate 1204, Arlington, VA 22202-4302, and to the Office of management and Budget, Paperwork Reduction Project (0

1. AGENCY USE ONLY (Leave Blank)	2. REPORT DATE	3. REPC
	December, 1995	Final

4. TITLE AND SUBTITLE
USAF Summer Research Program - 1995 High School Apprenticeship Program Final Reports, Volume 13, Phillips Laboratory

5. FUNDING NUMBERS

6. AUTHORS
Gary Moore

7. PERFORMING ORGANIZATION NAME(S) AND ADDRESS(ES)
Research and Development Labs, Culver City, CA

8. PERFORMING ORGANIZATION REPORT NUMBER

9. SPONSORING/MONITORING AGENCY NAME(S) AND ADDRESS(ES)
AFOSR/NI
4040 Fairfax Dr, Suite 500
Arlington, VA 22203-1613

10. SPONSORING/MONITORING AGENCY REPORT NUMBER

11. SUPPLEMENTARY NOTES
Contract Number: F49620-93-C-0063

12a. DISTRIBUTION AVAILABILITY STATEMENT
Approved for Public Release

12b. DISTRIBUTION CODE

13. ABSTRACT *(Maximum 200 words)*

The United States Air Force High School Apprenticeship Program's (USAF- HSAP) purpose is to place outstanding high school students whose interests are in the areas of mathematics, engineering, and science to work in a laboratory environment. The students selected to participate in the program work in an Air Force Laboratory for a duration of 8 weeks during their summer vacation.

14. SUBJECT TERMS
AIR FORCE HIGH SCHOOL APPRENTICESHIP PROGRAM, APPRENTICEDHIP, AIR FORCE RESEARCH, AIR FORCE, ENGINEERING, LABORATORIES, REPORTS, SCHOOL, STUDENT, SUMMER, UNIVERSITIES

15. NUMBER OF PAGES

16. PRICE CODE

17. SECURITY CLASSIFICATION OF REPORT	18. SECURITY CLASSIFICATION OF THIS PAGE	19. SECURITY CLASSIFICATION OF ABSTRACT	20. LIMITATION OF ABSTRACT
Unclassified	Unclassified	Unclassified	UL

UNITED STATES AIR FORCE

SUMMER RESEARCH PROGRAM -- 1995

HIGH SCHOOL APPRENTICESHIP PROGRAM FINAL REPORTS

VOLUME 13

PHILLIPS LABORATORY

RESEARCH & DEVELOPMENT LABORATORIES

5800 Uplander Way

Culver City, CA 90230-6608

Program Director, RDL
Gary Moore

Program Manager, AFOSR
Major David Hart

Program Manager, RDL
Scott Licoscos

Program Administrator, RDL
Gwendolyn Smith

Program Administrator
Johnetta Thompson

Submitted to:

AIR FORCE OFFICE OF SCIENTIFIC RESEARCH

Bolling Air Force Base

Washington, D.C.

December 1995

19981211 029

DTIC QUALITY INSPECTED 3

PREFACE

Reports in this volume are numbered consecutively beginning with number 1. Each report is paginated with the report number followed by consecutive page numbers, e.g., 1-1, 1-2, 1-3; 2-1, 2-2, 2-3.

This document is one of a set of 16 volumes describing the 1995 AFOSR Summer Research Program. The following volumes comprise the set:

VOLUME	TITLE
1.	Program Management Report
	Summer Faculty Research Program (SFRP) Reports
2A & 2B	Armstrong Laboratory
3A & 3B	Phillips Laboratory
4	Rome Laboratory
5A, 5B, & 5C	Wright Laboratory
6A & 6B	Arnold Engineering Development Center, Wilford Hall Medical Center and Air Logistics Centers
	Graduate Student Research Program (GSRP) Reports
7A & 7B	Armstrong Laboratory
8	Phillips Laboratory
9	Rome Laboratory
10A & 10B	Wright Laboratory
11	Arnold Engineering Development Center, Wilford Hall Medical Center and Air Logistics Centers
	High School Apprenticeship Program (HSAP) Reports
12A & 12B	Armstrong Laboratory
13	Phillips Laboratory
14	Rome Laboratory
15A&15B	Wright Laboratory
16	Arnold Engineering Development Center

DOCUMENTING A COMPUTER PROGRAM

Blake E. Ahrens

Albuquerque Academy
6400 Wyoming NE
Albuquerque, NM 87111

Final Report for:
High School Apprentice Program
Phillips Laboratory

Sponsored by:
Air Force Office of Scientific Research
Bolling Air Force Base, DC

and

Phillips Laboratory

August 1995

DOCUMENTING A COMPUTER PROGRAM

Blake E. Ahrens
Albuquerque Academy

Abstract

Documentation of a program used by the Electromagnetic Effects Division was almost completed. A valuable lesson and several software programs were learned. Organization was quickly developed. The foundation for the documentation of the BLWGN program was laid for those to follow.

DOCUMENTING A COMPUTER PROGRAM

Blake E. Ahrens

In October of 1990 Thomas A. Loughry wrote a computer program for the Electromagnetic Effects Division. The purpose was to control the instruments used to run the tests and to gather data from the tests. The data was then presented in a clear and precise fashion. The program was written to be easy to use while still being very flexible. The program was written specifically to perform these tests by someone familiar with the tests. This made it very useful for the user, any problems or complaints were taken directly to the programmer, unless he found them first, and were quickly fixed. The problem came when Capt. Loughry was no longer available for questions and repairs.

It was decided that the program needed documenting. I was to document the code. The first few weeks of the summer I worked on learning Microsoft C++, because this was the programming language used to write the program I was to document. Then I began looking at the code to determine which files did what. I ran into a few problems. It seemed that few people around me knew Microsoft C++. Also the program contained very few comments telling me what something was supposed to do. To help lessen my confusion I made lists. I had lists of questions, variables, included files, and file functions. These helped me to start on the actual documentation. My goal was then to make a flow chart of the program from a user angle. I started by making some lists of the menus and trying to determine what different things did.

After this was done I tried to figure out the keys that the program would listen to. Then I decided to walk through the program and map it out. I was trying to determine where different buttons would take me and which options gave me other options.

The lists of menus were helpful when I was drawing the flow chart because I could easily tell where a certain option was located. The list I made of all the constant keystrokes was very useful when I began to map out the program. I started by opening the first menu and trying keys. I kept a record of what each key did and where I was when it was done. Precise records are important and made my job a lot easier when I tried to consolidate my information. Then I made a flow chart of this. Flow charts are a way to present information in a clear manner. A flow chart uses boxes to represent an activity done by the computer, diamonds to represent a decision made by the user, circles to represent input from the user, and chopped off boxes ⬭ to represent computer output. Here is an example of the flow chart symbols and a flow chart.

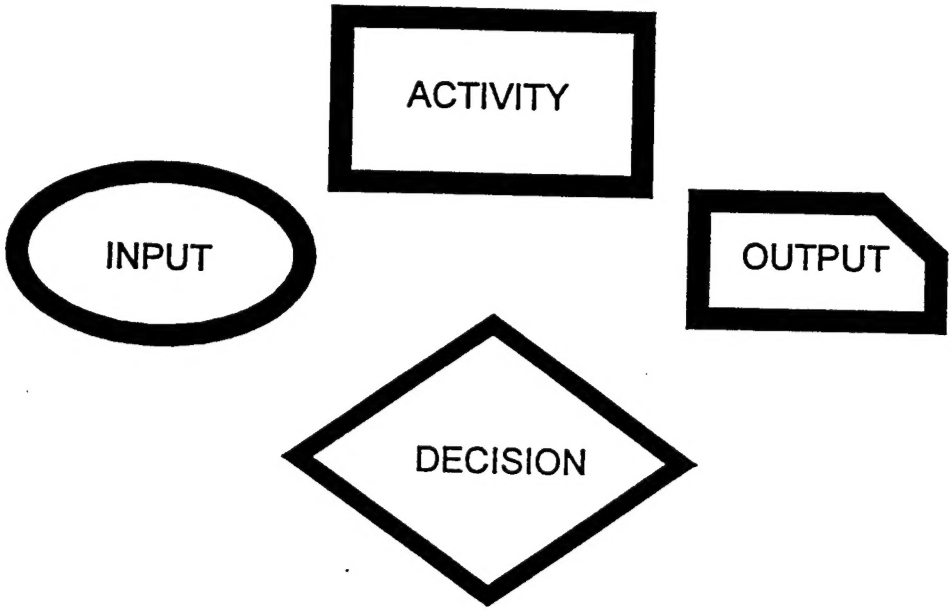

THE KEY STROKE USED IS PLACED NEXT TO THE ARROW →

THE ARROW IS USED TO TAKE YOU FROM ONE FUNCTION TO ANOTHER

Example Flow Chart

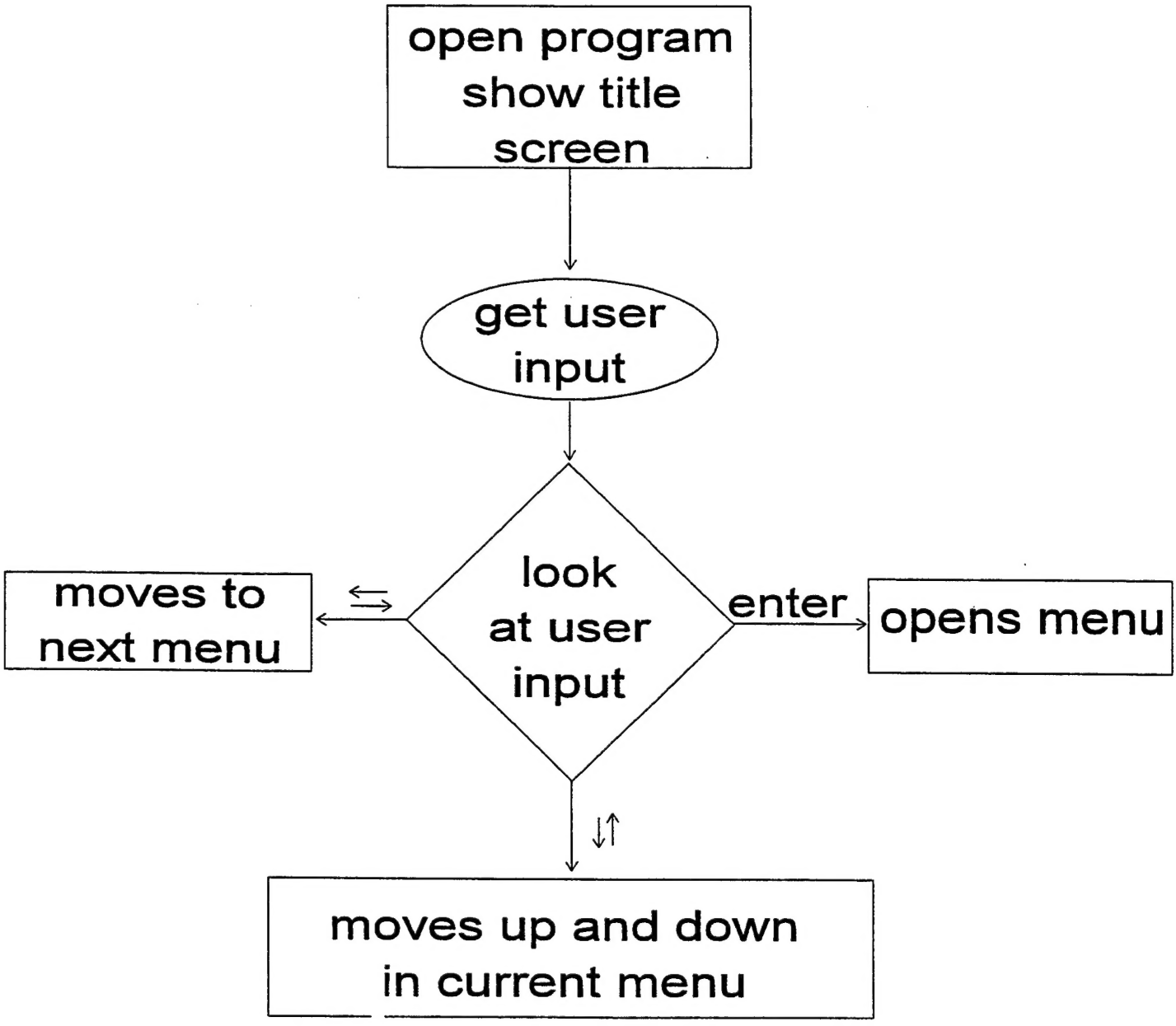

I was unable to complete the flow chart of the program in the time I had so I decided the best thing for me to do would be to organize all my notes. I tried to make it as easy as possible for someone else to finish what I had started. I wanted to make my notes easy to understand. I tried to organize them in the most efficient way. I also wrote down everything I could think of that had gone through my mind when I was working on this assignment. I learned from the program that if you do things in your head you should write them down because you will not always be there to answer questions. I also learned this lesson while doing something else.

For three days I worked for Hector Del Aguila. There were no other students to help him complete view graphs for a presentation. I learned Corel Draw when I did these view graphs. I had a problem when Mr. Del Aguila went out of town while I was finishing the view graphs. I learned once again how important it was to leave directions in written form. When you know what you want and you don't make it clear to the person doing the work it makes things difficult for them because they have to guess. I made a few mistakes on the view graphs because I didn't know what Mr. Del Aguila wanted. I did the same thing I had done with the program and wrote down my questions. When Mr. Del Aguila returned I asked him all the questions on my list and fixed the view graphs accordingly. The view graphs were better from this questioning process.

I learned many things this summer, Microsoft C++, the BLWGN program, Corel Draw, and the proper way to do a flow chart. None of these are as important what I learned from the program. If you make something you should write down why you did what you did and you should list any abbreviations you use with their meanings. These things should be with whatever you made when you leave so that the person

that comes behind you can very easily tell what you did and why. In this manner any mistakes you made can be fixed without to much trouble. This is easier said than done. However if you want your creation to be functional for years after you are gone it is important to write down what you did.

THE COLLECTIVE SUM OF MY WORK AT THE PHILLIPS LABORATORY

Michael A. Alfano
HSAP Summer Apprentice
Department of Tehachapi High School

Tehachapi High School
711 Anita Dr.
Tehachapi, CA 93561

Final Report for:
High School Apprenticeship Program
Phillips Laboratory (Edwards AFB)

Sponsored by:
Air Force Office of Scientific Research
Bolling AFB Washington DC

and

Phillips Laboratory (Edwards AFB)

August 1995

THE COLLECTIVE SUM OF MY WORK AT THE PHILLIPS LABORATORY

Michael A. Alfano
HSAP Summer Apprentice
Department of Tehachapi High School
Tehachapi High School

Abstract

A series of different projects where assigned to me during my time spent in the electric propulsion laboratory. For the majority of the time I was creating diagrams of flanges and plates that where to be used with the arcjet in the largest chamber in the lab. I also learned the LabVIEW programming language and created one program while assisting in the creation of another. I assisted in laboratory operations and clean-up. I monitored arcjet operations, including plume size, voltage and current values on a few occasions.

THE COLLECTIVE SUM OF MY WORK
AT THE PHILLIPS LABORATORY

Michael A. Alfano

Introduction

(1) It has become apparent that in coming years, certain space missions will need propulsion that can produce a specific impulse considerably higher than that that can be obtained with a chemical rocket. Specific impulse is the measure of how efficiently propellant is used to produce thrust. One way to represent specific impulse is as the thrust divided by the weight flow rate A device that is capable of producing this high specific impulse is an arcjet which heats propellant to a high temperature in an electric arc and then expands it in a conventional nozzle. To test the arcjets on earth a special containment unit is needed to simulate the vacuum of outer space. (2) One way to create those conditions is to use a sealed chamber with a vacuum pump that is able to remove most of the pressure within it. This chamber can also allow the use of water (cooling), electrical, and thermocouple feedthroughs with the use of flanges with a series of ports that give access to the inside of the chamber while keeping the chamber sealed.

LabVIEW is a computer programming language with a general-purpose programming system with an extensive library of functions and

subroutines for any programming task just as C or BASIC. LabVIEW differs from most other applications in one important respect. Other programming systems use text-based languages to create lines of code, while LabVIEW uses a graphical programming language to create programs in block diagram form.

Discussion of Problem

I was presented with a number of different tasks that mainly included drawing diagrams and programming in LabVIEW. It was required of me to complete each task within a certain amount of time, between a couple of hours and a week or two, depending on the individual assignment. With this now explained I will reveal in more detail the problems given to me.

On occasion I was asked to assist with the arcjet by observing a specific operation. It could include watching data coming from the arcjet. It sometimes included watching the plume from the arcjet itself. I also duplicated reference material and participated in laboratory clean-ups.

I was given the task of making a diagram of a plate made of aluminum that an arcjet could be mounted to. This plate would in turn have to be able to be mounted to the stand in one of the chambers so that the arcjet could be fired within it. I needed to make my own

measurements of where the holes would go for the mounting of the plate to the stand but I was also supplied with the measurements for the mounting holes for the plate to the arcjet. I also had to make a revised version of the diagram to include new measurements that I would receive about a month later.

Another diagram that I had made was one of a large flange that was to be place on the chamber. It had to include a large 4.5 inch port that would hold a sapphire window which would allow the temperature of the arcjet body to be determined. It would also have to accommodate six conflate flanges that would allow the use of various feedthroughs. I was given an example diagram that showed the same sized flange but all the ports on it were either too small or in the incorrect location.

I was also given the task of programming a computer to take an input and then output a signal from two different lines of a port which would create a specific voltage from the instrument that the port is hooked-up to. The input had to be supplied from a dial on the screen of the computer and each setting would correspond to a different input signal which would have to be converted to a Boolean value. It would also have to be represented graphically as do all things in a LabVIEW program. I provided some assistance in writing a program to control a stepper motors movement by inputting the

distance I want the motor to move in or out and the program tells it how many steps to move.

Methodology

To do the diagrams I first had to familiarize myself with Claris Draw. Then I measured the stand and received the measurements of the arcjet. After that I began drawing the thrust stand mount plate and as I went along I learned different drafting symbols [3] to assist the machine shop in understanding what it was asking for. For the revised version I measured the arcjet and altered the drawing to show the revised measurements and a few reference points.

For the flange I first took a number of conflat flanges and rearranged them on the full size example until I got down the arrangement that would work best. Then I drew-up the diagram and went back to finalize the exact measurements. These drawings were done on a Macintosh IIFX.

When I assisted in laboratory experiments, I observed the arcjet during operation watching for unstable conditions - such as sparks and overheating, so that shutdown could be initiated in the case of problems. I observed the plume for changes when they would transition between gases and report when the plume went out. I also took note of arcjet voltage during a start-up procedure.

For the programs I had to write in LabVIEW I first had to learn the language. After I had learned the rudiments of the language I assisted with the creation of a program that would tell a stepper motor how many steps to move but my technique mostly involved trial and error. Then I switched to another assignment and began by getting all the information that the program needs to run and planned out what the program would need to do. Finally, I finished the program after tracking down just what icons I needed to complete it.

Results

The diagram of the thrust stand mount plate accurately represented the data but unfortunately the information on the arcjet was incorrect and one of the holes were off. The revised diagram was successful in placing the hole in the right spot and also made the plate symmetrical again. The LabVIEW program I made allows you to turn a dial to what voltage you want and it outputs a signal in the form of a Boolean value from two lines of a port which in turn tells an instrument how many volts to produce. I completed most of the flange diagram before I was forced to stop because of time constraints and begin working on this report.

Conclusion

During my time at the Electric Propulsion Laboratory, I acquired a working knowledge of LabVIEW and used it in two separate programs. I picked-up some drafting skills and created three diagrams of things for the arcjet that would need to be machined. I also assisted in the laboratory operations and clean-ups Overall I enjoyed being here at the lab and was happy to work with the engineers. I would like to work here again next year and have the opportunity to help the lab out as best I can.

Appendix

Figure 1 shows the control panel of the program I made which you use to input the voltage that you want. Figure 2 includes the new holes that were needed to change the plate so that it would be able to mount all the necessary equipment to it and the old holes that were made as a reference. In Figure 3 is the diagram of how the LabVIEW program works. The input from the dial in the box at the left corresponds to a number which travels down the line into the two triangles. These triangles each decide if the input is equal to 0 or less than or equal to 1 depending on the triangle. This sends a true or false out of the port and into the instrument which produces the correct amount of volts from that information.

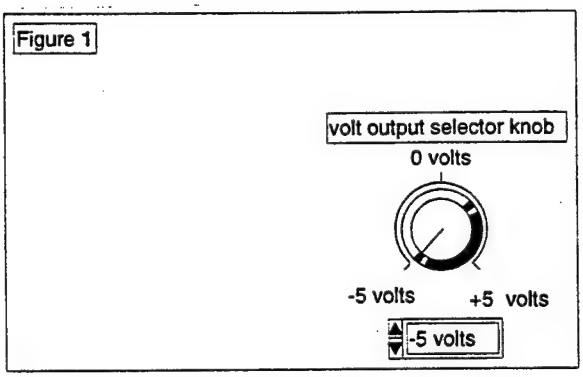
Figure 1
volt output selector knob
0 volts
-5 volts
+5 volts
-5 volts

Figure 2

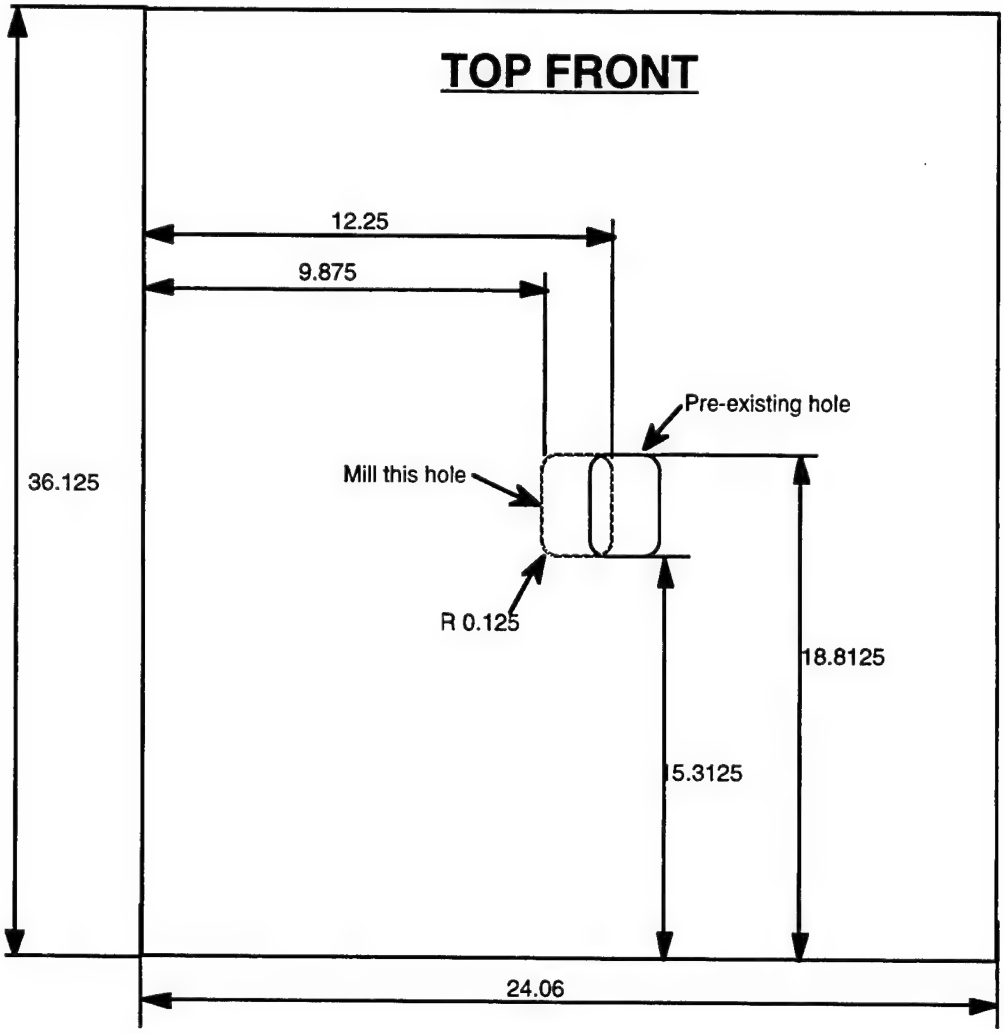

Thrust Stand Mounting Plate
Material: Aluminum
All Dimensions in Inches
Tolerances +/- 0.03
Quantity: 1

Requester: MCFALL/5502

Figure 3

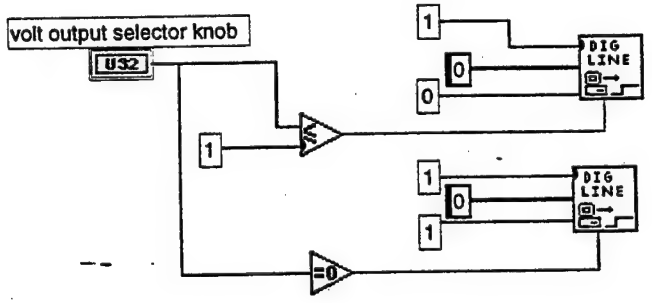

References

[1] Philip, H. G., Mechanics and Thermodynamics of Propulsion, Addison-Wesley Publishing Company, Reading, Massachusetts, 1970

[2] McFall, K., private communications, 1995

[3] Bromaghim, D., private communications, 1995

Jonathan Copp report not available at time of publication.

IMPLEMENTATION OF NETWORKING IN THE PHILLIPS LABORATORY INTEGRATED GROUND DEMONSTRATION LABORATORY

Alexander E. Duff

La Cueva High School
7801 Wilshire Blvd. NE
Albuquerque, NM 87122

Final Report For:
High School Apprenticeship Program
Phillips Laboratory

Sponsored By:
Air Force Office of Scientific Research
Bolling Air Force Base, DC

and

Phillips Laboratory

August 1995

IMPLEMENTATION OF NETWORKING IN THE PHILLIPS LABORATORY INTEGRATED GROUND DEMONSTRATION LABORATORY

Alexander E. Duff
La Cueva High School

Abstract

Phillips Laboratory has begun a new initiative to develop an Integrated Ground Demonstration Program jointly managed by the Space and Missile Technology Directorate (PL/VT) and the Space Experiments Directorate (PL/SX). In support of this effort, the Integrated Technology Development and Demonstration Office (PL/VT-I) is working closely with SX to build an infrastructure and laboratory for executing ground demonstration projects. Networking capability is an integral part of the ground demonstration infrastructure. Proper attention to networking during the build-up of the laboratory will ensure capabilities are not limited during future experiments. This paper will give a brief overview of networking in general, and then it will focus on the networking capabilities in the Integrated Ground Demonstration Laboratory (IGDL) which is located in building 467. Finally, this paper will look at a specific networking case and explore the options of connecting the IGDL at Kirtland AFB to the JPL Flight System Testbed (FST) in Pasadena, Ca.

Introduction to Networking

The concept of networking originated in the 1960's when companies wanting to increase productivity by allowing greater access to their computers designed remote input terminals for programmers. Since that time, many advances have been made in the area of networking, leading to the present ability for someone to download files from the other side of the world at a touch of a button on a home computer. The first networked system was called a remote batch access terminal. This system consisted of a remote terminal connected to a computer by a telephone company's line and two modems: one at each end of the line. Later, hardware was developed to process the communications to remove burden from the mainframe. Eventually, software was designed for minicomputers so that they could control communications functions. The networking of computers has evolved into two distinct areas: wide area networks (WANs) and Local Area Networks (LANs). WANs usually connect two different geographical areas. Also, WAN transmission rates are usually at the speed of 1.5 Mbps (Millions of bits per second) for a T1 connection, or 45 Mbps for a T3 connection. Local Area Networks typically only connect a small area: an office building, a campus, or a town. A LANs connection speed is usually between 4 and 16 Mbps. Local Area Networks are connected by WANs, allowing people hundreds or thousands of miles apart to exchange data, send e-mail, or connect in a video conference.

The backbone for today's extensive Internet network began when the National Science Foundation (NSF) connected many National Supercomputing sites across America. Gradually, more and more computing sites connected to this backbone, and then college campus' LANs were connected, resulting in the expansive Internet known today. Many wonder where the Internet is located, but the truth is that there is no central Internet computer or site, it is merely the connection of computers all over the world that makes the Internet. To access the resources on the Internet one needs only a computer terminal and a connection through a mainframe or a modem. This makes the Internet a very accessible resource for the public, and an easy way to get information.

Local area networks can be of several different types. First, there is the Ethernet network. Ethernet is very popular in LANs because it is relatively easy to install, cheap to

implement, and supports a broad range of technological characteristics. For these reasons, Ethernet dominates the market in terms of sales of adapter cards, currently representing a sixty-five percent market share. Another type of local area network is a fiber optic network. These networks are more difficult to install and more costly, but they offer an increased data rate and the possibility for longer lines, connecting areas farther apart. A third alternative is ProNET-10, a technology developed through research at universities. ProNET operates at the same speed as Ethernet, 10 Mbps, and is also limited to short distances

Regardless of the specific type of local network, there must be a bridge between a LAN and a WAN if an Internet connection is required. The bridge acts as a translator between the two types of networks, so that each can understand the other's messages. Other necessary hardware includes a router, which analyzes messages and determines the optimal way to send them, and a repeater, which simply amplifies data to increase the distance it may travel on the line. These components allow networks to communicate between themselves and also to the outside world.

Current PL Capabilities

Today, Phillips Laboratory has an extensive LAN, combining FDDI (Fiber Distributed Data Interface) Rings and Ethernet connections. Once connected to the LAN, messages are sent over the Internet through a T3 connection at a speed of 45 Mbps. The IGDL in B467 would send data through the ethernet to the 100 Mbps FDDI ring, at which point it would be transferred to an IBM RISC 6000 computer. The RISC 6000 then acts as a communications controller as well as a bridge to the Internet and outside organizations.

When analyzing the rate at which data is transferred, the theoretical limit is equal to the lowest transmission rate. As an example, assume an outside organization's connection is a T1 line at 1.45 Mbps and this link is the slowest in the path between the IGDL and the other organization. The theoretical data rate limit would be 1.45 Mbps, but in practice, many delays occur while waiting for lines to become clear and for the various

computers to process the signal and send it to the correct destination. As a result, the speed of the connection will probably average between 500 and 1000 Kbps.

As higher data transmission rates are required, the WAN connections become the limiting factor as compared to the LAN systems. As stated earlier, a WAN may transmit at up to 45 Mbps on a T3 link while a LAN may transmit at 100 Mbps in the case of a FDDI ring. This limited WAN transmission rate is because of the long distances traveled and the exposure of the transmission lines over these long distances. Accidents due to the elements are common and maintenance is more difficult, therefore delays are more likely.

Linking the IGDL to JPL

Projects executed in the IGDL may utilize spacecraft and mission simulation capabilities at the JPL Flight System Testbed (FST). Data collected in the IGDL would be sent through the PL LAN network to the IBM RISC 6000 computer. Next, the message would be sent over the T3 line to San Diego, a NSF supercomputing site. Finally, the message would travel to a California Bay area network, be transferred to a civilian network and then forwarded to Cal Tech and the Jet Propulsion Laboratory.

The JPL FST is connected to a JPL local area network, but a direct WAN connection is not available. In the future, the FST may lease a T1 line, enabling a data transmission rate of 1.45 Mbps. With this FST capability, the PL IGDL could also lease a T1 line and set up a direct connection to the JPL FST. These leased T1 lines would keep the transmission rate up because of the lack of traffic, but still could not exceed the limit of 1.45 Mbps. Accessing a T1 line includes a one time installation and set up fee of approximately $15,000. After the line is installed, it may be rented for one month periods, thus allowing flexible data sharing. The T1 line would not have to be paid for until an experiment requires network capability.

Emerging Technology

In addition to the T1 or T3 lines that connect to the Internet, some emerging technology could be considered for connection to JPL. One possible solution is an Integrated Services Digital Network (ISDN) connection. ISDN was developed 20 years

ago in the Bell Laboratories. This technology remained unpopular for many years because of its high cost and lack of applications. Now, with the increasing demand for networking resources, such as video conferencing and sharing of large graphics, ISDN has found its niche. ISDN allows video, voice, and data to be transmitted at speeds ten times faster than modems. However, ISDN is more difficult to install than modem connections and the ISDN products are proprietary. Also, ISDN is not available in all areas. Regardless, ISDN seems to be a good compromise when reasonable data transfer rates are needed at an affordable price.

Future Considerations

The need for increased data transfer speed will be dictated by what experiments are being performed in the IGDL and the application of the data. For real time processing and response, a faster connection may be needed. On a LAN, transmission rates are much faster, so the cost/capabilities of localizing components must be weighed against the cost/capabilities of a dedicated line. In the case of the IGDL, the best option may be to pay for the installation of a T1 line and then use it when experimental data are collected. This option would be more economical than trying to bring all the components of an experiment to PL.

Conclusion

Because of the variety of experiments which may be executed in the Integrated Ground Demonstration Laboratory and the potential need to exchange data with multiple organizations, the installation of a T1 line to the IGDL is recommended. This line would allow the laboratory a great deal of flexibility and would only have to be leased during periods of data collection. However, the systems that are currently in place are sufficient for low to moderate data transfer applications. The drawbacks are the data link may experience some unreliability because of the many legs the data must travel through and the delay time for the data to travel through these legs. The final decision must be based on the trade off between networking capabilities, cost and reliability.

References

Corbin, Lisa et al., "Integrated Services Digital Network," Government Executive: Communication Guide, June 1995

Held, Gilbert, Ethernet Networks, John Wiley & Sons, Inc., United States of America, 1994.

Daniel Fleisher report not available at time of publication.

Kyle Hunderman report not available at time of publication.

INFORMATION IN THE WORLD TODAY

Karl J. Iliev

Antelope Valley High School
44900 N Division
Lancaster, CA 93535

Final Report for:
High School Apprentice Program
Philips Laboratory
Edwards Air Force Base, CA

Sponsored by:
Air Force Office of Scientific Research
Bolling Air Force Base, DC

and

Philips Laboratory
Edwards Air Force Base, CA

August 1995

INFORMATION IN THE WORLD TODAY

Karl J. Iliev
Antelope Valley High School

Abstract

The applications and role of information in today's world were studied. How information is distributed and protected is a main focus in this report. The Internet and World-Wide Web were studied as different forms of disbursing information. These are compared and contrasted, and the inner workings of each are described. Also, different forms of safekeeping this information were studied. A sample break-in is described. In addition, different ways to guard against break-ins were examined.

INFORMATION IN THE WORLD TODAY

Karl J. Iliev

Introduction

We are living in the electronic revolution and in the age of information. Everything is electronic or digitized. Computers control the world with their great sources of information. The greatest source of information is the Internet. The Internet can carry information all around the world quickly and cheaply. The availability of this information is too great. A variety of methods of protecting this information from unauthorized personnel are available, and many are still under development. Virtually everything today is stored on computers.

The Internet vs. The World-Wide Web

From 1973, when only 40 computers were the Internet (or 'Net), to today with thousands of computers and 35 million users world-wide, the Internet has shown just how popular it has grown. Now the World-Wide Web (WWW or just Web) has made the 'Net even more popular. The WWW consists of 10,000 servers in 84 countries world-wide. With the presence of so many computers linked together, the security of each computer is even more difficult to control. Every network and system is at risk. Someone can break into your computer without leaving a trace. Is your computer secure?

The Internet is the physical medium used to transport data, while the WWW is a collection of protocols and standards used to access information off the Internet. E-mail is the most popular application on the Internet, while the WWW is the second largest source of traffic on the Internet. The

WWW was developed by Tim Berners-Lee at the Conseil Europeen pour la Recherché Nucleaire (a French acronym: CERN) Particle Physics Laboratory in 1990. He designed it to be the user friendly portion of the 'Net. It only requires you to know one server address when previously the Internet required you to know each address as you wanted to telnet to a new server. Now you don't even need to connect directly to the server or even know its name on the Web. Previously with the Internet, a menu-based *gopher* was used to change the location on the net. Now, the Web is a windows-like interface that uses interactive graphical hyperlinks. These hyperlinks allow you to "surf" the 'Net with a push of a button.

The WWW is called the Web because it has no beginning, middle, or end; everything is tangled together which makes it much easier to reach your destination. The Web was designed with three standards in mind: Uniform Resource Locators (URLs), HyperText Transmission Protocol (HTTP), and HyperText Markup Language (HTML). All of which are jumbled together in this thing called the World-Wide Web.

URL is the location identifier. This tells the computer where the document is located. Its syntax consists of protocol://server-name:port/path. The type of protocol is usually HTTP or File Transmission Protocol (FTP), depending on the type of the document. The server-name, port, and path tell the browser the document's name and where it is. URLs are imbedded in the hyperlinks. Each time you click on a hyperlink, a URL is activated and a document appears on your screen.

HTTP is the standard language of the Web used for communicating between computers. Transmission Control Protocol/Internet Protocol (TCP/IP) is the standardized protocol of choice on the Internet. Protocol is what allows different computer systems (PCs, MACs, and UNIXs) to communicate. All computers require some type of protocol to transfer data. All computers also have an IP source address which tells other computers who they are communicating with. In an attempt of securing data many companies only check the IP address of the client before allowing the transfer of data. This is a very

risky way of authenticating the client (a *client* uses a *browser* to request data from a *server*).

A simple transaction contains four parts. First, the client establishes the connection and then issues this request to the server specifying a particular document. Next, the server sends a response and finally disconnects. FTP is what allows the file transfer across the Internet. Within HTTP there are three types of common request methods: Get, Head, and Post. Get is what the user uses to ask for a specific document. Head is used to ask only for certain information on the document, such as size or last updated date. Post is used to transfer data from the client to the server. Post can be very useful to businesses who perform surveys to obtain information from the client. HTTP flexibility was also very important to the Web's development; each server needs to be able to allow a wide range of responses to these requests. The first section of the response contains the status code. The main message of the status code is whether or not the request was successful. The second contains information about the object being returned, such as the last modified date or the type of language it was written in. The last portion contains the object itself.

HTTP is a 'stateless' protocol; it doesn't retain information about the connection from request to request. State can be maintained outside of protocol in a hidden form. Yahoo (**http://www.yahoo.com/**), for example, has a bar of links across the top of each page containing the current location on their outline of places to go and documents to see. Common Gateway Interface (CGI) scripts can be used to save state in databases, and FTP remembers the current directory for the next request. HTTP is also a 'connectionless' protocol; the user doesn't stay connected from request to request. After the browser receives the document it disconnects, unlike the previous Internet's TCP. Each graphic requires a separate connection to be made. Some browsers open multiple connections at a time, such as Netscape (**http://www.netscape.com/**), while others wait for each connection to finish, such as NCSA (National Center for Supercomputing Applications) Mosaic

(http://www.ncsa.uiuc.edu/SDG/Software/Mosaic/NCSAMosaicHome.html).

HTML is the language that the Web documents are written in. HTML is similar to the previously used Standard Generalized Markup Language (SGML). HTML provides the capability of hypermedia and hyperlinks. Hypermedia is one of the main reasons for the Web's success. Hyperlinks take you to another document just by clicking on special text, and sometimes pictures. "These links are the threads that bind the Web together" (Richard, 1995). Hyperlinks can lead you to anywhere in the world. The first document seen is called a 'homepage'. This HTML document allows instant access to most places on the 'Net. Through a homepage you can reach almost any document you wish. Anyone can make a homepage, and most major businesses have one. The homepage you see is originally that of your browser.

HTML tags areas of text with a specific format. Tags determine how the text will be displayed, whether it will be large or small, for example. Tags are defined functionally, not visually; the browser determines how large the largest text will be. The tag <H1> is the largest headline</H1>, while the tag <H6> is the smallest</H6>. The <...> tells the browser what to do with the text that follows, and </...> tells the browser that is all of the text for the current tag. Not only can text be displayed, but graphics can be displayed as well. Most browsers are able to display graphics in the GIF format. HTML can also create forms which asks for information from the client. This can be used to gain the user's opinion or as a searching tool like WebCrawler. If you're interested in seeing a script of a actual file, just open a Web document and use your browser to view the source. You can create your own Web documents or even your own homepage. HTML is plain text that can be edited by any text editor, and it's easy to understand too.

Networks provide a cheap and effective way to exchange information. Businesses can use the Internet or WWW for advertising, online publishing, customer support, and electronic shopping. The

Wide Area Network (WAN) provides for interactive market research both between business partners and between customers and business. Companies can post 'Help Wanted' signs, questionnaires, or even contests and coupons. A Local Area Network (LAN) can be used to transfer files and documents within a company. Within a LAN, mail can be sent between employees, and bulletins can be posted that will reach all employees. LAN provides an effective way to monitor employees. Also, hard drive space and memory can be conserved if a 'supercomputer' is set-up to contain most of the information.

Although very different, the WWW would be nothing without the Internet. The Internet created the WWW. The WWW has helped the Internet immensely.

The Security Issue

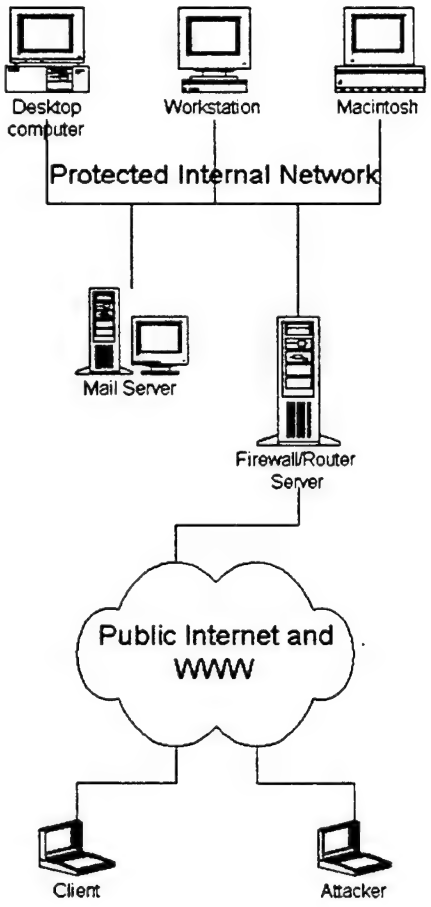

Refer to this diagram for any examples in the following text.

A major problem with all this information floating around is that some of it is too easy to obtain. There are many different forms of hacking. IP address spoofing and TCP hijacking are two examples. Major businesses need to secure their information from their competition. The government has to keep its secrets. How do we keep this vital information secure? There are different ways to fight against each attack, but all precautions should be taken into account.

IP address spoofing is when the hacker attempts to trick the victim into believing that he is

trusted. A major example of successful IP address spoofing occurs when a user level authentication isn't used. TCP Hijacking is when the hacker taps into existing TCP sessions and replaces the data being sent. TCP hijacking is regarded as requiring local 'root' access. With this 'hijacking tool,' it is possible to disable the trusted host and spoof a TCP establishment from that host. Here is an example of an attack in which both of these were used.

This attack has many specific and distinct phases. The first phase is to penetrate the screening router. The hacker spoofs his IP source address to trick the router. This can be stopped if the router uses ACLs bound to physical interfaces rather than solely checking IP source address, or if a peer site router was configured with ACLs to filter packets independent of ENSS. Also a firewall or an InterLock should be obtained to provide authentication prior to allowing access. This spoofing only allows for packets to travel into the protected network, but won't allow for responses to be sent to the attacker. All phases are like this. Without a firewall, the attacker can send packets directly to the target host and receive responses.

The goal of the second stage is to gain root access on the trusted machine using these injected packets. First the hacker uses a TCP password or sequence number prediction to hijack the connection with the trusted. This positions the hacker onto a machine that the target machine trusts. This extremely simplifies the final attack against the target machine. Next the hacker needs to disable this machine so it can't respond to the reply packets coming from the target machine. Now with the trusted machine disabled, the attacker has to blindly (remember that this is not a interactive session) inject packets simulating the trusted machines half of the TCP negotiation. This stage shows that "the strength of your network is only as strong as your weakest link" (Sangster, Paul); all computers within a network must be equally and strongly protected. Also, monitoring the protected side computers and duplicating the audit logs helps. A firewall would help immensely.

Now the attacker needs to hijack a connection from the trusted machine to the target machine. This stage involves loading a STREAMS kernel extension allowing the attacker to tap into existing TCP sessions directly. This program permits the attacker to inject commands into any existing TCP session. Now packets can be sent containing viruses or requesting desired information. The hacker can request these files by running targets FTP client and sending it transfer file commands.

Similar to IP spoofing is ICMP redirecting. An ICMP redirect tells the recipient to disregard something in its redirect table. This is used by routers to tell hosts that they are using an extinct route to a particular destination. An ICMP redirect packet that contains the correct address is sent back. ICMP redirect packets can be forged. This can cause the host to alter its redirect tables and cause traffic to flow through an unintended path. ICMP traffic should be screened from your network, therefore limiting the ability of outsiders to ping hosts, or modify their routing tables.

Firewalls are also good ways to protect your internal network. A firewall is a computer set up to protect organizations from the outside Internet world. Hackers may want to access files, phone lines, or storage. A good firewall will keep out these unwanted hackers. Good firewalls will also be transparent to inside users while giving them use of the Internet.

The firewall that is right for your business depends on how your company wants to operate its system. Does your company want to deny everyone except those directly involved, or does your company just want to meter calls? There is also the level of monitoring and control and the financial aspect that needs to be taken into account. If you run a top secret agency, you probably shouldn't even hook up to the 'Net at all; there are safer means of transporting information. All that a firewall protects against is unauthenticated logins from the Internet. Firewalls can't protect a network from viruses hidden in programs that are sent, then executed. A firewall can't protect against internal theft, such as an employee steeling a magnetic tape or disk from the office.

There are many different types of firewalls. A Proxy server uses an application that forwards application traffic through a firewall. Proxies must know the application protocol, and may increase the access control or audit level by implementing protocol specific security. With proxies you can permit or deny specific applications, FTP, or Telnet. These can also be controlled by setting up a router to restrict connections using something like 'established' screening rules. This requires modifying the client and client application on internal hosts. A proxy-based firewall, with security clearance at the application level, differs from a router-based firewall, with security implemented at the network level. A router-based firewall uses screening routers to protect the network. Screening routers are configured to selectively control traffic between networks. Cisco is one possible filtering router. The problem with router-based firewalls is that they only check to see where the packet has been routed from. It is too easy for an attacker to generate a packet claiming to be from a trusted machine, this is called 'source routing'.

A common type of firewall is the host-based firewall. This is where the security is implemented in software on a computer devoted to this firewall server. With this, security is generally at the application level rather that at the network level. These firewalls may have a bastion host, or *gateway host*, acting as the platform on which the firewall program is run. This is referred to as a *strong point* in the network's security system. A dual-homed gateway refers to a bastion host with two network interfaces, one connected to the Internet and the other connected to the protected network. This restricts traffic to whatever passes through some kind of application proxy. A screened subnet is when a network is set up between the Internet and the protected network. This *demilitarized zone* blocks traffic between the two networks similarly to the way that a dual-homed gateway works. The difference is that the dual-homed server only uses a single computer host that is reachable from the 'Net, while the screened subnet uses an entire network of computers.

Sometimes corporate policy mandates hiding domain names. You do this by setting up a Domain

Name Server (DNS) on the bastion host for the outside world to talk to, and a DNS on an internal machine. Now you set up all of your DNS clients to use the internal DNS. All communications originating from internal machines are routed through the internal DNS which gives a truthful response of the host's DNS name. All external computers would communicate with the bastion host will only receive a restricted answer, usually the address of the server instead of the actual host. Remember that there needs to be packet filtering between the two servers in order to communicate DNS between each other and restrict DNS between other hosts.

One of these host-based firewalls generates one-time passwords. Each user is issued a security card-token and a PIN (Personal Identification Number). After the user telnets to the firewall server he is prompted for his user name and a user specific challenge. The user then enters his PIN onto the electronic card and is given his one-time password. He then enters this password as a response to the challenge. The next telnet session would require a different password.

These passwords are not random; however, it would be impossible for the firewall server to predict a random number generated from a separate electronic card. Actually these numbers are pseudo random numbers, which means that each one-time password is some increment of an initial sequence number. "This initial sequence number increases at a fixed rate of 128/sec and 64 every connection for BSD 4.3 based OSs" (Sangster, Paul). If an experienced hacker obtains this initial sequence number he can predict each of the one-time passwords. These passwords are much harder to crack than permanent passwords. Any firewall is better than no firewall at all. Servers are not limited to one of the previous types of firewalls. Some firewall servers give you a choice between the types of firewall security you wish to use, but the better servers are composed of several types of firewalls.

One network tool called SATAN, or SANTA for the kids, scans UNIX systems and reports back their weaknesses. This program only reports back well-known security vulnerabilities and then shows

pointers on how to fix the weaknesses. The release of this program also has its pitfalls. There is a potential security problem if you use SATAN while browsing the WWW. Also, the SATAN program can be used to detect vulnerabilities on other systems; once these vulnerabilities are reported, that person can use his new knowledge to his advantage. These scans leave 'fingerprints' if your system is correctly configured. A number of logging tools can be acquired to detect the abnormal patterns of network activity. A properly configured firewall in place would protect against the release of this sensitive information.

Other internet services include finger, whois, gopher, archie, and X-Windows. Finger and whois permit connections to the finger port from only trusted machines which can issue finger requests. This only works with standard UNIX versions of finger. Also, there have been security bugs in finger servers, such as sensitive information being revealed in the user's finger information. Gopher and arhie are Internet search tools that retrieve information from multiple remote servers. These transmit data with only minimal security. X-Windows is a useful network tool but has many security flaws. Attackers can gain access to a workstation's X display and monitor keystrokes that a user enters (like a password), download copies of their windows content, or simply interfere with the X display. All of these services should be blocked or restricted with application proxies.

Over the Internet any thing can happen. You can send E-mail, download a file, or just play a game with a friend hundreds of miles away. You can also break into a top secret area and discover plans for a secret weapon or have your bank account drained by a hacker. Whichever the case, the Internet is a great source of information.

Conclusion

Each new invention sets the stage for the next. No invention is flawless. It takes years to make an invention almost perfect; nothing is perfect. Most of the 'Net is still in the developmental stages. Most inventions improve the world while some cause misfortune. The Internet can be used for good or evil, as you can see. We must push towards the discovery of favorable uses of our inventions.

INFORMATION IN THE WORLD TODAY

Karl J. Iliev

Acknowledgments

Before this program I was only interested in working in the area of computers. Now I have experienced it. Over the summer I've learned plenty about the Internet and the security involved. I had no idea that so much was involved. Now I am even more interested in computer science. I want to thank the Research and Development Laboratories (RDL) High School Apprenticeship Program and Phillips Laboratory for sponsoring my work. I would also like to thank my co-workers for their encouragement, help, and friendship.

Karl J. Iliev

References

Coast Homepage. (**http://www.cs.purdue.edu/coast/coast.html**)

Firewalls FAQ. (**http://www.cis.ohio-state.edu/hypertext/faq/usenet/firewalls-faq/faq.html**) Dec. 1994 (**mailto:Fwalls-FAQ@tis.com**)

Kantor, Andrew. "Home Sweet Home Page." Internet World, April 1995.

Richard, Eric. "Anatomy of the World-Wide Web." Internet World, April 1995.

Sangster, Paul. (**mailto:sangster@reston.ans.net**). "IP Spoofing and TCP Hijacking." (**mailto:ans-security@ans.net**).

Wiggins, Richard W. "Webolution: The evolution of the revolutionary World-Wide Web." Internet World, April 1995.

CHAOS AND THE DIODE RESONATOR

Rebecca Kalmus

Sandia Preparatory School
532 Osuna Road NE
Albuquerque, NM 87113

Final Report for:
High School Apprentice Program
Phillips Laboratory

Sponsored by:
Air Force Office of Scientific Research
Bolling Air Force Base, DC

and

Phillips Laboratory

August 1995

CHAOS AND THE DIODE RESONATOR

Rebecca Kalmus
Sandia Preparatory School

Abstract

The periodic and chaotic properties of the diode resonator were investigated. Liquid nitrogen was used to study the effects of temperature on the resonator. Different combinations of frequency, amplitude, DC offset, and temperature were used as control parameters of the resonator driver. The goal of the experiment was to find high periods and antimonotonicity. By the end of the summer, both high periods and antimonotonicity had been observed.

CHAOS AND THE DIODE RESONATOR

Rebecca Kalmus

INTRODUCTION

The system under study is a diode resonator, a driven nonlinear circuit composed of a diode, an inductor, and a resistor in series. It has in the past been used to study various chaotic phenomena. It has displayed the period doubling route into chaos, tangent bifurcations, intermittent route into chaos, hysteresis, period bubbling, crisis, and antimonotonicity. Other studies of the circuit have revealed forward and reverse bifurcations with respect to the drive voltage, drive frequency, wave bias, and diode temperature. Theoretically, periods should double to infinity. In reality, doubling rarely reaches higher than period 16 before noise obscures the high periodic orbits.

The diode resonator has a long history of characterization. It was originally studied as a chaotic system by Linsay in 1981 who put together a varactor diode, inductor, and resistor. Linsay observed, in the frequency domain, the period doubling route into chaos. Subsequent studies of the circuit were performed by Testa, Perez, and Jeffries who first obtained bifurcation diagrams of the current with respect to the drive voltage. Perez and Jeffries observed tangent bifurcations and the intermittent route into chaos. Rollins and Hunt, and later Hilborn, studied the onset of crisis in the resonator as the chaotic attractor collided with the stable period 3 orbit. Extensive characterization of the resonator and resistively coupled resonators were made by Buskirk and Jeffries who modeled the circuit as a damped driven oscillator. They obtained and compared numerical and experimental bifurcation diagrams and return maps and observed reverse bifurcations out of chaos as the drive frequency increased.

Monotonicity is either the creation or the destruction of periods. Periods that are created and not destroyed experience period doubling but never reverse period doubling. Doubling of periods does not destroy the lower periods because the higher periods contain the lower periods as well. For example, when a dynamic system bifurcates from period 2 to 4, period 2 still exists in period 4, but it is not visible because it is unstable. Figure 1 shows a logistic map, an example of monotonicity. In a logistic map, periods double into chaos but never reverse the doubling. The destruction of periods is the opposite of a logistic map. Beginning at a high period,

reverse period doubling occurs, destroying the higher period. For example, when a system bifurcates from period 4 to 2, period four no longer exists.

Antimonotonicity is the creation and destruction of an infinite number of periods. A bifurcation diagram showing antimonotonicity begins with period one and, after going through period doubling, chaos, and reverse period doubling, ends with period one. Diagrams illustrating antimonotonicity appear later in this report.

EQUIPMENT

The experiments were conducted with a diode resonator consisting of a diode, inductor, and resistor in series. The diode and inductor give rise to the nonlinear resonator while the resistor influences the quality factor. Two resonator were used. Resonator 1 had a resistor with a resistance of 90.9Ω and an inductor with an inductance of 46mH and a resistance of 417Ω. Resonator 2 had a resistor with a resistance of 330Ω and an inductor with an inductance of 47mH and a resistance of 368Ω. The resonator was driven sinusoidally by a function generator. The voltage across the resistor was amplified by a low noise preamplifier, then recorded by a digitizer. Data was collected on a PC and analyzed on an HP workstation.

EXPERIMENTS

In the first experiment resonator 2 was used. A potentiometer, which served as a voltage divider, was attached to the preamplifier in order to shift the signal within the range of the digitizer. In this experiment, the drive frequency was 110kHz and the amplitude was 5V; the DC offset increased in increments of 4mV. The resulting bifurcation diagram is shown in figure 2. The gray tones represent peak density, or the number of peaks at a given coordinate. The gray tone diagram has two advantages over a black and white diagram. It is much easier to see the periodic orbits in the chaos and it is possible to see where the wave spends most of its time. The only problem with the bifurcation diagram in figure 2 is it jumps at -0.8 and -0.3V. When a bifurcation diagram was taken of only the area of the jumps, no shifts occurred. The shifts could be the result of using AC coupling to the digitizer rather than DC coupling. However, subsequent bifurcation diagrams using DC coupling also showed jumps. Alternatively, the shifts could have resulted from hysteresis, which occurs when there are two paths for the signal to follow. The path taken depends upon the direction from which the signal is coming, that is, whether the DC offset (or amplitude or frequency or whatever variable is changing) is increasing or

decreasing. The signal follows one path until it becomes unstable, then jumps to the other path. A bifurcation diagram similar to figure 2 is shown in figure 3. It was taken at a frequency of 38kHz and an amplitude of 8V while the DC offset increased in increments of 1mV. It also shows period doubling, reverse period doubling, chaos, periodic windows, and period adding. However, the diagram in figure 2 shows points that were taken only above the average, thereby cutting off some of the lower points. The diagram in figure 3 shows all the points the signal produced.

Liquid Nitrogen

In the next experiment resonator 1 was first cooled in liquid nitrogen. When the resonator was placed directly in the liquid nitrogen the signal never bifurcated above period two, even when an amplifier was used to multiply the function generator's amplitude by three. The resonator was then left in liquid nitrogen until it had cooled to the same temperature, then taken out and allowed to warm to room temperature. The settings on the function generator were a frequency of 150kHz, an amplitude of 9.5V, and a DC offset of 0.0V. The signal doubled from period 1 to 2 to 4 to 8 to 16 to chaos. Because the resonator warmed to room temperature very quickly, it was difficult to catch the high periods. Periods higher than 16 may have appeared for an extremely short time. Figure 4 (a) shows a time series taken as the resonator was warming up at period 8. A Fourier transform and a reconstruction of the attractor are shown in figures 4 (b) and (c). These show that the signal is actually just above period 8 and starting to go into chaos.

Another liquid nitrogen experiment was done with the identical setup described in the preceding experiment, except resonator 2 and a driving amplifier were used. In this experiment frequency and amplitude were held constant while DC offset was changed. The resonator was set about five inches above liquid nitrogen, making the temperature of the resonator below room temperature but not as cold as liquid nitrogen. The resonator was insulated to keep its temperature constant. Figure 5 shows the observed bifurcation diagrams using this setup. Figure 5 (a) shows periods 1-2-1 taken at a frequency of 60kHz and an amplitude of 5.01V while the DC offset increased in increments of 10mV. Figures 5 (b) and (c) show periods 1-2-4-2-1 taken at a frequency of 60kHz and an amplitude of 9.09 and 15V, respectively, while the DC offset increased in increments of 10mV. Figures 5 (d) and (e) show periods 1-2-4-chaos-4-2-1 taken at a frequency of 60kHz and an amplitude of 30 and

24V, respectively, while DC offset increased in increments of 10mV. These figures are examples of period doubling and reverse period doubling. Figure 5 (f) shows a bifurcation diagram taken at a frequency of 150kHz and an amplitude of 30V while the DC offset increased in increments of 10mV. Figure 5 (f), which was taken at a higher frequency in order to get higher periods, also shows period doubling, reverse period doubling, chaos, period adding, and periodic windows.

Driving the Resonator with Two Sine Waves

In another experiment resonator 2 was hooked up to a driving amplifier, two function generators, and a signal analyzer instead of a digitizer. One function generator was set at a low frequency (30 to 70kHz) and amplitude. The other function generator was set at a frequency of 30 to 100kHz. The amplitude of the second function generator was set at the point that the signal had just bifurcated from period 1 to 2. The voltage difference between the highest and lowest points of the signal in period two was measured. The results, expressed in mV, are shown in the table below.

	30kHz	**40kHz**	**50kHz**	**60kHz**	**70kHz**	**80kHz**	**90kHz**	**100 kHz**
30kHz	222	112	67.2	47.2	28	23.2	18.8	16
40kHz	240	128	84	48	34.4	22.4	19.6	17.2
50kHz	256	128	68.8	52	36.8	30.4	24.8	16
60kHz	236	141.6	82.4	56	37.6	28.4	24.4	22.4
70kHz	220	110	65.6	51.2	34.4	26.4	22	20

A second experiment with resonator 2 and two function generators but no preamplifier was designed to determine how the second function generator affected the amplitude at which the resonator bifurcated from period 1 to 2. In this experiment the main function generator was set to a frequency of 50 or 60kHz and the amplitude was changed until the signal bifurcated from period 1 to 2. The second function generator was then turned on to a frequency between 20 and 120kHz and its lowest amplitude. The amplitude of the main function generator was again varied to see where the signal bifurcated from period 1 to 2 with two function generators attached to the resonator. A table of the results, measured in volts, is shown below.

	main amp.	20 kHz	30 kHz	40 kHz	50 kHz	60 kHz	80 kHz	100 kHz	120 kHz
50kHz	0.967	1.04	1.15		1.927		1.93	1.932	1.929
60kHz	0.781	1.552		1.556		1.556	1.557	1.557	1.557

The second function generator caused the amplitude at which the signal bifurcated from period 1 to 2 to increase by a factor of two, except for the 20 and 30kHz readings when the main function generator was set to 50kHz. If those two readings are ignored, than the increase in frequency of the second function generator did not affect the amplitude at which the signal bifurcated. As long as the second function generator was turned on to any frequency, the amplitude at which the signal bifurcated doubled; the particular frequency of the second function generator did not matter.

Synchronization

The next experiment involved synchronizing two chaotic resonator. They were mutually coupled with a capacitor or potentiometer from between the diode and inductor of one resonator to between the diode and inductor of the second resonator or between the inductor and resistor of one resonator to between the inductor and resistor of the second resonator. Using a 10k potentiometer between the resistors, the resonators synchronized at 0.4Ω; between the diodes they synchronized at 37.3Ω, although not as well as between the resistors. When a capacitor was placed between the diodes of the resonators, synchronization occurred for 0.011mf and higher. When the capacitor was placed between the resistors, however, the resonators never synchronized.

Antimonotonicity

The last experiments demonstrate antimonotonicity in the diode resonator. Resonator 2 was placed in ice for all these experiments to reduce noise. A low-impedance line driver was connected between the waveform generator and the resonator to reduce feedback into the function generator. A potentiometer, which served as a voltage divider, was attached to the preamplifier in order to shift the signal within the range of a 16-bit resolution digitizer card with a one megabyte per

second sampling rate. The first bifurcation diagrams, shown in figure 6, are signal peaks (arbitrary units) vs. DC offset, taken at a frequency of 40kHz and an amplitude of 0.75V, 0.3V, and 0.5V, respectively. They show period doubling and reverse period doubling without chaos. Another bifurcation diagram, shown in figure 7 (a), illustrates antimonotonicity. The diagram displays signal peaks (arbitrary units) vs. DC offset and was taken at a frequency of 40kHz and an amplitude of 8V. Figure 7 (b) is a close up of figure 7 (a) showing period 4, 8, 6, and 12 windows and reverse period doubling out of chaos. Figure 7 (c) is a close up of figure 7 (a) showing the destruction of periods from chaos to periods 4, 2, and 1. Figure 8 shows return maps of the bifurcation diagrams in figure 7 (a). All the return maps except (b) show chaos at their DC offset; (b) shows a period 5 window. The diode resonator is a three dimensional system. However, in a phase space with current as the x-axis, voltage across the diode as the y-axis, and time as the z-axis, the graph looks like curled string. In parts of the phase space the "string" (the attractor) can be considered one dimensional. (b) and (g) are one dimensional while the rest of the return maps indicate higher dimensionality. It is only at a DC offset of close to 0.0V that the return maps are almost one dimensional. As the DC offset moves away from 0.0V, the diode resonator becomes higher dimensional. The ticks that appear at the beginning and end of (a) are due to the folding over of the bifurcation diagram in figure 7 (a) which occurs at a DC offset of approximately -0.54 to -0.39V. Finally, figure 9 contains a bifurcation diagram of signal peaks (arbitrary units) vs. DC offset showing antimonotonicity. Frequency was 40kHz, and amplitude was 3 V. Figure 9 shows even more clearly than figure 7 the destruction of periods from chaos to periods 4, 2, and 1.

CONCLUSION

The purpose of putting the resonator in liquid nitrogen was to reduce noise in order to observe high periods. Resistors generate noise voltage across their terminals. This is called Johnson noise, whose formula is $V_{noise}=(4KTRB)^{1/2}$, where T is temperature in degrees Kelvin. Based on this formula, noise should be reduced as temperature decreases. When the resonator was placed above liquid nitrogen, high periods were seen. However, at lower temperatures the amplitude and frequency of the function generator had to increase in order to observe high periods. Data taken at high frequencies will have fewer points per period than data taken at low frequencies due to the fixed sampling rate of the digitizer. While bifurcation

diagrams taken at low temperatures and high frequencies were less noisy than those taken at room temperature, they did not contain as many points and were less accurate. This problem can be corrected, however, by either using a driving amplifier to increase the amplitude of the function generator or by using a digitizer with a higher sampling rate.

Antimonotonicity, illustrated in figures 7 and 9, was observed in the last few bifurcation diagrams. Earlier bifurcation diagrams show period doubling and reverse period doubling, but in those the signal bifurcates directly from chaos into period 1. Only in the diagrams in figures 7 and 9 is the bifurcation from chaos to period 4 to 2 to 1 obvious. Reverse period doubling is seen not only at the end of the diagrams, into period 1, but also in the middle, where it bifurcates from period 8 to 4 to 2. These diagrams prove that antimonotonicity, which is seen numerically, is also seen experimentally in the diode resonator.

REFERENCES

S. P. Dawson and C. Grebogi, Chaos, Solitons, and Fractals, **1**, 137 (1991).

S. P. Dawson, C. Grebogi, J. Yorke, I. Kan, and H. Koçak, Physics Letters A, **162**, 249 (1992).

P. Horowitz and W. Hill, *The Art of Electronics* (Cambridge University Press, Cambridge, 1980).

A. P. Malvino, *Electronic Principles, 4th Edition* (McGraw Hill Book Company, New York, 1989).

T. C. Newell, Thesis, 1994, University of North Texas.

R. Van Buskirk and C. Jeffries, Physical Review A **31**, 3332 (1985).

Figure 1

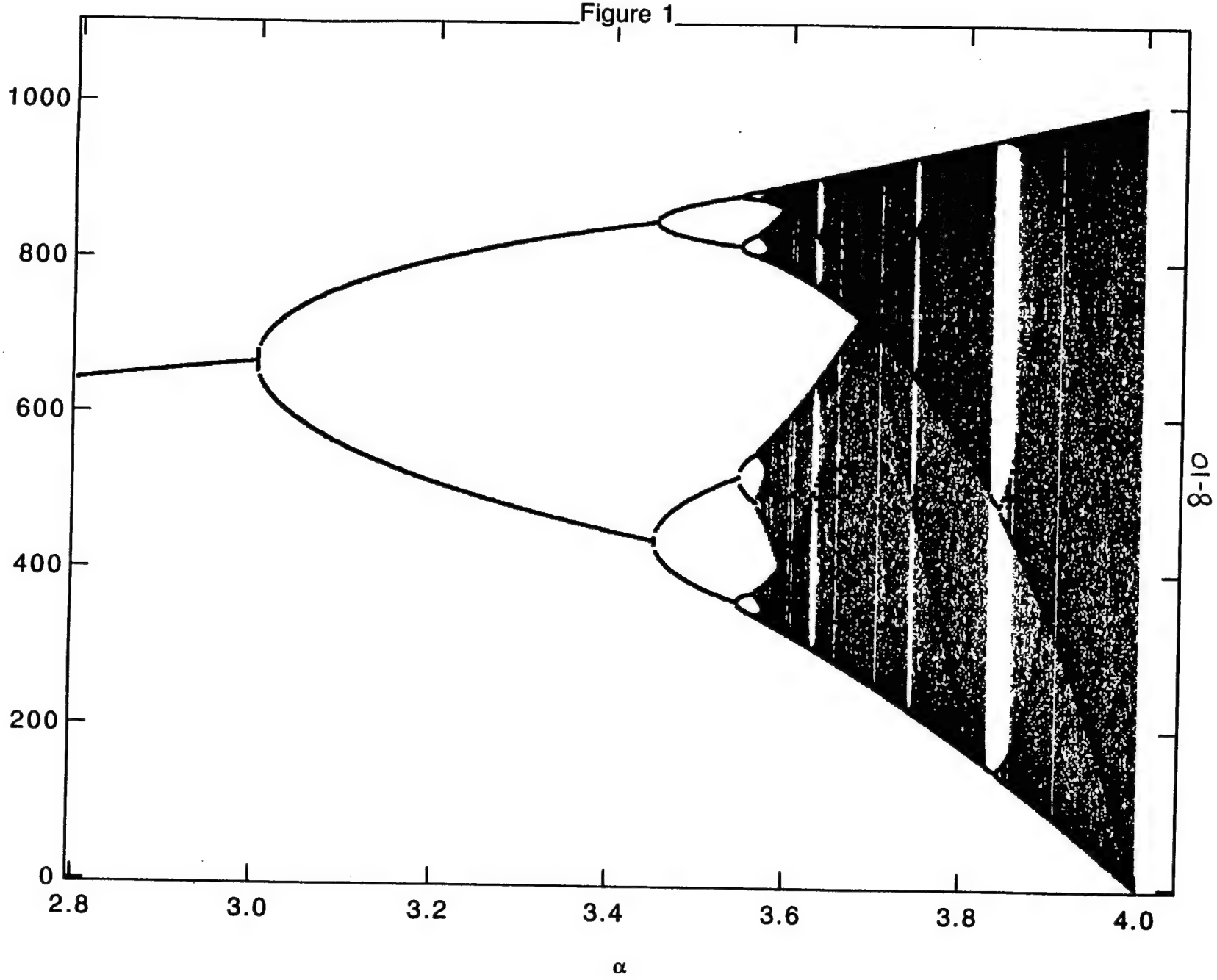

Figure 2

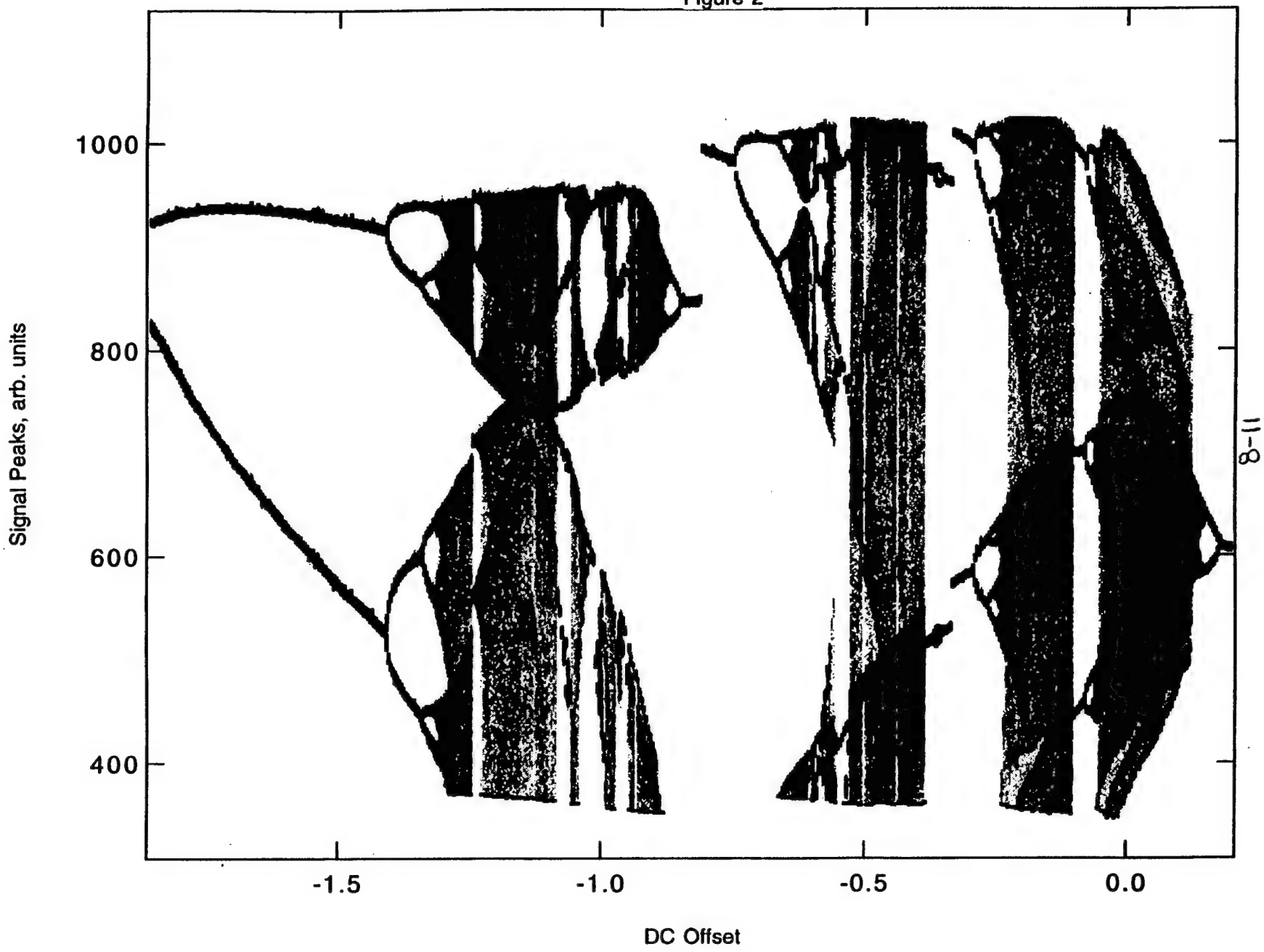

Figure 3

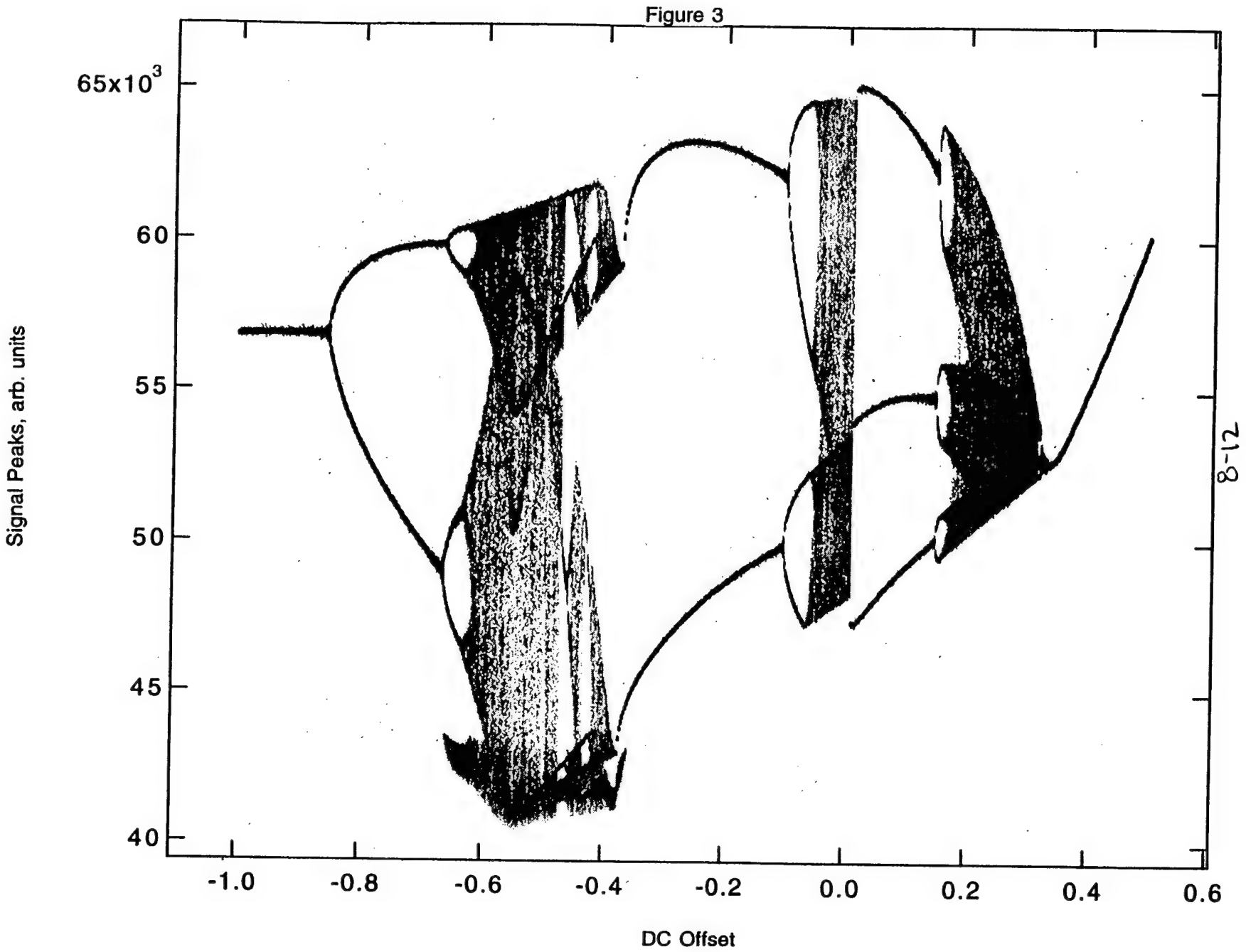
65x10^3
60
55
50
45
40
Signal Peaks, arb. units
-1.0
-0.8
-0.6
-0.4
-0.2
0.0
0.2
0.4
0.6
DC Offset

Figure 4

16 June, 1995
Diode Resonator just above period 8 crygenically cooled.
f=105kHz, A=9.5V, DC = 0.0V
(a) Peaks of time series (b) Fourier transform
(c) Reconstruction of the attractor.

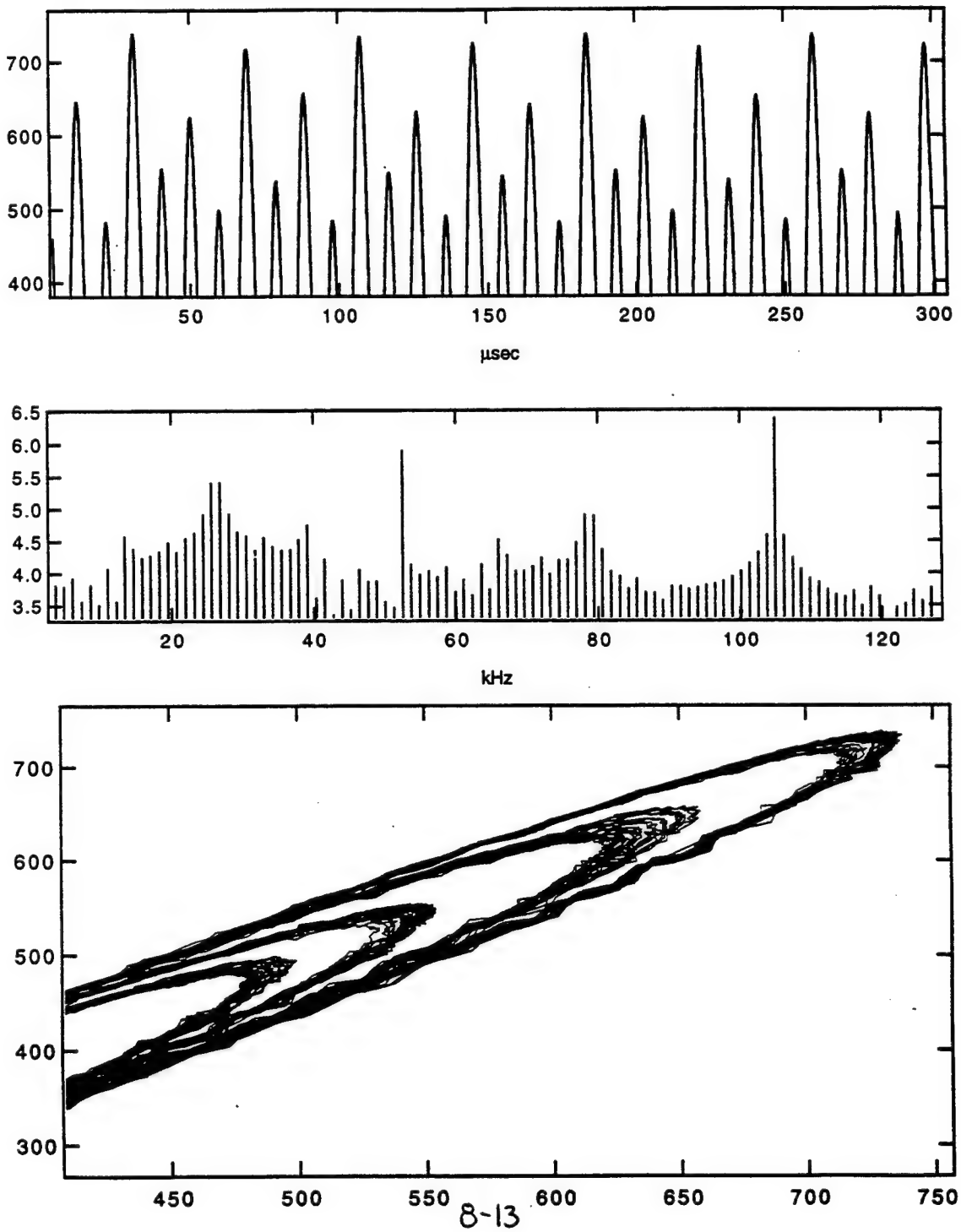

Figure 5

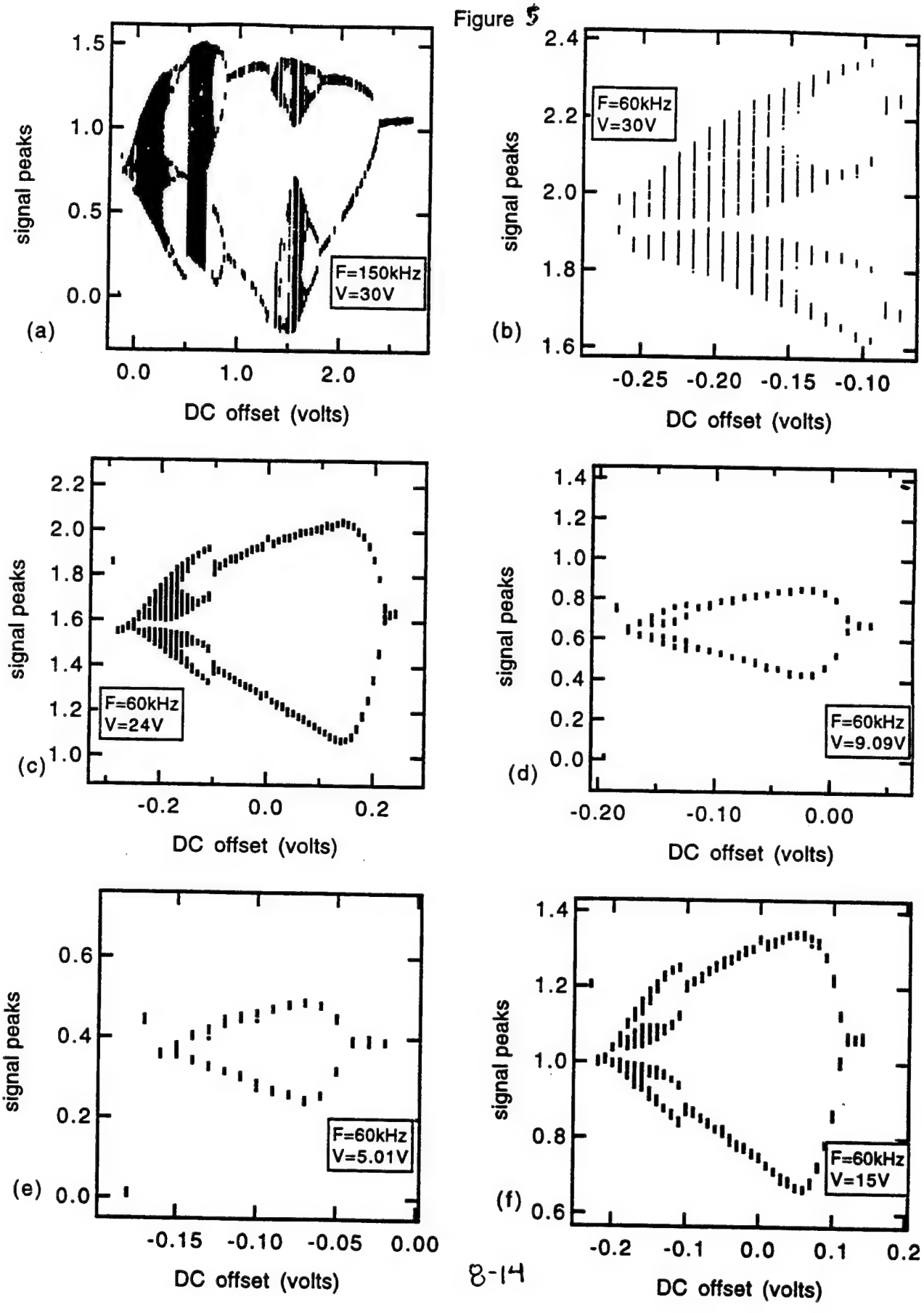
signal peaks
DC offset (volts)
F=150kHz
V=30V
(a)
F=60kHz
V=30V
(b)
F=60kHz
V=24V
(c)
F=60kHz
V=9.09V
(d)
F=60kHz
V=5.01V
(e)
F=60kHz
V=15V
(f)

Figure 6

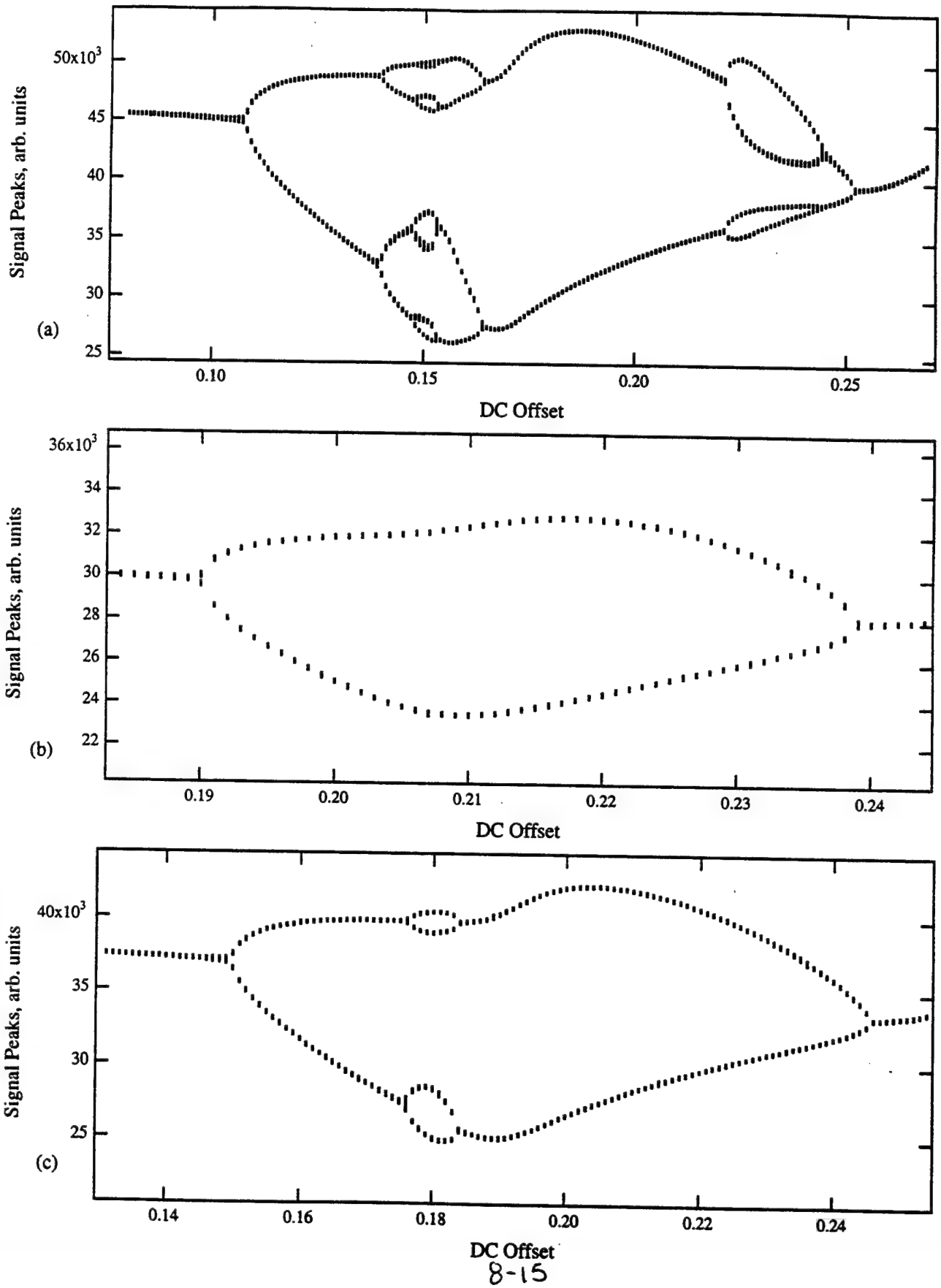
50x10^3
45
40
35
30
25
Signal Peaks, arb. units
(a)
0.10
0.15
0.20
0.25
DC Offset
36x10^3
34
32
30
28
26
24
22
Signal Peaks, arb. units
(b)
0.19
0.20
0.21
0.22
0.23
0.24
DC Offset
40x10^3
35
30
25
Signal Peaks, arb. units
(c)
0.14
0.16
0.18
0.20
0.22
0.24
DC Offset

8-15

Figure 7 (a)

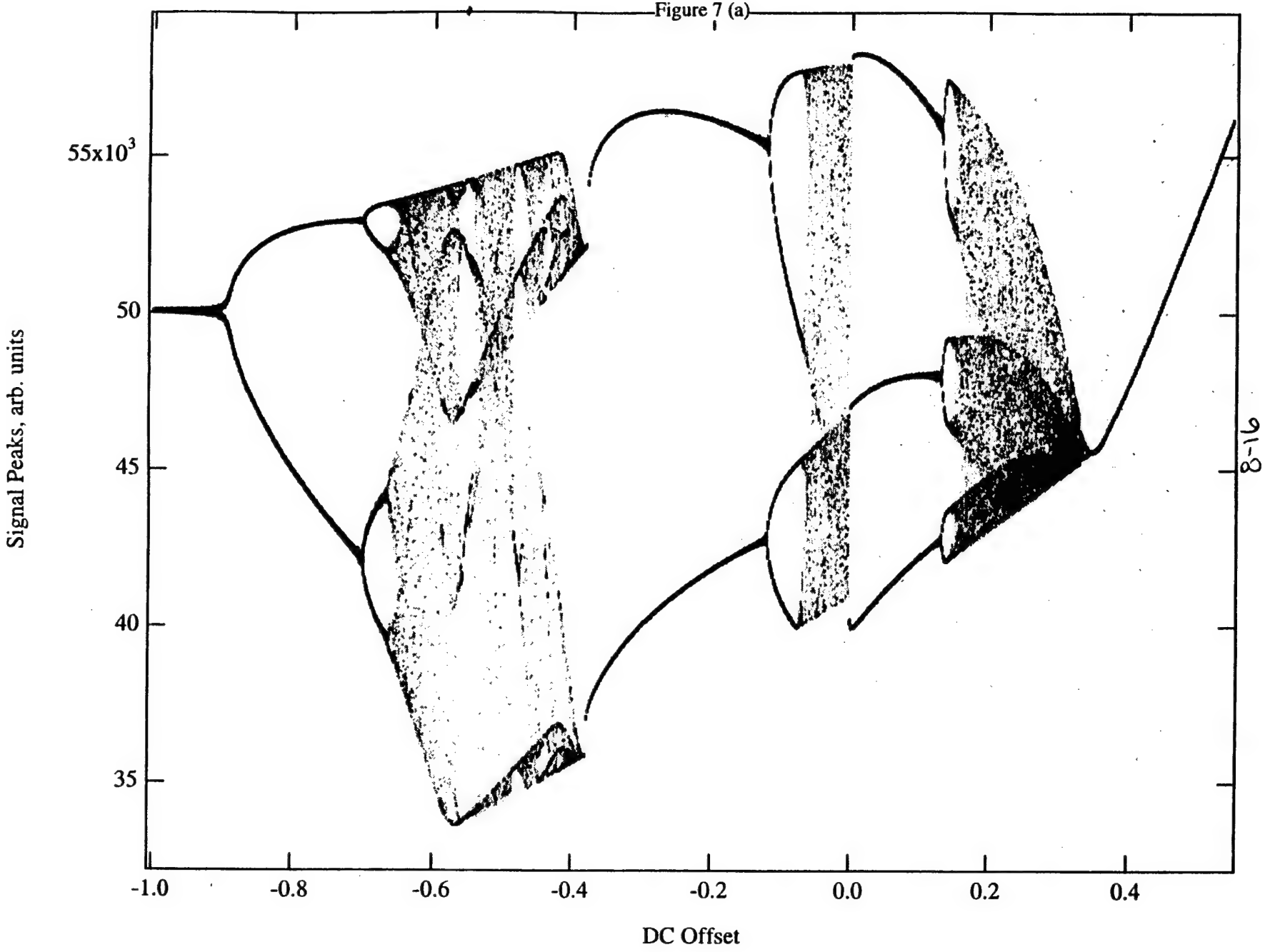
55x10^3
50
45
40
35
Signal Peaks, arb. units
-1.0
-0.8
-0.6
-0.4
-0.2
0.0
0.2
0.4
DC Offset

Figure 7 (b)

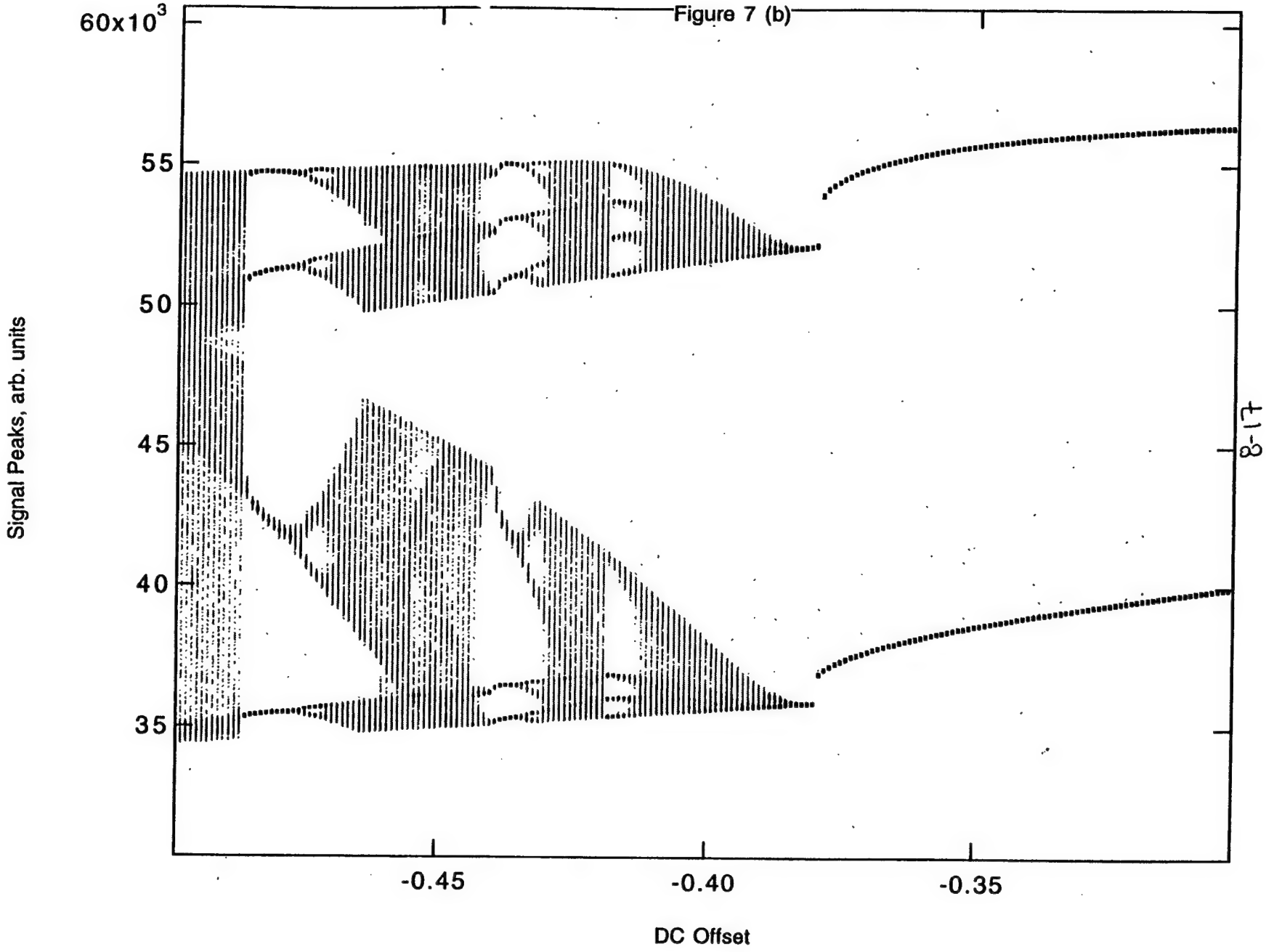
60x10^3
55
50
45
40
35
Signal Peaks, arb. units
-0.45
-0.40
-0.35
DC Offset

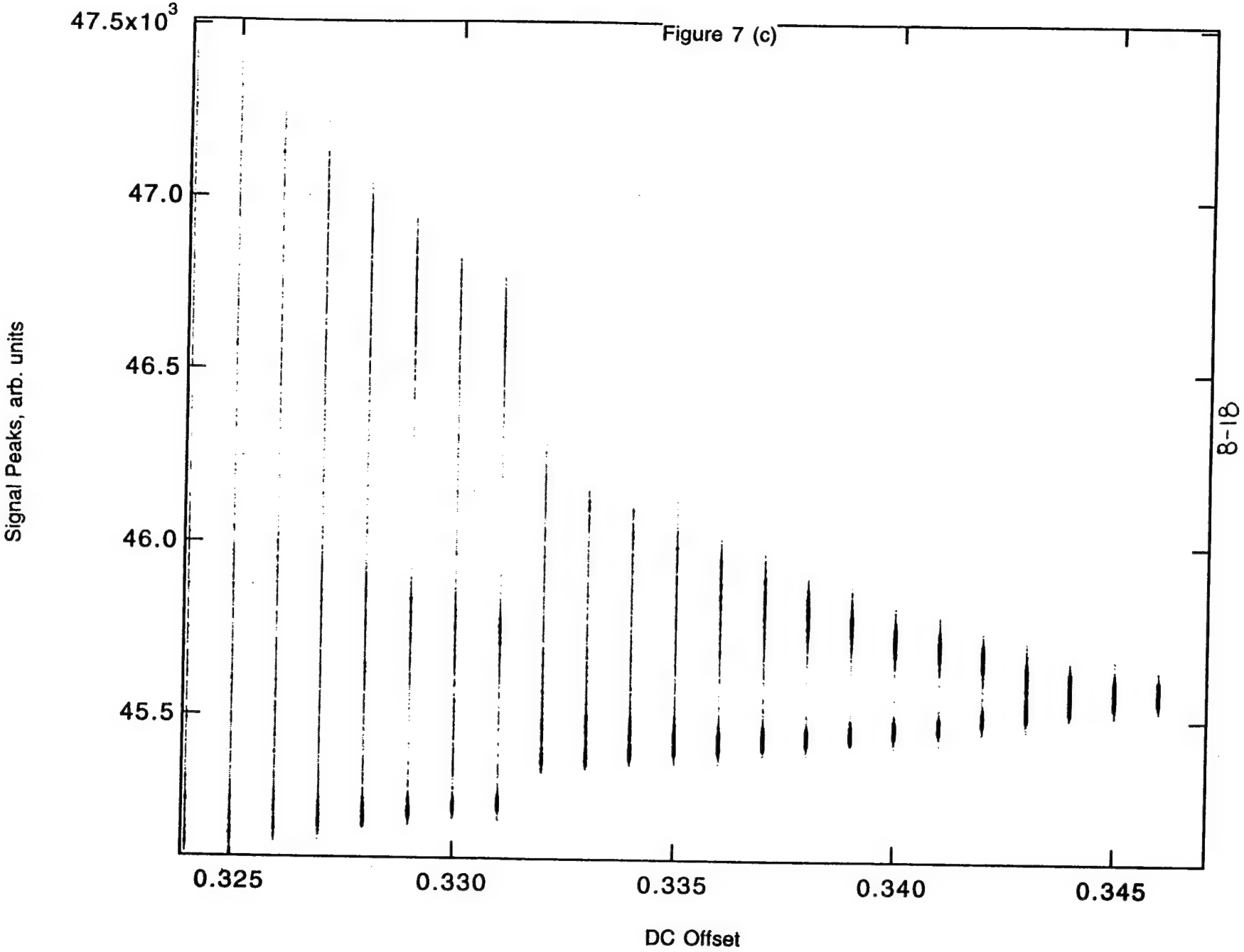
47.5x10^3
47.0
46.5
46.0
45.5
Signal Peaks, arb. units
0.325
0.330
0.335
0.340
0.345
DC Offset
8-18

Figure 7 (c)

Figure 8

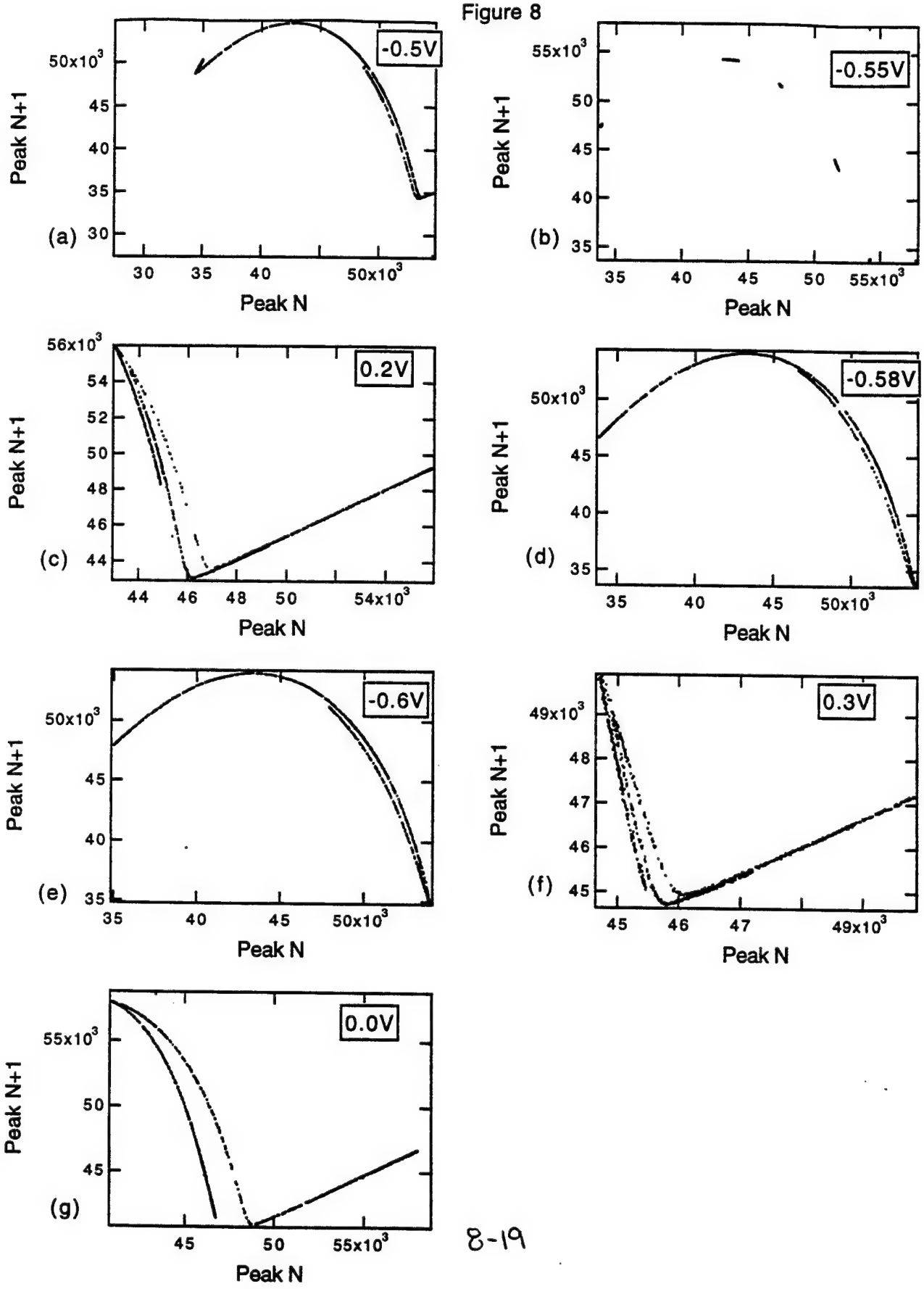
-0.5V
50x10^3
45
40
35
30
(a)
30
35
40
50x10^3
Peak N+1
Peak N
-0.55V
55x10^3
50
45
40
35
(b)
35
40
45
50
55x10^3
Peak N+1
Peak N
0.2V
56x10^3
54
52
50
48
46
44
(c)
44
46
48
50
54x10^3
Peak N+1
Peak N
-0.58V
50x10^3
45
40
35
(d)
35
40
45
50x10^3
Peak N+1
Peak N
-0.6V
50x10^3
45
40
35
(e)
35
40
45
50x10^3
Peak N+1
Peak N
0.3V
49x10^3
48
47
46
45
(f)
45
46
47
49x10^3
Peak N+1
Peak N
0.0V
55x10^3
50
45
(g)
45
50
55x10^3
Peak N+1
Peak N

Figure 9

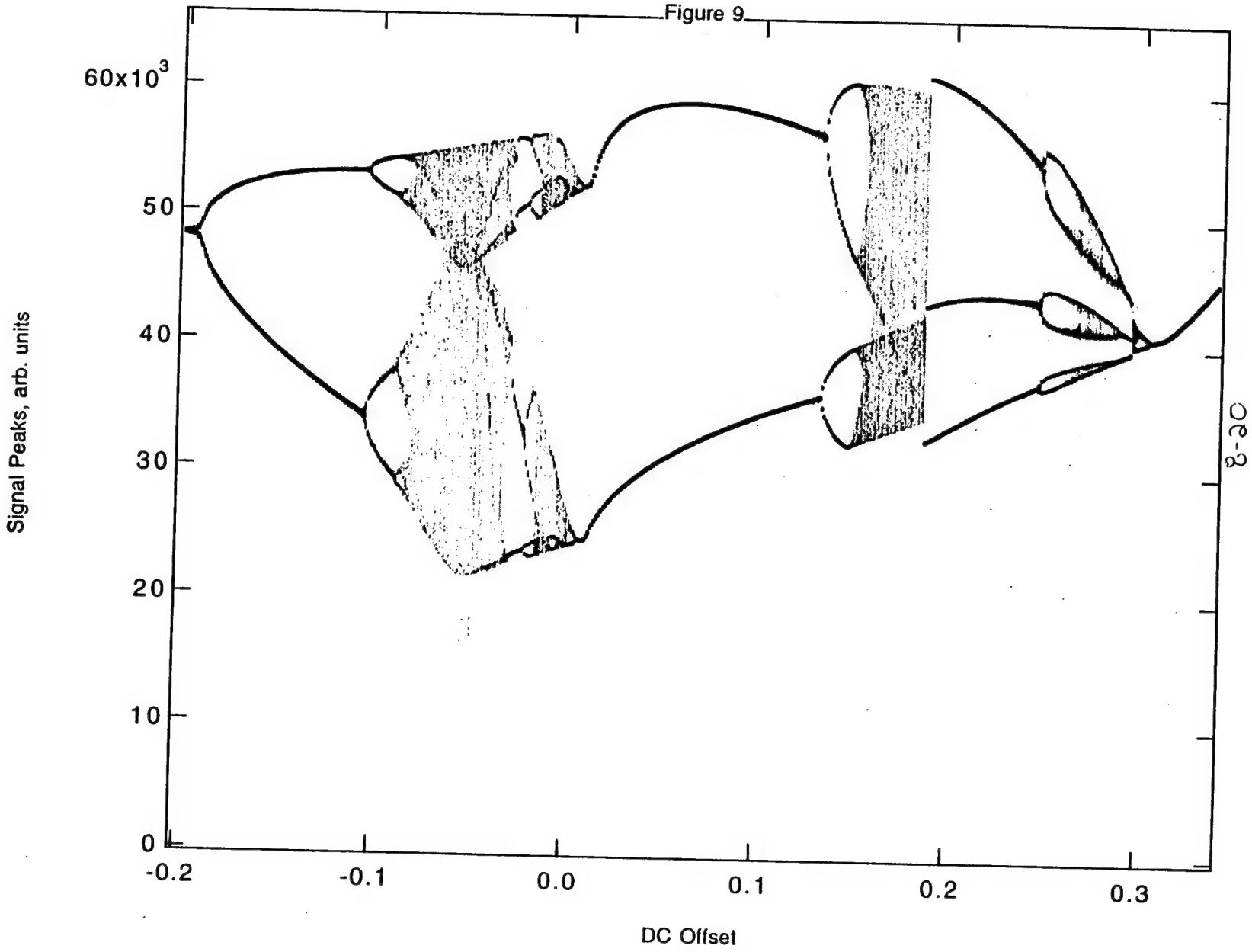
60x10^3
50
40
30
20
10
0
Signal Peaks, arb. units
-0.2
-0.1
0.0
0.1
0.2
0.3
DC Offset

A MOS APPROACH FOR THE PREDICTION OF SUMMERTIME CLOUD COVER OVER NEW ENGLAND

Hong Van M. Le

Chelmsford High School
200 Richardson Road
Chelmsford, MA 01863

Final Report for:
High School Apprentice Program
Phillips Laboratory
Geophysics Directorate

Sponsored By:
Air Force Office of Scientific Research
Hanscom AFB, Boston, MA
and
Phillips Laboratory

August 1995

A MOS APPROACH FOR THE PREDICTION OF SUMMERTIME CLOUD COVER OVER NEW ENGLAND

Hong Van M. Le
Chelmsford High School

ABSTRACT

Model Output Statistics (MOS) is an objective weather forecasting technique that determines a statistical relationship between the predictand (cloud amount) and predictors (forecast variables) by using a numerical model at some projection time. This research project focused on the generation of MOS equations and the analysis of those regression statistics. Four cities were chosen to conduct the project: Boston, MA; Concord, NH; Burlington, VT; Caribou, ME. The forecast data was collected from the Eta Model, an operational weather prediction model that carries out forecast information to forty-eight hours. The variables used to predict cloud amount in New England during the summer included: U and V wind components, vertical velocity, lifted index, six-hour precipitation amount, and relative humidity at three levels in the troposphere. A multiple linear regression was performed to calculate correlation coefficients that are a measure of the relationship between a predictor and cloud amount. Significance testing was done to determine the degree of confidence in the correlation. Results showed that the degree of correlation generally decreased with forecast length. Verification tests showed that at certain stations, the MOS equations showed some skill at forecasting cloud amount.

A MOS APPROACH FOR THE PREDICTION OF SUMMERTIME CLOUD COVER OVER NEW ENGLAND

Hong Van M. Le

I. Introduction

A. Phillips Laboratory

Phillips Lab is one of four laboratories that conducts R&D for the US Air Force. There are branches at Kirtland AFB, NM; Space and Missiles Systems Center, Los Angeles AFB, CA; Air Force Material Command, Wright-Patterson AFB, OH; and Hanscom AFB, MA. At Hanscom AFB, MA, Geophysics is the focus of Phillips Laboratory. There are research departments in space and ionospheric physics, atmospheric and earth sciences, and optical and infrared technologies. The lab develops geophysical models and databases, design standards, and prototype hardware and software.

In the Atmospheric Sciences Division of the Geophysics Directorate, scientists and researchers are dedicated to the investigation of atmospheric effects on AF (Air Force) systems and operations. The search for better methods of observing and predicting meteorological conditions continues to be a vital part of the geophysical research program of the AF because many operations and systems past, present, and future depend on atmospheric conditions and changes {11}.

B. Forecasting Cloud Amount

Focusing on the important effects of cloud amount in many military operations illustrates the need for accurate cloud forecasts. In daily operations, successful use of electro-optical communication and sensor systems of the AF greatly depends on the knowledge of the probability of the cloud-free line-of-site from one level of the atmosphere to another at selected angles of elevations. Fogs and clouds also affect the propagation of electromagnetic radiation through the atmosphere as well as decrease visibility at and around airfields. The presence in the atmosphere of clouds that generate precipitation is a critical input for the deployment of systems which operate surveillance radar and for selecting microwave frequencies used in communication systems. In addition, leading edges of aircrafts and missiles are subject to erosion by precipitation particles {11}.

With precise cloud forecasts, many of the problems and risks mentioned above can be prevented or eliminated. This motivated the goal of the project which was to generate statistical relationships to forecast cloud amount in the summer from the forecast variables of a Numerical Weather Prediction (NWP) model. In this project, four New England cities were observed during late June, July, and early August. Using the data collected during the six weeks, a MOS equation was generated for each city for twelve, twenty-four, thirty-six, and forty-eight hour forecasts from 0000 UTC and 1200 UTC model runs.

C. New England Summertime Climate

New England is characterized by the unique elements of each of its four seasons. With a moderately cold winter and wet spring, New England residents have come to cherish and value their summer. Showers and thunder storms are the major sources of precipitation. New England summer is basically associated with long, warm, and sunny summer days and cool and pleasant summer nights. In addition, because the relative humidity is usually at its highest in the summer, the climate is generally temperate and humid. Even though the weather seems to follow a pattern for each season, New England weather is also famous for being unpredictable. Drastic changes can occur over a very short period of time. Therefore no one can complain that New England weather is dull.

1. Boston, Massachusetts

Being situated in a zone with prevailing west to east atmospheric flow, both the polar and the tropical air masses influence the Boston region. In addition, Boston is frequently on or near the tracks of many low pressure storm systems. The extreme temperatures of the summer and winter months are moderately influenced by the Atlantic ocean because Boston is on the east coast. Cooling sea breezes often relieve the hot summer afternoons when air flows inland from cool water surfaces to displace warm air over the land. The average summer temperature ranges from 67.1 to 72.7 degrees, the hottest month being July. Boston also experiences heavy fog on an average of two days in a month with its prevalence increasing eastward from the interior of Boston Bay to the open waters beyond.

2. Burlington, Vermont

On the eastern shore of Lake Champlain at the widest part of the lake, and near the peaks of the Adirondacks and the Green Mountains, lies Burlington, Vermont. As a result of its geographical location, Burlington experiences the variety and vigor of New England weather. The city is one of the cloudiest in the US because Burlington is also situated in the path of the St. Lawrence Valley storm track. Despite this factor, Burlington residents can still enjoy delightful summer weather. There are few days higher than ninety degrees. Precipitation is generally plentiful and well distributed throughout the year. Overall Burlington experiences moderate summer climates.

3. Caribou, Maine

Caribou, Maine is influenced by the Summer Polar front because of its location high up in the St. Lawrence Valley. As a result, Caribou has cool summer months with a growing season of only one hundred and twenty days. Caribou has sparkling visibility and relatively pollen-free air in the late summer months. With an abundance of precipitation, there are practically no dry periods of more than three to four days during the growing season.

4. Concord, New Hampshire

Near the geographical center of New England lies Concord, New Hampshire. Concord is characterized by the hilly and wooded countryside and the surrounding lakes and ponds. Northwesterly winds are prevalent, bringing pleasantly cool and dry air in the summertime. Occasionally stronger southerly winds also come in during July and August. Generally, the summers are not very hot. Precipitation occurs on an average of one out of every three days of the year. The most significant rain is associated with northeasterly winds during the months of April and May.

D. Current Forecast Tools

The National Meteorological Center (NMC) acquires, processes, and distributes meteorological and oceanographic information to users throughout the Northern Hemisphere. A major focus of NMC is the production of weather summaries, short and extended range forecasts, and developing methods to improve forecasting techniques. The three major numerical weather prediction models that forecast New England weather are the Eta, NGM, and the MRF models. These NWP models are run on the NMC's high-speed computers. NMC distributes data to the National Weather Service forecast offices, the US Air Force, the Federal Aviation Administration, and other governmental and non-governmental offices.

1. Eta Model

The Eta model was implemented in June, 1993, replacing the LFM (Limited-area Fine Mesh) model in providing early forecast guidance over North America after elaborate testing. The current Eta model that the NMC operates is a thirty-eight level version with a horizontal resolution of eighty kilometers {2}. It provides daily forecasts out to forty-eight hours beginning at 0000 UTC and 1200 UTC. The vertical coordinate (called eta) is a generalization of the terrain-following sigma coordinate. Both the eta and sigma coordinates are pressure-based and normalized from zero to one, but the Eta is normalized with respect to sea-level pressure instead of surface-level pressure. The result is eta surfaces that are quasi-horizontal, which eliminates errors in pressure gradient force computation over steeply sloped terrain which occur in sigma coordinates {2}. The Eta model runs in NMC's Early slot which is intended to provide timely first looks at forty-eight hour forecasts. Initial data for the Eta Model is provided by NMC's Global Data Assimilation System (GDAS). Currently the Eta model is one of the most hi-tech and sophisticated NWP models available, yet improvements and developments are still being applied to the model.

2. Nested Grid Model Forecast (NGM)

As a forecast model component of RAFS (Regional Analysis and Forecast System), the NGM was introduced operationally on March 27th, 1985 {7}. The model runs on a two-grid configuration. The outer grid is hemispheric, and the inner grid—centered over the United States—has twice the resolution of the grid surrounding it. NGM's inner grid has a horizontal resolution of eighty-four kilometers, and a vertical resolution of sixteen

layers {8}. The NGM is used to provide twice daily forecasts of up to forty-eight hours, and runs in NMC's Regional slot. The task of initializing the NGM Model is carried out by the Regional Data Assimilation System (RDAS) {2}. Eventually, the NGM will be phased out and replaced by the Eta model.

3. Medium Range Forecast Model (MRF)

In March of 1991, forecasts from the MRF GDAS (Global Data Assimilation System) forecast model-became routinely available {5}. It is started about six hours after the collection of 0000 UTC data and is integrated out to two hundred and forty hours (ten days) {10}. Like NGM, the global forecast model uses sigma coordinates (normalized pressure) for the vertical. In the horizontal, MRF uses the spectral method for the representation of fields {9}. The model has eighteen layer vertical resolution, and a horizontal resolution of 126 waves with triangular truculation (T126) in the east and west direction. The T126 resolution corresponds to about eighty kilometers horizontal resolution. In the "Aviation Run" mode, the MRF is also run twice daily to produce 72 hour forecasts that provide timely guidance to the US aviation community {3}.

E. Model Output Statistics (MOS)

MOS is an objective weather forecasting technique that determines a statistical relationship between the predictand and the forecast variables (predictors) by using a numerical model at some projection time. Applications of MOS and screening regression may be used to develop an objective method to forecast surface weather variables {6}. The MOS technique defines a statistical relationship between the numerical values from the models and the actual weather {1}. MOS requires an archive of dynamical model forecasts. With the archive of data, usually a multiple linear regression statistics method is used to determine relationships among various observed weather elements (predictands) and numerical model weather elements (predictors) {4}.

Using the multiple linear regression method, a line is fitted through a set of observations using the "least squares" method. This method also determines the coefficient of each independent variable called the regression coefficient. The equation also has a constant coefficient (called the regression constant). The regression coefficients represent the relative role each predictor plays in determining the predictand. With these regression coefficients and the regression constant, new forecast values for the predictors obtained from a dynamical model can be input into the equation to calculate the new forecast predictand. As a result, the MOS equation accounts for some of the bias and systematic errors that can be found in dynamical models {4}.

II. Methodology

A. Data

Before a MOS equation can be created using the multiple linear regression method, an archive of forecasts over a period of time must be obtained. Over a six week period, forecast data from the Eta Model were saved and kept in a database. The observational data were taken from Aviation Surface Airways Reports accessible through

the University of Illinois Gopher. These airway weather observations are taken every hour on the hour at most of the world's principal airports. Each day, observations for 0000 UTC and 1200 UTC were selected. The significant observation for the project was the cloud amount. The greatest observed cloud fraction amount among the various reported layers at 0000 UTC and 1200 UTC served as the predictand. Each type of observation was assigned to a number to convert the predictand into a numerical format to be able to perform the regression (see Table 1).

Table 1. Symbolic and Numerical Representation of Observed Cloud amount

Observed Cloud Amount	Symbol	Numerical format
clear	clr	0
light obscuration	-X	1
light scattered	-sct	2
scattered	sct	3
light broken	-bkn	4
broken	bkn	5
light overcast	-ovc	6
overcast	ovc	7
obscured	X	8

The forecast data were taken from the Eta Model runs of 0000 UTC and 1200 UTC each day. From the Eta Model, the twelve, twenty-four, thirty-six, and forty-eight hour forecasts data were chosen. Selected predictors were taken and organized into the spreadsheet for each city. There were a total of thirty-two spreadsheets (4 cities x 2 initial or start time x 4 output times).

B. Data Source

The days of digging through mountains of files in a storage room are over. The best place to get access to any type of data quickly and easily at the push of a button is the information super-highway. The World Wide Web (WWW) pages and gophers that many universities and institutions maintain are in many cases dedicated to weather and meteorology and can be accessed from the Internet. One useful source is the University of Illinois Weather Gopher. This is a gopher server operated by the University of Illinois Atmospheric Department. The gopher server contains up-to-date observations and forecasts. Other sites on the Internet were used from time to time as back-up or research sources. Data from these sites were retrieved and saved locally.

The AF Interactive Meteorological System (AIMS), running the VAX/VMS system at Phillips Lab also served as a source of forecast data and observations, but only as a backup source. AIMS has an archive, in which past observations or Eta model forecasts can be called up. This is useful, because the University of Illinois Gopher only displays current Eta model forecasts, and observations for the most recent thirty-six hour period. Therefore any missing data can be retrieved from AIMS, if the information is available.

C. Database and Computing Environment

In order to carry out the data collection process, an essential tool was the workstation. A UNIX workstation was the main repository for data collected and maintained in the database of observations and Eta model forecasts. The data organization, analysis, and word processing tasks were carried out on a PC.

At the Geophysics Directorate, various mainframes, workstations, and PC's are all connected to a high capacity Local Area Network (LAN). The LAN permits interconnectivity between these host computers as well as enabling high speed data transfer. The network conforms to Ethernet, which is a type of network cabling and signaling standard. Both DECNET and TCP/IP protocols are being concurrently utilized by the LAN, with the latter facilitating connectivity with the Internet and the outside world. The X-Windows standard is supported by many applications in this computing environment. Using X-Windows allows a user to work with multiple programs simultaneously, regardless of the native operating system and network protocol. Each application can be viewed in a separate window on any workstation or any other X-Window device that is connected to the network. This means that a user can run a process on remote machine while displaying the results on their own screen. This facilitates the use of several different host computers and applications that were required to carry out this project effectively.

III. Analysis

A. Selection of Predictors

In selecting the predictors to forecast cloud amount, the individual components that influence the formation of clouds have been taken into account. The movement of moisture from one level of the atmosphere to another often causes H_2O in the atmosphere to change phase, which can result in cloud formation or dissipation. Therefore, factors related to the movement of moisture in the atmosphere have been chosen as predictors. These predictors include the U and V wind components, vertical velocity, and lifted index. Vertical velocity is a measure of the movement of air masses in the atmosphere in the vertical direction. The lifted index is a measure of the static stability of the air masses. Before it rains, clouds have to form; therefore precipitation has also been chosen as a predictor. The last three predictors are the relative humidity in the low, middle, and highest levels in the Eta Model. The amount of moisture in the atmosphere is very much related to cloud amount, because clouds form from condensation of water vapor in the atmosphere. All together, there were eight predictors.

B. Regression

The Data Analysis Tool in Microsoft Excel 5.0 uses the LINEST function to carry out the regression task. The function uses the "least squares" method to calculate a straight line that best fits the given data and returns an array that describes the line in the form:

$$Y = m_1X_1 + m_2X_2 + m_3X_3 + m_4X_4 + m_5X_5 + m_6X_6 + m_7X_7 + m_8X_8 + b$$

In the equation, Y is the predictand, m_n are the regression coefficients, X_n are the eight predictors, and b is the regression constant.

There are many statistical output factors that must be analyzed in order to determine the validity of the regression equation. (Refer to Table 2.) ANOVA (which means Analysis of Variance) partitions the total variance into an explained component (the regression) and the error component (the residual). Table 2 displays the degrees of freedom (df), sum of squares (SS), and the mean of squares of the regression and residual (MS), along with the necessary information to perform a significance test (F-test).

Table 2. Sample ANOVA Chart

ANOVA	BOS 00Z	12HR. FCST			
	df	*SS*	*MS*	*F*	*Significance F*
Regression	8	81.97084218	10.24635527	2.471078438	0.0556649
Residual	17	70.49069628	4.146511546		
Total	25	152.4615385			

The R^2 value, called the coefficient of determination, is the ratio of the explained variance (regression sum of squares) to the total variance (total sum of squares) {12}. Ranging from zero to one, there is a perfect correlation in the sample (meaning there is no difference between the predicted and the actual Y-value), if the R^2 value equals one. If the R^2 value is zero, then the regression equation is irrelevant in predicting the Y-value.

Excel 5.0 also calculates the standard error for each variable and for the equation in general. The standard error measures the scatter of the data. A small standard error indicates that there is less scatter in the sample. In a similar way the P-value also indicates the validity of the forecast. The P-value is the probability that the observed relationships between predictor and predictand occur just by chance. A small P-value indicates that the relationship between the variables and the forecast has some skill, and a large P-value indicates that any relationship between the variables and the forecast is probably the result of chance. If the correlation is high, but the P-value is large, chances are the good result is a product of luck.

In order to differentiate the skill the regression has from the probability that the results occur by chance, two types of tests can easily be done to prove that the regression equation is valid for the model forecast. The F-test and the t-test can determine the level of confidence in the regression. Both the F-observed value and the F-critical are given by Excel's ANOVA table (see Table 2) with Alpha equal to 0.05. F-critical values can also be found in a statistics textbook. There is a valid correlation among the variables in forecasting cloud amount if the F-observed value is greater than the F-critical value. By passing the F-test, assumptions can be made that the results from the regression equation did not occur purely by chance.

The second test that must be done, the t-test, determines whether each regression coefficient is useful in forecasting cloud amount. Once again there is an observed and a critical value. T-observed of a predictor is equal to its regression coefficient divided by the standard error. The t-critical value is obtained from a statistics textbook. The variable is a good predictor if the absolute value of its t-observed value is greater than the t-critical value. Essentially, both the F- and the t-test determine whether the relationships between the predictors and the

predictand calculated by the regression occurred by chance or not, in order to determine the credibility of the regression.

IV. Regression Results

The results from the project varied from good to not so good (that was a litotes). The R^2 values were generally satisfactory for 0000 UTC twelve, twenty-four, thirty-six hour forecasts and 1200 UTC twelve and twenty-four hour forecasts. The accuracy of the cloud cover forecasts seemed to diminish with forecast time. Forty-eight hour forecasts at 0000 UTC and 1200 UTC had low R^2 values. Therefore the combination of the predictors that produced good results for the twelve hour forecasts were less successful in forecasting cloud cover forty-eight hours later. The most likely contributor to this problem is the inadequate representation of moist physical processes in the Eta model, resulting in decrease in forecast skill with forecast time.

In addition to the temporal variation of results was the spatial variation. Out of the four cities chosen, Burlington, VT (BTV) had the highest R^2 value for the twelve hour forecasts at 1200 UTC. In general, Concord, NH (CON) had the best results (relative to the other cities). Boston, MA (BOS) was worse, but the R^2 values for Caribou, ME (CAR) were even lower (see Table 3).

Table 3. Coefficient of Determination (R^2 value)

	0000 UTC				1200 UTC			
City	12 hr.	24 hr.	36 hr.	48 hr.	12 hr.	24 hr.	36 hr.	48 hr.
BOS	0.537649	0.533173	0.548732	0.26701	0.613375	0.484547	0.251371	0.44985
BTV	0.449821	0.378396	0.614011	0.04999	0.660204	0.589041	0.442342	0.289631
CAR	0.458793	0.549707	0.275937	0.352317	0.528374	0.339593	0.372158	0.22112
CON	0.609876	0.568127	0.610141	0.202804	0.435776	0.606637	0.268435	0.277188

Analysis of the standard error (SE) and the P-value of the eight variables revealed a different aspect of the results. Despite the fluctuating results of the R^2 value, the SE values were more consistent. The variables with the least SE were the three levels of relative humidity. The data for three levels of relative humidity had the least scatter relative to the other variables used. Hence the relative humidity variables were more consistent in forecasting cloud amount than the other variables.

To validate the SE values, the P-value of each variable was compared. All variables with a P-value of less than 0.1 also passed the t-test. In comparing the SE values with the P-values, predictors number six and eight still had acceptable P-values, whereas predictor seven did not. The results implied that the low SE of the middle level of relative humidity (predictor #7) most likely occurred by chance. On the other hand, the P-values of predictors six and eight confirmed that the surface level (#6) and the upper level of relative humidity (#8) were important in the model forecast, but more analysis must be done in order to conclude confidently that #8 and #6 were the best predictors out of the eight predictors chosen.

In performing the F-test, only three regressions failed the test, all being forty-eight hour forecasts. The twenty-nine other regressions passed, verifying that the predictors did correlate with the predictand. Even though most of the stations had passed the F-test, the test casts some doubt because some regressions with low R^2 values also passed the F-test. Remember that the F-test only determined whether the results occurred by chance, therefore implying whether there was a valid correlation between the predictors and the predictand; but the confidence in the correlation was not determined.

Table 4. Variables Passing t-test

	0000 UTC				1200 UTC			
City	12 hr.	24 hr.	36 hr.	48 hr.	12 hr.	24 hr.	36 hr.	48 hr.
BOS	1,4,8	8	1,2,6,7	X	8	X	8	3
BTV	8	X	2,6	X	4,6,8	2	X	8
CAR	8	7	X	X	1	X	X	X
CON	8	X	8	X	X	1,2	8	X

(1= U wind component, 2= V wind component, 3= vertical velocity, 4= lifted index, 5= precipitation, 6= surface level relative humidity, 7= second level relative humidity, 8= highest level relative humidity, X=no variables passed t-test)

Unlike the F-test, the results of the t-test were less optimistic. Despite the fact that both the t-test and the F-test determined whether the results were dependable or not, the t-test was more specific. The F-test applied to the whole regression equation in general, whereas the t-test applied to each individual variable. In testing the variables, most passed the t-test one time or another except for six-hour precipitation amount (see Table 4). Therefore, we concluded that precipitation is not an appropriate predictor for cloud amount. The best correlated predictor was the highest level of relative humidity (#8). This predictor passed the t-test eleven out of thirty-two times, and it consistently passed the t-test for all four cities for twelve hour forecasts at 0000 UTC. Other good predictors included the U and V wind components, lifted index, and the surface level relative humidity. In the regression equations with a R^2 value greater than 0.6, the variables that passed the t-test were vertical wind component, lifted index, and surface level relative humidity, and the highest level relative humidity (See Table 4) . Overall, because most of the regression results passed the F-test there was a relationship between the predictors and the predictand, but the poor results in the t-test showed that confidence in the correlation between the chosen predictors and the model forecast of cloud amount were not enough to validate the generated MOS equations .

V. CONCLUSION

A. Verification

To verify regression results, we used the Excel 5.0 TREND function. TREND used the LINEST functions to extract the regression equation. Then new values for the predictors were incorporated into the regression equation, and a predicted Y-value (forecast cloud amount) was acquired after solving the regression equation. Plots of the forecast cloud amount obtained from the TREND function verses the actual observed cloud amount for

Boston are illustrated in Figure 1. The graphs showed how the actual cloud amount converged and diverged with the predicted cloud amount obtained from the linear regression.

B. Source of Error

Clearly there are many factors that could have contributed to the incoherence of the regression output. Foremost, the basis for a reliable MOS equation is an adequate statistical sample of forecast data and observations. A good MOS equation is generated using a minimum of two or more years of data. In this project, data was collected over a six week period. There is no need to hire a mathematician to figure out that there is a big difference between six weeks of data and two or more years of data. Without data over a long period of time, the sample is not an accurate representation of the population as a whole.

For example, this summer Boston and New England in general have experienced an unusually dry summer. Hence, the model is predisposed to forecasting cloud amount for dry weather conditions, and not for "normal" weather conditions. The model is vulnerable to certain changes and fluctuation in the weather because the sample is limited. Samples taken over a long period of time can allow the model to incorporate the differences and variation in the weather. In other words, a large sample is also a more accurate representation of the population, thus the model can then make more accurate forecasts.

Without more time and a bigger sample, it is difficult to say what other factors have contributed to the disparate results. As mentioned earlier, limitations of the Eta model's representation of moist physical processes is another factor that surely stood in the way of better results. No coherent inference should be made from the results of this project, unless the sources of error can be eliminated to produce reliable results. Any analyses or inferences made are only as good as the regression results. An analogy can be made to baking a cake: If there is not enough sugar and eggs, then the cake will not be very tasty. Hence, without more complete data samples, the results and analysis of the project is limited. One important point the results of the project do confirm is that a very large sample is indispensable in generating a suitable MOS equation to forecast cloud amount.

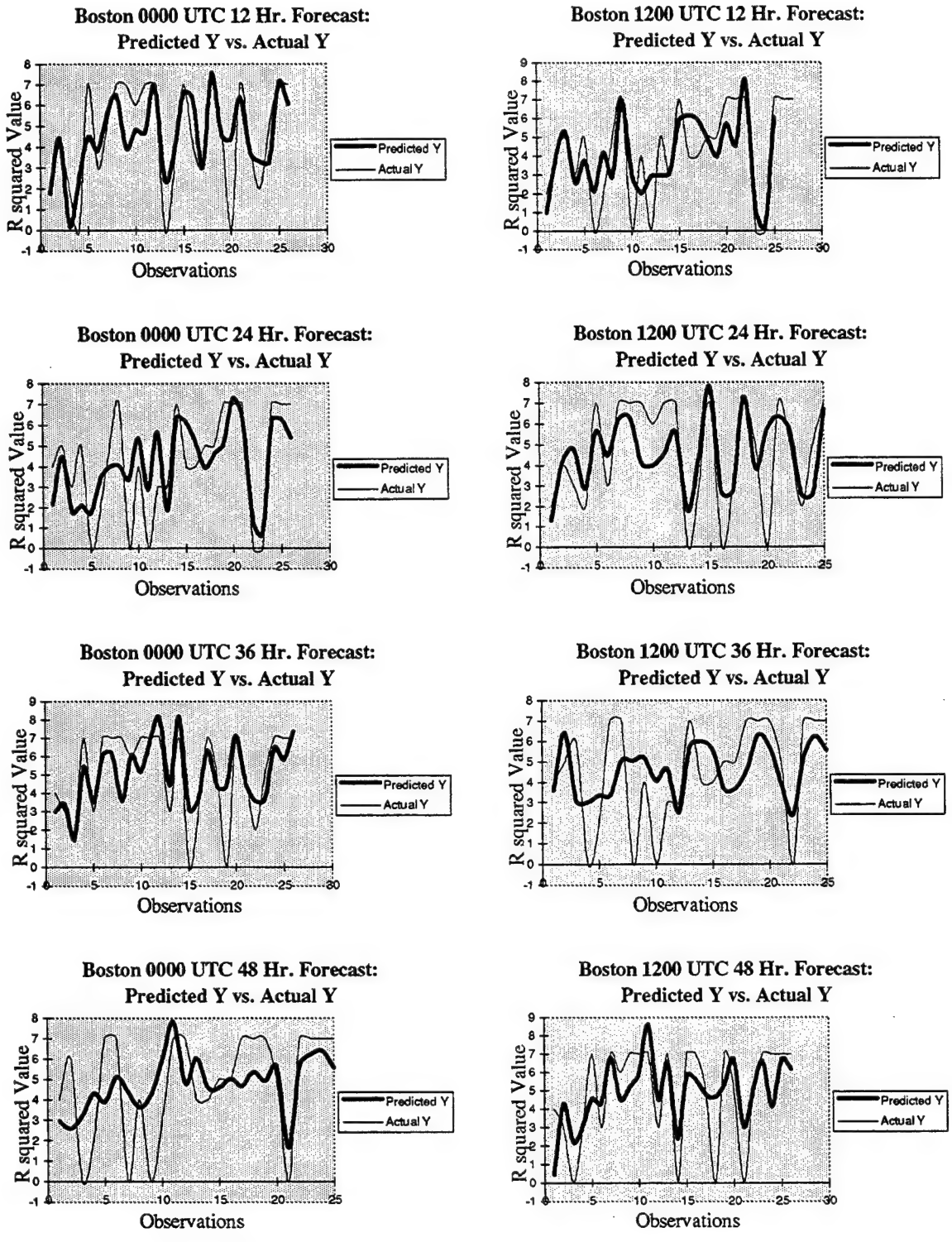

Figure 1. Predicted vs. Actual Cloud Amount

VI. REFERENCES

1. Aakjaer, P., T. S. Pedersen, and C. Simonsen. 1984: *Statistical Interpretation of the ECMWF Model Using MOS to Predict Surface Wind and Temperature*. Weather Service Report No. 2., Danish Meteorological Institute, pp. 1-15.

2. Baldwin, M., T, Black, D, Deaven, G. DiMego, Y. Lin, N. W. Junker, E. Rogers, and Q. Zhao. 1985: *Changes to the Operational Eta Model Analysis/Forecast System.* Technical Procedures Bulletin.

3. Caplan, P. M., and G. H. White. 1989: *Performance of the National Meteorological Center's Medium-Range Model.* J. Weather and Forecasting.

4. Carter, G. M., J. P. Dallavalle, and H. R. Glahn. 1989: *Statistical Forecasts Based on National Meteorological Center's Numerical Weather Prediction Systems.* J. Weather and Forecasting. p. 401.

5. Colucci, S. J., A. J. Cristaldi III. and D. S. Wilks. 1994: *An Analysis of the Accuracy of 120-h Predictions by the National Meteorological Center's Medium Range Forecast Model.* J. Weather and Forecasting.

6. Glahn, H. R. and D. A. Lowry. 1972: *Use of Model Output Statistics (MOS) in Objective Weather Forecasting*. Journal of Applied Meteorology. pp. 1203-1208.

7. Grumm, R. H., J. E. Hoke, and N. W. Junker. 1989: *Performance of NMC's Regional* Models. J. Weather and Forecasting.

8. Hoke, J. E., N. A. Phillips, G. J. Dimego, J. J. Tuccillo, J. G. Sela. 1989: *The Regional Analysis and Forecast System of the National Meteorological Center*. J. Weather and Forecasting.

9. Kanamitsu, M . 1989: *Description of the NMC Global Data Assimilation and Forecasting System.* J. Weather and Forecasting.

10. Livingston, R. L. and J. T. Schaefer. 1990: *On Medium-Range Model Guidance and the 3-5 Day Extended Forecast.* J. Weather and Forecasting. p. 362.

11. Modica, G. D. 1989: *Mesoscale Modeling Studies at the Air Force Geophysics Laboratory.* Proceedings of the DOD Environmental Technical Exchange Conference on Mesoscale Phenomena.

12. Panofsky, H. A. and G. W. Brier. Some Applications of Statistics to Meteorology. College of Earth and Mineral Sciences The Pennsylvania State University: Pennsylvania 1968.

13. Weather of US Cities. 1992: Gale Research Inc., Detroit.

VI. APPENDIX

BOSTON, MA REGRESSION COEFFICIENT

	0000 UTC				1200 UTC			
	12 hr. fcst	24 hr. fcst	36 hr. fcst	48 hr. fcst	12 hr. fcst	24 hr. fcst	36 hr. fcst	48 hr. fcst
Intercept	6.483056	-2.45195	-1.91712	-1.78645	-1.27839	-0.25882	0.556029	4.460831
X Variable 1	-0.15243	-0.01567	0.111236	0.021674	-0.05161	0.007555	-0.03342	-0.07707
X Variable 2	0.115479	0.015708	-0.08746	-0.0837	-0.02895	-0.05681	-0.03489	0.023295
X Variable 3	-1.02593	-0.39752	0.103711	0.058541	-0.58684	0.228345	-0.37604	-1.52095
X Variable 4	-0.36724	-0.08379	0.253684	0.03913	-0.12906	0.086425	-0.08462	-0.3698
X Variable 5	-27.2385	-12.0461	-29.7151	-12.4444	8.430245	-2.47216	0.90555	-11.0599
X Variable 6	-0.04858	-0.00013	-0.089	-0.00269	0.02797	-0.02577	0.029522	-0.0173
X Variable 7	0.027098	0.054218	0.188747	0.087037	0.004006	0.100539	-0.01207	0.018482
X Variable 8	0.049	0.085761	0.033243	0.047393	0.096406	0.033395	0.061949	0.032781

BURLINGTON, VT REGRESSION COEFFICIENTS

	0000 UTC				1200 UTC			
	12 hr. fcst	24 hr. fcst	36 hr. fcst	48 hr. fcst	12 hr. fcst	24 hr. fcst	36 hr. fcst	48 hr. fcst
Intercept	-0.02968	0.511851	-2.80218	3.245453	-2.44805	-2.44805	-1.17203	6.198485
X Variable 1	-0.02386	0.056356	-0.04513	-0.03483	0.005358	0.005358	0.028337	-0.01044
X Variable 2	-0.0052	0.05415	-0.10223	-0.01589	0.047416	0.047416	-0.02063	0.003053
X Variable 3	0.119885	0.062759	-0.10693	-0.01087	0.305975	0.305975	0.565688	-0.81075
X Variable 4	-0.03458	0.18574	0.173435	-0.00819	0.245047	0.245047	-0.19168	-0.15923
X Variable 5	-0.73153	-1.54612	0.728122	1.067289	-2.11523	-2.11523	-9.53148	2.707217
X Variable 6	0.042196	0.013989	0.060261	0.020805	0.095791	0.095791	0.021574	-0.04242
X Variable 7	-0.00067	0.015123	0.052023	-0.00314	-0.02497	-0.02497	0.047447	-0.01031
X Variable 8	0.047182	0.042269	0.018714	0.011661	0.054836	0.054836	0.032241	0.049413

CARIBOU, ME REGRESSION COEFFICIENT

	0000 UTC				1200 UTC			
	12 hr. fcst	24 hr. fcst	36 hr. fcst	48 hr. fcst	12 hr. fcst	24 hr. fcst	36 hr. fcst	48 hr. fcst
Intercept	-1.59895	-4.75905	-6.12266	3.323393	0.010681	-5.43853	4.597119	-1.26606
X Variable 1	-0.04255	-0.00496	0.054317	-0.00527	-0.06272	0.012978	-0.01177	0.081525
X Variable 2	-0.05447	-0.05973	-0.07408	-0.02402	-0.09387	-0.03448	0.013028	-0.01049
X Variable 3	0.392407	0.400014	0.729991	0.200281	0.12815	-0.36612	0.214738	0.756597
X Variable 4	0.023775	0.114615	0.514175	-0.23138	-0.14062	0.32729	-0.19909	0.419942
X Variable 5	-8.69365	-2.25869	-8.22942	-2.33486	-1.34811	-2.23891	4.039384	5.389145
X Variable 6	0.063501	0.060665	0.079662	0.0188	0.042322	0.069062	-0.01547	0.057216
X Variable 7	-0.01162	0.098838	0.064903	0.004333	0.034762	0.044128	0.018967	0.01085
X Variable 8	0.056801	0.010103	0.015509	0.004474	0.01889	0.03943	-0.00325	0.009983

CONCORD, NH REGRESSION COEFFICIENTS

	0000 UTC				1200 UTC			
	12 hr. fcst	24 hr. fcst	36 hr. fcst	48 hr. fcst	12 hr. fcst	24 hr. fcst	36 hr. fcst	48 hr. fcst
Intercept	5.495102	5.257374	0.105608	2.517211	6.327916	0.240183	2.681815	4.831302
X Variable 1	-0.22407	-0.08881	-0.07071	-0.04061	-0.14523	-0.16163	-0.00068	-0.04643
X Variable 2	0.067661	0.030455	-0.17056	0.00389	0.057442	-0.13964	-0.05303	-0.0184
X Variable 3	-0.55312	0.636507	0.769437	-0.18176	0.111759	0.271263	0.917877	-0.26499
X Variable 4	-0.34116	-0.38949	0.110243	-0.24523	-0.24504	0.174028	-0.25725	-0.11361
X Variable 5	-2.00597	0.97941	2.866728	5.682154	4.745279	4.522552	-4.70242	1.873548
X Variable 6	0.008701	-0.00364	0.018916	0.008441	-0.03833	0.003765	0.030409	-0.05413
X Variable 7	-0.04114	-0.05942	0.041519	-0.00625	-0.01082	0.083492	-0.05331	0.032183
X Variable 8	0.067276	0.063207	0.044483	0.031955	0.032704	0.019448	0.066654	0.048623

BOS 00Z 12 HR FCST

ANOVA TABLE

	Coefficients	*Standard Error*	*t Stat*	*P-value*
Intercept	6.483056248	3.7169263	1.744198223	0.09917662
X Variable 1	-0.152430634	0.061147929	-2.492817608	0.023287495
X Variable 2	0.115478856	0.075964484	1.52016903	0.146848983
X Variable 3	-1.02593497	0.597499615	-1.717047082	0.10413233
X Variable 4	-0.367236619	0.188519294	-1.948005492	0.068120842
X Variable 5	-27.23850959	34.3839237	-0.792187356	0.439166794
X Variable 6	-0.048583534	0.043714459	-1.11138363	0.281874821
X Variable 7	0.027098337	0.053173197	0.509623983	0.616866797
X Variable 8	0.049000316	0.025358382	1.932312393	0.070160119

ANOVA 12Z 24 hr. fcst BOS

	df	*SS*	*MS*	*F*	*Significance F*
Regression	8	87.112253	10.889032	2.4270067	0.05922047
Residual	17	76.272363	4.4866096		
Total	25	163.38462			

ANOVA 00z 36 hr. fcst BOS

	df	*SS*	*MS*	*F*	*Significance F*
Regression	8	75.640662	9.4550827	2.5839584	0.047563289
Residual	17	62.205492	3.6591466		
Total	25	137.84615			

ANOVA 00z 48 hr. fcst. BOS

	df	*SS*	*MS*	*F*	*Significance F*
Regression	8	42.871122	5.3588902	0.7285501	0.665533456
Residual	16	117.68888	7.3555549		
Total	24	160.56			

ANOVA 12z 12 hr. fcst BOS

	df	*SS*	*MS*	*F*	*Significance F*
Regression	8	102.68358	12.835448	3.5695986	0.011876166
Residual	18	64.723823	3.5957679		
Total	26	167.40741			

ANOVA 12z 24 hr. fcst BOS

	df	*SS*	*MS*	*F*	*Significance F*
Regression	8	80.255405	10.031926	2.1150958	0.089124538
Residual	18	85.374225	4.7430125		
Total	26	165.62963			

ANOVA 12z 36 hr. fcst BOS

	df	*SS*	*MS*	*F*	*Significance F*
Regression	8	39.75535	4.9694188	0.7135236	0.677125479
Residual	17	118.3985	6.9646174		
Total	25	158.15385			

ANOVA	12z	48 hr. fcst		BOS
	df	*SS*	*MS*	*F*	*Significance F*
Regression	8	76.405356	9.5506695	1.7375856	0.160949692
Residual	17	93.440798	5.4965175		
Total	25	169.84615			

ANOVA	00z	12hr. fcst.		BTV
	df	*SS*	*MS*	*F*	*Significance F*
Regression	8	45.817465	5.7271831	1.9417756	0.112257184
Residual	19	56.039678	2.9494567		
Total	27	101.85714			

ANOVA	00Z	36HR. FCST		BTV
	df	*SS*	*MS*	*F*	*Significance F*
Regression	8	65.852733	8.2315916	3.778033	0.008258433
Residual	19	41.397267	2.1788035		
Total	27	107.25			

ANOVA	12Z	12 HR. FCST		BTV
	df	*SS*	*MS*	*F*	*Significance F*
Regression	8	44.893896	5.611737	4.1287588	0.006720869
Residual	17	23.106104	1.3591826		
Total	25	68			

ANOVA	12Z	36 HR. FCST		BTV
	df	*SS*	*MS*	*F*	*Significance F*
Regression	8	31.070107	3.8837634	1.586428	0.205471529
Residual	16	39.169893	2.4481183		
Total	24	70.24			

ANOVA	00Z	12 HR. FCST		CAR
	df	*SS*	*MS*	*F*	*Significance F*
Regression	8	54.273561	6.7841951	1.9073773	0.121639544
Residual	18	64.022736	3.5568186		
Total	26	118.2963			

ANOVA	00Z	36 HR. FCST		CAR
	df	*SS*	*MS*	*F*	*Significance F*
Regression	8	35.830986	4.4788733	0.8574663	0.567591298
Residual	18	94.020866	5.2233814		
Total	26	129.85185			

ANOVA	00z	24hr. fcst		BTV
	df	*SS*	*MS*	*F*	*Significance F*
Regression	8	26.095337	3.2619171	1.3696702	0.274180359
Residual	18	42.867626	2.3815348		
Total	26	68.962963			

ANOVA	00Z	48 HR. FCST		BTV
	df	*SS*	*MS*	*F*	*Significance F*
Regression	8	3.8140374	0.4767547	0.1183957	0.997765269
Residual	18	72.482259	4.0267922		
Total	26	76.296296			

ANOVA	12Z	24 HR. FCST		BTV
	df	*SS*	*MS*	*F*	*Significance F*
Regression	8	55.097974	6.8872468	3.0458301	0.025501817
Residual	17	38.440488	2.2612051		
Total	25	93.538462			

ANOVA	12Z	48 HR. FCST		BTV
	df	*SS*	*MS*	*F*	*Significance F*
Regression	8	25.621174	3.2026467	0.8664016	0.561948468
Residual	17	62.840365	3.696492		
Total	25	88.461538			

ANOVA	00Z	24 HR. FCST		CAR
	df	*SS*	*MS*	*F*	*Significance F*
Regression	8	54.767152	6.845894	2.7467518	0.0357372
Residual	18	44.862478	2.4923599		
Total	26	99.62963			

ANOVA	00Z	48 HR. FCST		CAR
	df	*SS*	*MS*	*F*	*Significance F*
Regression	8	14.919249	1.8649061	1.1559235	0.378471167
Residual	17	27.426905	1.6133473		
Total	25	42.346154			

ANOVA 12Z 12 HR. FCST CAR

	df	SS	MS	F	Significance F
Regression	8	52.139177	6.5173971	2.6607682	0.038171438
Residual	19	46.539395	2.4494418		
Total	27	98.678571			

ANOVA 12Z 24 HR. FCST CAR

	df	SS	MS	F	Significance F
Regression	8	44.3775	5.5471875	1.221266	0.339148073
Residual	19	86.301071	4.5421616		
Total	27	130.67857			

ANOVA 12Z 36 HR. FCST CAR

	df	SS	MS	F	Significance F
Regression	8	22.439764	2.8049705	1.3337056	0.289325132
Residual	18	37.856532	2.1031407		
Total	26	60.296296			

ANOVA 12Z 48 HR. FCST CAR

	df	SS	MS	F	Significance F
Regression	8	26.471166	3.3088958	0.6742484	0.708176466
Residual	19	93.243119	4.9075326		
Total	27	119.71429			

ANOVA 00Z 12 HR. FCST CON

	df	SS	MS	F	Significance F
Regression	8	108.73857	13.592321	3.517392	0.012696902
Residual	18	69.557725	3.8643181		
Total	26	178.2963			

ANOVA 00Z 24 HR. FCST CON

	df	SS	MS	F	Significance F
Regression	8	87.659917	10.95749	2.9598669	0.026599452
Residual	18	66.63638	3.7020211		
Total	26	154.2963			

ANOVA 00Z 36 HR. FCST CON

	df	SS	MS	F	Significance F
Regression	8	98.210064	12.276258	3.5213137	0.012633146
Residual	18	62.752899	3.4862722		
Total	26	160.96296			

ANOVA 00Z 48 HR. FCST CON

	df	SS	MS	F	Significance F
Regression	8	30.451738	3.8064673	0.5405915	0.810261357
Residual	17	119.70211	7.0413005		
Total	25	150.15385			

ANOVA 12Z 12 HR. FCST CON

	df	SS	MS	F	Significance F
Regression	8	69.288409	8.6610511	1.8343223	0.132473795
Residual	19	89.711591	4.7216627		
Total	27	159			

ANOVA 12Z 24 HR. FCST CON

	df	SS	MS	F	Significance F
Regression	8	96.433631	12.054204	3.6626816	0.009588811
Residual	19	62.530654	3.2910871		
Total	27	158.96429			

ANOVA 12Z 36 HR. FCST CON

	df	SS	MS	F	Significance F
Regression	8	40.344858	5.0431072	0.8256002	0.591171282
Residual	18	109.95144	6.1084132		
Total	26	150.2963			

ANOVA 12 Z 48 HR. FCST CON

	df	SS	MS	F	Significance F
Regression	8	45.647001	5.7058751	0.9107804	0.528246391
Residual	19	119.03157	6.2648195		
Total	27	164.67857			

COMPUTER-ASSISTED LASER POWER MEASUREMENT

Eric McEuen

(recent graduate of:)
Albuquerque High School
800 Odelia Rd. NE
Albuquerque, NM 87102

Final Report for:
High School Apprentice Program
Phillips Laboratory

Sponsored by:
Air Force Office of Scientific Research
Bolling Air Force Base, DC

and

Phillips Laboratory

August 1995

COMPUTER-ASSISTED LASER POWER MEASUREMENT

Eric McEuen
Institutionless

Abstract

Work was done on a computer program designed to provide power vs. current (LI) curves for semiconductor lasers. At the beginning of the summer tour, existing LI programs at PL/LIDA assumed a "magic ratio" relationship between voltage sent to the circuit and resulting current flow. Work was underway, separately, on an algorithm to measure current flow from an oscilloscope reading. Both programs were organized in a way that made them difficult to use, and their output was limited to raw numbers. At the time of this writing (3 Aug), the current algorithms have been finished and incorporated with the LI software, with menus and graphs making the program more friendly.

COMPUTER-ASSISTED LASER POWER MEASUREMENT

Eric McEuen

Introduction

One important reference for a scientist in laser research is the power-versus-current (LI) curve, which gives basic information about the performance of any individual laser. These can be slow and tedious to calculate by hand. Automated LI facilities are not uncommon, but until this summer, researchers in the Semicontuctor Laser branch of Phillips Laboratory (PL/LIDA) have not had this capability. In late 1994, an 80286 computer and several instruments, including power supplies and various detectors, were set aside with the goal of producing this function. Since early 1995, work has been underway on various aspects of the interfacing and programming tasks. The apprentice began work in middle June, when rudimentary algorithms had been established, and contributed mostly to the program's user interface, but this paper will describe the work as a whole.

Methodology

After some preliminary attempts at learning to communicate with the equipment on hand (an important part of the task, but not significant from a research standpoint), simple LI programs were constructed, repeatedly incrementing voltage and measuring power, which worked for the first lasers tested. However, these programs computed current as a fixed ratio of the voltage input (in pulsed fashion) to the circuit, which was not always accurate, depending on the laser tested. Therefore, much time has been spent on an algorithm to read current vs. time information from an oscilloscope, search through these data for the actual current pulse, and average several of these data points to obtain the current pulse amplitude. Several test programs were developed until this algorithm was in a useful form, and it was then combined with the previous LI software; eventually both parts of the program even worked together.

Another major drawback of the initial LI programs was the user interface. These early programs simply prompted the user for various numeric values employed in the computation of the LI curve, and output only raw numbers. Improving the interface has been the major task for this summer apprentice,

who is much better versed in programming than in laser optics. The program is now largely menu-driven; some menus include options that display numbers for acceptance or modification, replacing the tedious, occasionally cryptic prompts. As each LI curve is computed, the program's progress is displayed on a graph screen, allowing users to stop the program prematurely if something does not seem right.

The third major task related to this program has been debugging. Aside from countless small problems that have been relatively easy to fix, the program has often been plagued by symptoms arising from the method of its construction, with separate pieces of code sometimes simply combined and then tested. The most insidious of these have related to the fact that the program was originally designed to provide only one curve; the user was required to start over in order to do another test. The menu structure, however, has made it possible for users to compute several LI curves without completely restarting the program. Therefore, bugs have arisen from variables not being reset to their initial values, from disabling instruments before the user is really finished, and from the complicated setup routines that have greatly enhanced the program's speed, just to name a few. The program seems to work entirely correctly at the moment, but as with any computer program, an attempt at something slightly outside of normal operating parameters could still cause problems. Therefore, as with any program, the debugging might go on and on.

Results/Conclusion

At the moment, the computer program in question, as completed so far, seems to work as intended. It is still very much a work in progress (hence the continual use of qualifiers such as "at the moment" in this report), but it is now complete enough to be a usable tool. Though the author (the high-school apprentice) is not well versed in laser optics, he has been able to learn many of the basic aspects that the program deals with, and his programming experience proved extremely valuable in his attempts to make the program more "user-friendly."

APPENDICES

Contents

(Sample graph of program output)
1 August
Using Oscgood.bas

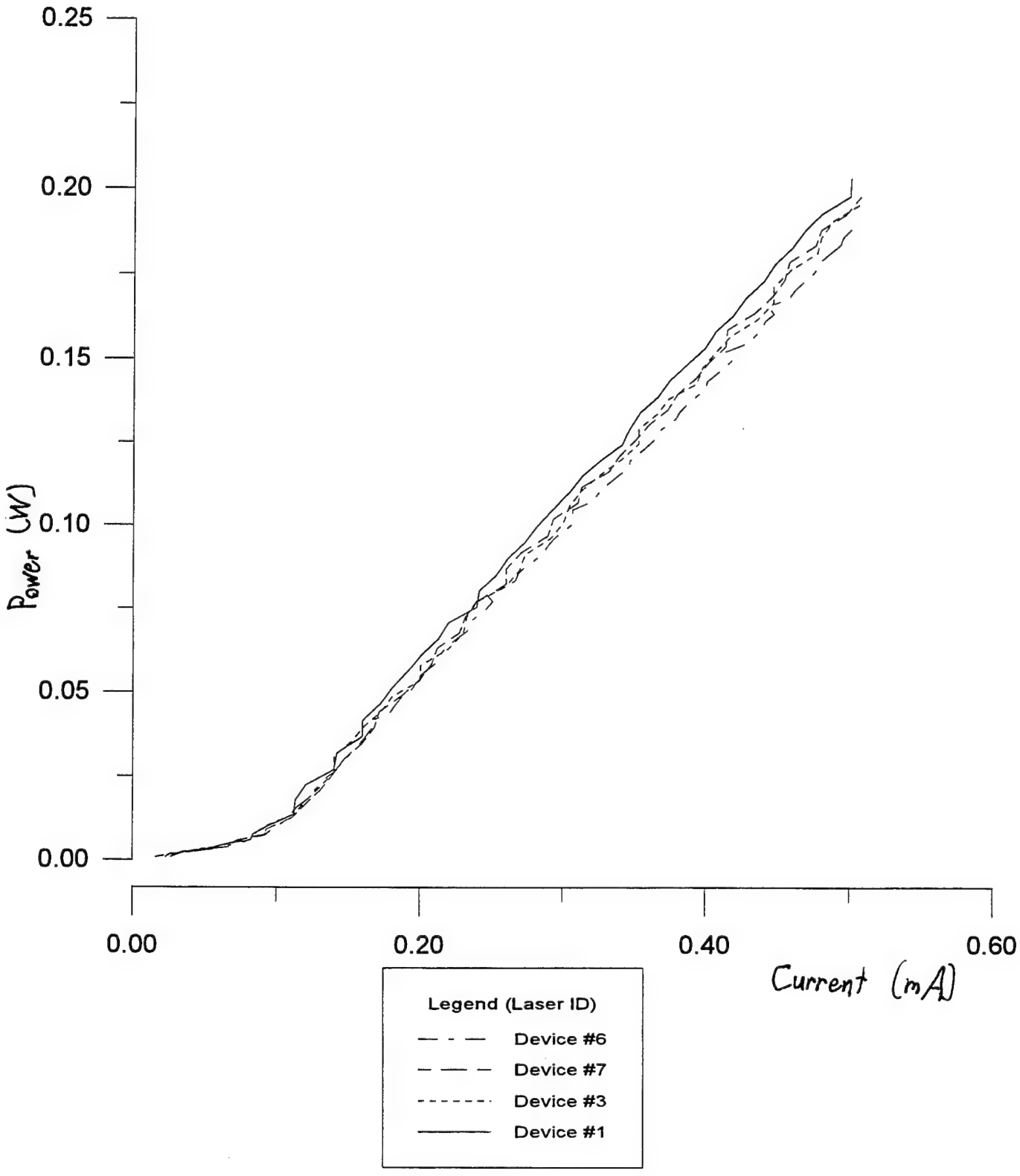

Appendix B
Diagram of Equipment and Connections

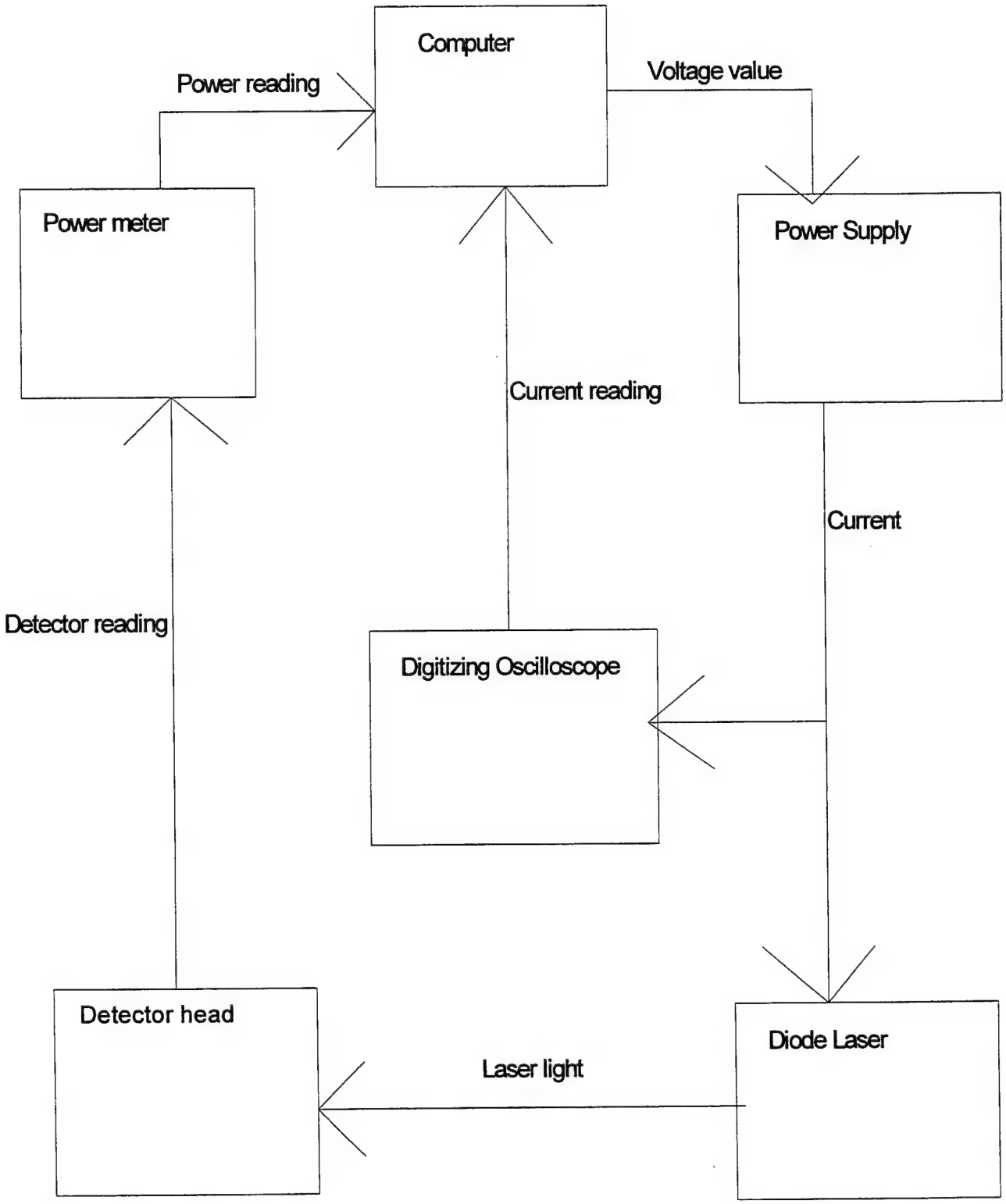

A DATABASE FOR RADIATION INTERACTION MODELING

Jerome C. Michelback

Highland High School
4700 Coal Avenue
Albuquerque, NM 87108

Final Report for:
High School Apprentice Program
Phillips Laboratory

Sponsored by:
Air Force Office of Scientific Research
Bolling Air Force Base, DC

and

Phillips Laboratory

August 1995

A DATABASE FOR RADIATION INTERACTION MODELING

Jerome C. Michelback
Highland High School

Abstract

The Phillips Lab Satellite Assessment Center performs satellite survivability/vulnerability analyses on radiation interactions with spacecraft. Their analyses include the effects of nuclear weapon produced radiation, primarily high energy electrons, the effects of high energy lasers, and radio frequency effects. They base these analyses on high fidelity models of spacecraft. Essential to their analyses is a well documented and flexible database of material properties. The formats for this database were developed and population of the database was started.

A DATABASE FOR RADIATION INTERACTION MODELING

Highland High School

Introduction

The Phillips Lab Satellite Assessment Center performs satellite survivability/vulnerability analyses on radiation interactions with spacecraft. Their analyses include the effects of nuclear weapon produced radiation, primarily high energy electrons, the effects of high energy lasers, and radio frequency effects. They base these analyses on high fidelity models of spacecraft. These models include many different types of materials. Properties of a specific material that are of importance vary with the application. Bulk properties are important for shielding high energy electrons, surface properties are important for the coupling of laser energy into materials, and electrical properties are important for RF analyses. This effort was to convert a linear "flat-file" into a true database that would allow many different access methods.

Methodology

The goal of this effort was to convert the currently available "flat-file" of material properties into a database for multiple routes of access. This database could then produce any number of "flat-files" to be used by the complete variety of codes available at the Satellite Assessment Center. Since IBM PC's are inexpensive and widely available, the ACCESS program from Microsoft Office was chosen as the software most suitable for implementation of this effort. Data input forms were identified. The format of the current "flat-file" was defined as one of the outputs. A dump of all of the property and identifier fields for a particular material was defined as another output. Additional output forms can be added easily and almost at will. Some sample material output data is attached.

A modest amount of data entry was accomplished to demonstrate the system worked. Additional information fields can be added very easily including material on property measurement uncertainties and references to the experimental efforts that determined the properties used in the database.

Sample Work

This is some of the work that I have acomplished during the eight week research program.

Surface Material Properties

Material- Aluminum Alloy
Surf. Mat. Code- 1
Type- 2024-T3 (Polished)
Lot #- 184261
Ingot #- ****
Solar Absorptance- ****
Thermal Emissivity @ 300K- ****

Wavelengths-	**10.6**	**5.0**	**3.8**	**2.7**	**1.3**	**1.06**	**.411**	**.34**	**.25**
Matter.Dat-	0.03	0.04	0.05	0.06	0.09	0.14	0.235	0.306	0.461
Tracor Gie.-	****	****	****	****	****	****	0.235	0.306	0.461
Matter Dat. Abs. Coeff. cm-1-	-1	-1	-1	-1	-1	-1	-1	-1	-1

Material- Aluminum Alloy
Surf. Mat Code- 2
Type- 2024-T3 (Mill Finish)
Lot #- 184261
Ingot #- ****
Solar Absorptance- 0.264
Thermal Emissivity @ 300K- 0.097

Wavelengths-	**10.6**	**5.0**	**3.8**	**2.7**	**1.3**	**1.06**	**.411**	**.34**	**.25**
Matter.Dat-	0.107	0.122	0.115	0.139	0.09	0.14	0.235	0.306	0.461
Tracor Gie-	****	****	****	****	****	****	****	****	****
Matter Dat. Abs. Coeff. cm-1-	-1	-1	-1	-1	-1	-1	-1	-1	-1

Material- Aluminum Alloy
Surf. Mat Code- 3
Type- 360 (Cast)
Lot #- ****
Ingot #- ****
Solar Absorptance- ****
Thermal Emissivity @ 300K- ****

Wavelengths-	**10.6**	**5.0**	**3.8**	**2.7**	**1.3**	**1.06**	**.411**	**.34**	**.25**
Matter.Dat-	0.19	0.22	0.25	0.27	0.32	0.343	0.379	0.378	0.433
Tracor Gie-	****	****	****	****	****	****	****	****	****
Matter Dat. Abs. Coeff. cm-1-	-1	-1	-1	-1	-1	-1	-1	-1	-1

Material- Aluminum Alloy
Surf. Mat Code- 4
Type- 2024-T3 (Black Anodized)
Lot #- 184261
Ingot #- ****
Solar Absorptance- 0.646
Thermal Emissivity @ 300K- 0.875

Wavelengths-	**10.6**	**5.0**	**3.8**	**2.7**	**1.3**	**1.06**	**.411**	**.34**	**.25**
Matter.Dat-	0.97	0.6	0.67	0.73	0.145	0.201	0.941	0.944	0.929
Tracor Gie-	0.958	0.438	0.551	0.464	0.193	0.247	0.949	0.952	0.938
Matter Dat. Abs. Coeff. cm-1-	-1	-1	-1	-1	-1	-1	-1	-1	-1

Material- Aluminum Alloy
Surf. Mat Code- 5
Type- 2024-T3 (Clear Anodized)
Lot #- 184261
Ingot #- ****
Solar Absorptance- 0.398
Thermal Emissivity @ 300K- 0.846

Wavelengths-	**10.6**	**5.0**	**3.8**	**2.7**	**1.3**	**1.06**	**.411**	**.34**	**.25**
Matter.Dat-	0.94	0.301	0.399	0.314	0.073	0.1	0.581	0.811	0.914
Tracor Gie-	0.933	0.371	0.485	0.402	0.157	0.19	0.703	0.888	0.925
Matter Dat. Abs.Coeff. cm-1-	-1	-1	-1	-1	-1	-1	-1	-1	-1

Material-Aluminum Honeycomb
Surf. Mat Code- 6
Type- 2024-T3 (Bare)
Lot #- ****
Ingot #- ****
Solar Absorptance- ****
Thermal Emissivity @ 300K-

Wavelengths-	**10.6**	**5.0**	**3.8**	**2.7**	**1.3**	**1.06**	**.411**	**.34**	**.25**
Matter.Dat-	.100	.130	.160	.180	.270	.380	.000	.780	.940
Tracor Gie-	****	****	****	****	.443	.435	.813	.905	.923
Matter Dat. Abs. Coeff. cm-1-	-1	-1	-1	-1	-1	-1	-1	-1	-1

Material- Magnesium Alloy
Surf. Mat Code- 7
Type- AZ31B-H24 (Anodized)
Lot #- 190014
Ingot #- ****
Solar Absorptance- .633
Thermal Emissivity @ 300K- .656

Wavelengths-	**10.6**	**5.0**	**3.8**	**2.7**	**1.3**	**1.06**	**.411**	**.34**	**.25**
Matter.Dat	.855	.279	.307	.397	.523	.529	.874	.941	.958
Tracor Gie-	.855	.279	.307	.397	.523	.529	.874	.941	.958
Matter. Dat. Abs. Coeff. cm-1-	-1	-1	-1	-1	-1	-1	-1	-1	-1

Material- Steel
Surf. Mat Code- 8
Type- A36 (Mild)
Lot #- ****
Ingot #- ****
Solar Absorptance- .656
Thermal Emissivity @ 300K- .694

Wavelengths-	**10.6**	**5.0**	**3.8**	**2.7**	**1.3**	**1.06**	**.411**	**.34**	**.25**
Matter.Dat-	.050	.100	.140	.200	.838	.832	.784	.834	.846
Tracor Gie-	.710	.801	.799	.818	.838	.832	.784	.834	.846
Matter. Dat. Abs. Coeff. cm-1-	-1	-1	-1	-1	-1	-1	-1	-1	-1

Material- Steel (Stainless)
Surf. Mat Code- 9
Type- 304-2B (Unoxidized)
Lot #- ****
Ingot #- ****
Solar Absorptance- .395
Thermal Emissivity @ 300K- .066

Wavelengths-	**10.6**	**5.0**	**3.8**	**2.7**	**1.3**	**1.06**	**.411**	**.34**	**.25**
Matter.Dat-	.064	.165	.206	.278	.350	.363	.466	.543	.713
Tracor Gie-	.064	.165	.206	.278	.350	.363	.466	.543	.713
Matter. Dat. Abs. Coeff. cm-1-	-1	-1	-1	-1	-1	-1	-1	-1	-1

FERROELECTRIC LIQUID CRYSTALS FOR SATELLITE COMMUNICATIONS

Fawn R. Miller

Manzano High School
12200 Lomas Blvd, NE
Albuquerque, NM 87112

Final Report for:
High School Apprentice Program
Phillips Laboratory

Sponsored by:
Air Force Office of Scientific Research
Bolling Air Force Base, DC
and
Phillips Laboratory

September 1995

FERROELECTRIC LIQUID CRYSTALS FOR SATELLITE COMMUNICATIONS

Fawn R. Miller
Manzano High School

Abstract

The nature and operation of liquid crystals was studied. Ferroelectric liquid crystal devices were evaluated for use in satellite laser communications. Performance of the ferroelectric liquid crystals was measured by ON-OFF modulation of a laser beam. Measurements were taken from 10 to 500 hertz and results inducate potential future applicaion.

Ferro-electric Liquid Crystals for Satellite Communications

For only a few years, liquid crystals have been used by and for science and technology. Liquid Crystal Display (LCD) technology is used in wrist watches, pocket calculators, air craft, and many devices to transfer alphabetic and numerical information to the user. Now we are testing liquid crystal technology for possible use in satellite communications.

The previous and currently used methods for satellite communication transmitting and receiving have been with radio frequency (RF) systems using microwave frequencies.

Liquid crystals are being experimented with because they switch from transparent to opaque at fast speeds, effectively modulating a laser beam. A large laser on the ground could be used to illuminate a satellite. The light hitting the satellite would pass through a liquid crystal and then be reflected back to the ground. The data from the satellite would be used to create a modulation pattern for the liquid crystal. The reflected, modulated laser beam would be received on the ground by a telescope where an optical detector would be used to retrieve the satellite data.

The Phillips Laboratory has been working on laser communications technology for many years and recent laser technology advances make this appear to be a feasible alternative to RF systems. With the new discoveries of laser communications on satellites, the liquid crystal appears to be an effective device to be used to transmit data from the satellite. This laser and liquid crystal technology team up to give many advantages to data transmission. Some advantages include:

-Low weight of the satellite

-Little power is needed on satellite because there are no moving parts to be operated

-The setup is fairly simple

-The transmitting is more secure because the laser transmits to a smaller area

-There is still a moderate data transmitting rate

Ferroelectric Liquid Crystals (FLC)

The FLC was the main study of the experiment this summer. Understanding how liquid crystals (LCs) work and what made them work was a large part of the summer research.

Liquid crystals are unlike ordinary crystals nor ordinary liquids, they have a classification of their own. Yet, they have some characteristics of both solid crystals and liquids.

In liquids, such as water, the molecules run into each other and move around. In a solid crystal, such as ice, the molecules are no longer free to move, they are arranged regularly and oriented in the same direction. Liquid crystals consist of rod-shaped organic molecules about 25 Angstroms (10^{-10} meters) in length. See Figure 1. These molecules are free to move around, as in an ordinary liquid, but they all point in the same direction, like in a solid crystal.

Figure 1. Ferroelectric Crystal Molecule.

There are several types of liquid crystals. The nematic phase liquid crystal, for example, is characterized by the orientational order of the constituent molecules. The molecular orientation (and hence the material's optical properties) can be changed by temperature or by having an electric current applied to it. The nematic LC has a cloudy appearance or is blocked when cold. Then when heated up, the state changes and appears to melt, the plate clears up and can be looked through. The nematic phase can be controlled by an electric current. The effect of the current is an opening and shutting of the liquid crystal.

Nematics are (still) the most commonly used phase in liquid crystal displays (LCDs).

The smectic phases, which are found at lower temperatures than the nematic, form well-defined layers that can slide over one another like soap. The smectics are thus positionally ordered along one direction. In the Smectic A phase, the molecules are oriented along the layer normal, while in the Smectic C phase they are tilted away from the layer normal. These phases, which are liquid-like within the layers, are illustrated in Figure 2. Unlike nematic liquid crystal technology, FLC devices are not voltage tunable, they have only two states.

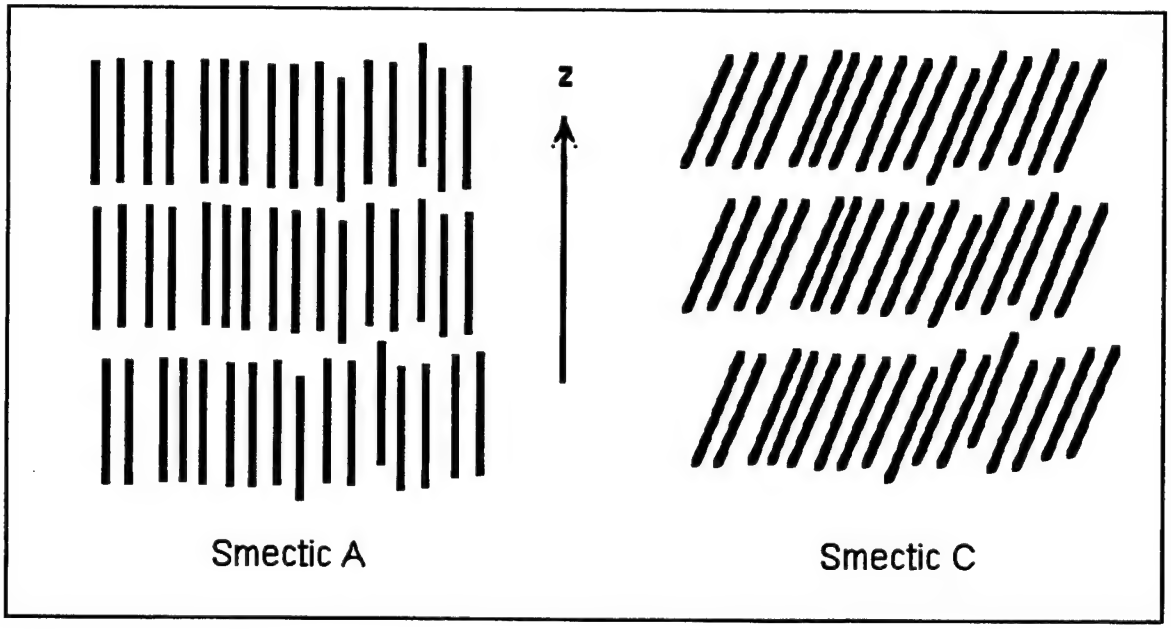

Figure 2. Orientation of Smectic Phases.

Liquid crystal's states can be changed by temperature or by having an electric current applied to it. The LC has a cloudy appearance or is blocked when cold. Then when heated up, the state changes and appears to melt, the plate clears up and can be looked through. The nematic phase can be controlled by an electric current. The effect of the current is an opening and shutting of the liquid crystal.

The FLC is only about a micrometer thick. The FLC is covered by two glass plates on both sides of it. The glass is then coated with a transparent conducting material, usually indium tin oxide (ITO). Two voltage wires are connected to this conducting material and the current sent to the glass effects the FLC's stage. Control of the FLC is straight forward, to hold the FLC OPEN or CLOSED, five volts is applied between the leads. To change the state of the FLC, the polarity of the voltage is reversed. The study this summer was to determine how fast the FLC could be opened and shut.

As stated before, the laser's light beam goes through the FLC and then into a detector. The FLC's different states affect the light beam and the detector reads this information.

Experiment

The setup used was as follows: A polarized Helium Neon (HeNe) laser was put at one end of the setup. A neutral density filter was placed where the laser light went through it to act as an attenuator. The laser beam then passed through the ferroelectric liquid crystal (FLC) modulator and finally, the beam went into a detector. The information from the detector went to a computer and was stored on a program called LabView. A function generator was connected to the FLC and to the computer program. The generator sent an electric current to the FLC to open and shut it.

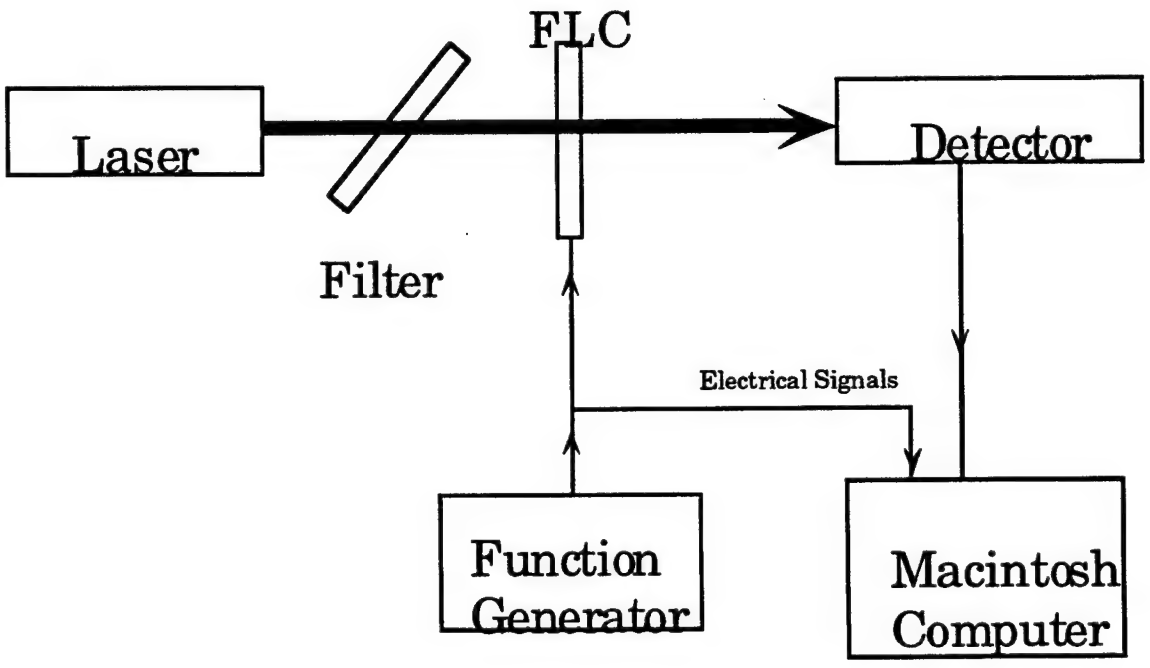

Figure 3. Experiment Schematic

The information received by the detector and the electric current sent to the FLC was also sent to the computer on two different channels. The program that picked up the two channels on the computer was LabView. This program displayed the data and stored it. In LabView, a VI (virtual instrument) had to be programmed to do what was necessary before data could be displayed and stored.

We used a Macintosh computer for data acquisition and analysis. Data entered the computer through a 12-bit analog-to-digital converter card using a program called LabView. Within LabView we created an object oriented program, called a virtual instrument or VI. This was used to read two channels of data at 1000 data points a second and store the data to disk. After data acquisition, we were able to plot the data to determine the performance of the FLC.

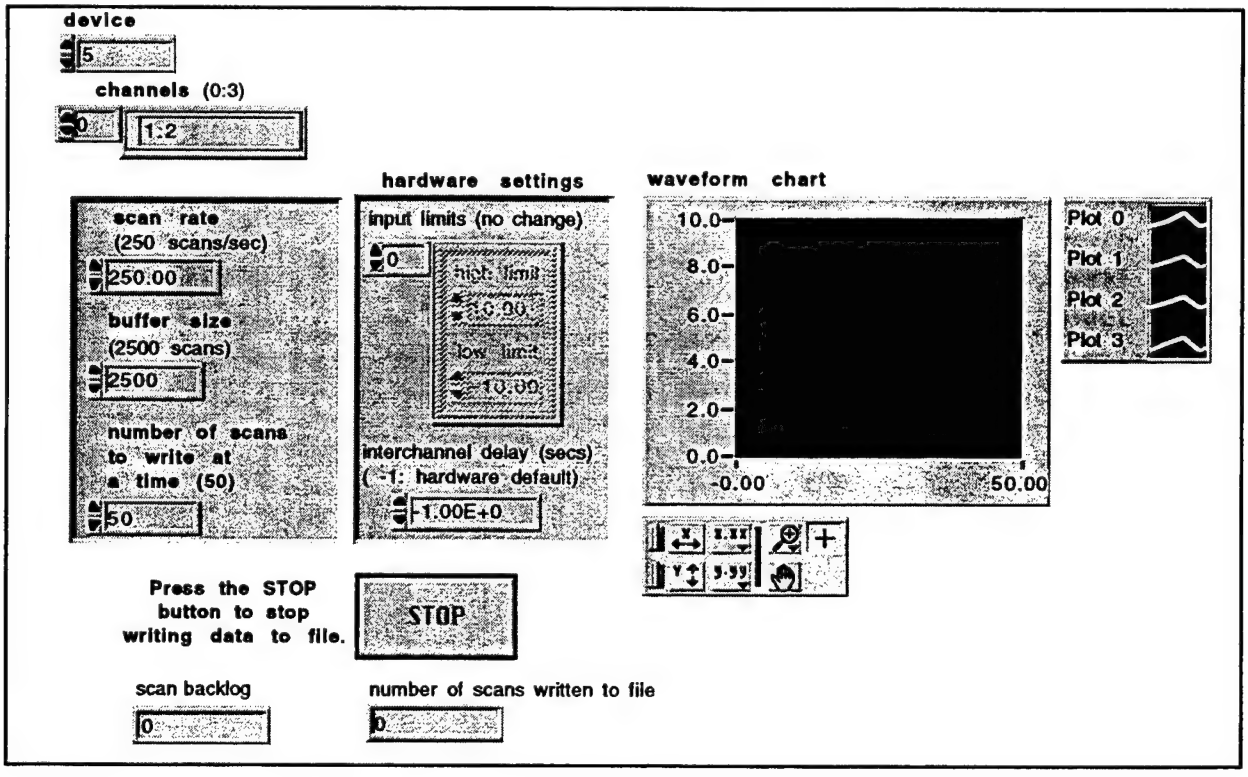

Figure 4. LabView Screen

Results

The results were recorded in a square wave frequency. Since the square wave has a tall boxy look, it is easy to tell how much laser light, or information, is going through the FLC at different speeds. Again, the effect wanted is totally open and completely shut at the fastest speed. The slowest test (10 Hz) showed the FLC opened and closed almost completely; about 95% open and 95% shut.

The 20 Hz test was about 85% open and shut. The 50 Hz test was about 75% open and shut. The FLC was unable to open a quick as the 10 Hz response and no longer has the square wave look; the appearance is now of a triangle. Now, less information is being sent through the FLC. The fastest test was at 500 Hz and the response was about 10% open and 10% shut. The results that were taken from the FLC testing were reasonable, but hopefully can be improved. See results on the FLC Response page.

FLC Response

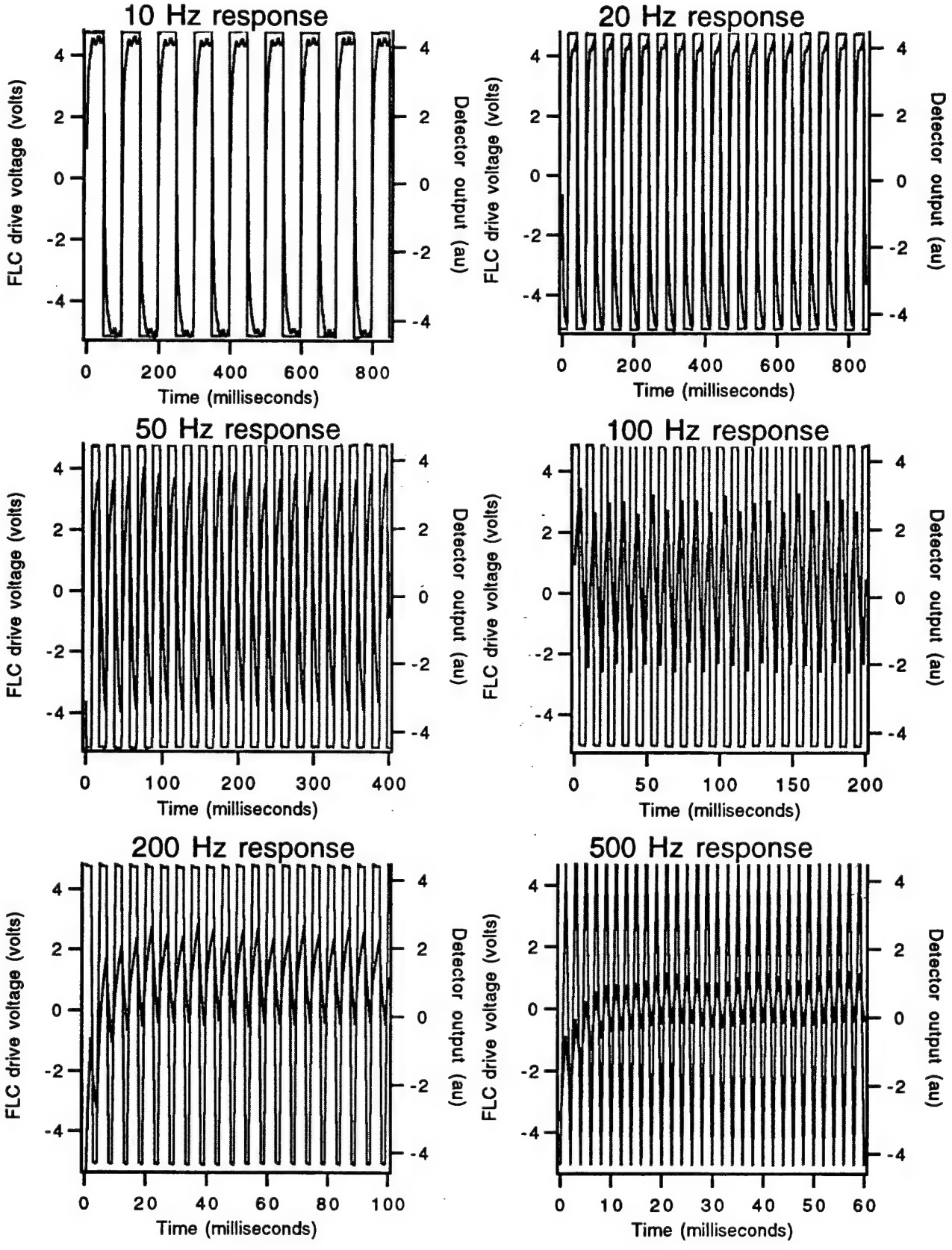

Conclusion

The ferroelectric liquid crystal technology is hopefully going to have an effective use in satellite technology. The FLC has many advantages over other laser or RF communiction techniques on the satellite. The FLC can receive information from a large angle. The FLC is also fairly inexpensive, around $150 for each modulator. The total estimated weight of the communication system with the FLC, is less than 10 pounds. Another large benefit of using the FLC and the laser is the smaller area it transmits to on the ground, making it more secure for Air Force applications.

The use of liquid crystals is a fairly new technology and the AFOSR research program has allowed my work with this new and upcoming technology. The knowledge of an unexplored field of technology is very beneficial. The ideas that can come to this technology are endless. The use of lasers and ferroelectric liquid crystals on satellites have a future of improvement and success.

There are other tests that can be run on the FLC and the setup. Different temperatures could be applied to the FLC. Different types of liquid crystal material could be used. Polarizers could effect the results, and many other variables could and should be tested at Phillips Lab next summer. The testing of these other variables could be the success for using lasers and liquid crystals.

References

Halliday, David, and Robert Resnick, Physics, John Wiley & Sons, 1978.

Pedrotti, Frank L., and Leno S. Pedrotti, Introduction to Optics, Prentice-Hall, 1987.

WWW pages from the Clark Research Group at the University of Colorado at Boulder.

MOSAICS OF ASTRONOMICAL IMAGES

Mark Nesky

Lincoln Sudbury Regional High School
390 Lincoln Rd.
Sudbury MA 01776

Final Report for:
High School Apprentice Program
Phillips Laboratory

Sponsored by:
Air Force Office of Scientific Research
Bolling Air Force Base, DC

and

Phillips Laboratory

August 1995

Abstract

To facilitate research at Phillips Lab, mosaic software that would combine images from the Infrared Astronomical Satellite (IRAS), was needed. Responding to the need, we wrote software that would work with any Flexible Image Transport System (the FITS file format), handle missing data points, and limit dstortions. We also wrote software that removes the zodiacal dust bands that contaminate the IRAS data. At every step we measured the level of uncertainty for any given pixel.

Introduction

In various projects, astronomical researchers in Phillips Laboratory work with data from the IRAS satellite. To make this data set more manageable, researchers needed specialized software that combines individual images into an image covering a wider field of view. The software would need to work with the FITS file format, handle missing data points, and limt distortions. Software that could remove the zodiacal dust bands that contaminated the IRAS data was also developed. A measure of uncertainty was associate with every step of the processing.

Mosaicking

Mosaicking is the process of putting together small pictures to make a larger picture. This process was originally developed to map large areas of land photographically. Early maps of the moon were also created using the mosaicking technique. The process must be able to line up the pictures correctly and it must account for the view point from which the picture was taken. Accounting for the viewpoint requires warping the pictures so they have the same spacial distortions. Originally this was all done optically. Presently computers can do the same job digitally with less picture degradation.

At Philips Lab, in the Geophysics Optical Background division, mosaicking software specialized for IRAS satellite images was needed to combine images and make large maps of the infrared sky. These mosaicked images will be used in astronomical research. To make the processed data useful, the software needed to be accurate.

concepts

In order for a computer to manipulate an image, it needs to be stored digitally. This is done using a two dimensional array with intensity values stored in each element. When displayed, each

element in the array has a corresponding pixel on the screen. The bigger the intensity value for that element, the brighter the corresponding pixel will be. In this way the computer can easily display and manipulate monochrome images. To increase the image's brightness, a constant can be added to each element in the array. To double the contrast, each element can be multiplied by two.

Warping is a more complicated manipulation requiring interpolation between pixels. Interpolation is the process of estimating points where no points exist. A simple example requiring interpolation is doubling an image's size, which requires doubling the array's dimensions. What intensity values belong in the new array elements? By fitting polynomials across data points, computers can calculate apropriate values for any location.

Images need to be warped because, like photographs, the arrays are three dimensions represented in two. Mathematically, the warping is done by mapping the two dimensional array onto a sphere and then mapping it back onto a plane from a different viewpoint. This can be conceptualized by imagining the view due north from the center of the map below, and comparing it with the view due east. The building northeast of the center can be seen from both viewpoints. However, if photographs were taken from each viewpoint and put side by side, the rectangular face of the building would not appear rectangular. Projecting the images onto a sphere and back to a plane, results in images like the ones on the next page. After warping the images can be combined.

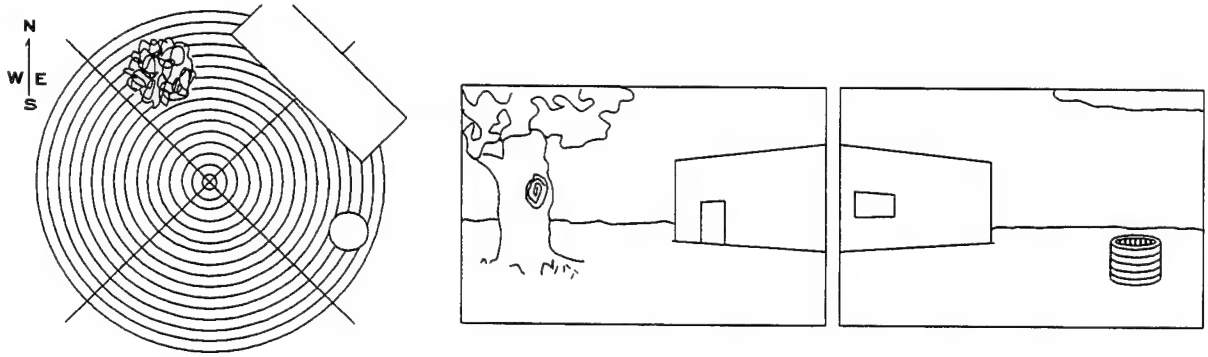

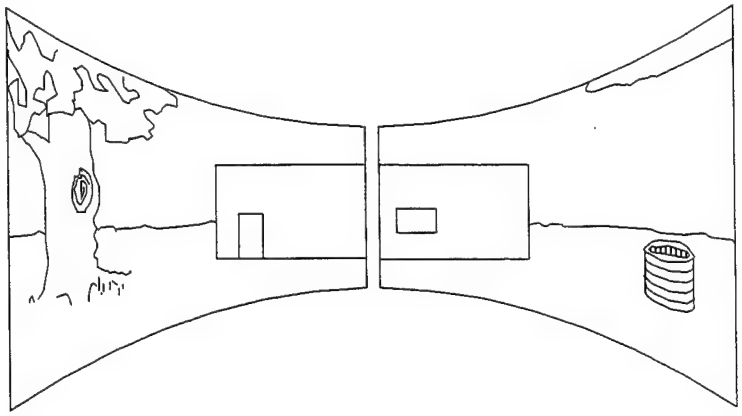

The side affects in this two dimensional representation are stretched sides. It is the same plane-to-sphere distortion that causes Greenland to appear large on a world map and small on a globe. Though the stretching makes 2D pictures appear a little bit odd, the above picture in its 3D state would appear perfectly distortionless to a person standing at its focus. However, maps of the earth or of the stars represented on a plane are inherently distorted due to its representation of three dimensions in two.

Accuracy

There are several aspects of acuracy of conceren. For example, one concern is the spacial acuracy of the coordinates for a given point source before and after processing. But for the researchers, a greater concern is the intensity acuracy; the difference between a point's actual intensity and its measured intensity.

Spacial acuracy, is accomplished by making the correct distortions using the equatorial coordinates stored in the header of each image. The header is part of the FITS file format used in the IRAS data set containing specifications including like size, scale, and center coordinates. One way the accuracy of warping was determined was looking at how well the stars in overlapping regions matched. Spacial accuracy was also checked using the header to convert the pixel coordinates of

bright stars into equatorial coordinates before and after the mosaic. This test showed that the information in the header and the mathematical algorithms were accurate enough to keep errors less than the size of a pixel.

One problem with the satellite images was they had different brightness offsets. Compensation for such relative intensity errors was made using the average intensity difference between images calculated from overlapping regions. In this fashion the center image in the mosaic was defined as having the correct intensity and all neighboring images were adjusted to the same level.

Implementation of the above correction system exposed dificulties. For a pair of images the system worked well, but for multiple images it would be optimum to find a way that already corrected images did not affect the corrections of subsequent images. Otherwise, the error in intensity correction could grow with the distance from the central image. Unfortunately not all images overlapped the central image and the computers could not simultaneously manipulate all eight images anyway. Thus, only two images can be manipulated at a time. Due to this limitation the program would take the output of a previous mosaic and mosaic another picture on. In this way the program could keep mosaicking pictures on until a suitably large picture was created. Because the computer was only working with pairs, images that did not overlap the central image had their intensity correction based on an already corrected image. Fortunately, most pictures overlapped the center picture and the necessary corrections were small to begin with, so the intensity correction system proved sufficient.

The fact that the computer was only working with two images at a time caused other problems because the original image would repeatedly go through the interpolation algorithms each

time it ran through the mosaic code. Since the first picture was defined to be correctly spatially distorted, it was unnecesary to interpolate the first image. To mosaic a series of images, the revised program would warp the central image once, mosaic the first and second images, and then mosaic each successive image to the previous mosaicked output. Because the central picture was defined as having the correct spacial distortions, it really did not need to be warped. However, by running it through the warping code and warping it to its original coordinates, it was forced it through the interpolation algorithms. This meant all of the data would be treated consistently because every data point would go through the same algorithms the same number of times.

Continuing with the concept of consistancy, the program does not to average the overlap data. Any combining algorithm for the overlap would be treating the data inconsistently. This was visually evident when the overlap data was averaged because it made a well defined band of smoothed data in the overlapping region. If one does not subject all of the data to the same distortions, nonexistent trends in the data may show up. Maintaining this philosophy, the mosaic code uses data points from the first image in the overlapping area instead of averaging or otherwise combining the overlap data.

The mosaic code required a great deal of testing and tweaking before the acuracy of its computations maximised, its distortions had been minimized, and all of the data were being treated consistently. Intensity corrections were monitored by plotting the intensity of the overlapping region in one image against the intensity of the same region in the next image. This plot allowed the effectiveness of our intensity correction to be diagnosed. A slope of one indicates that the images have the same contrast. A slope of two would indicate a diference in contrast. In such a case adding an offset to the image would not make the images match. The slope of the plots were nearly one for

most mosaics. The Y intercept of the plots represents an offset. Adding an offset compensates for brightness. Since the satellite images using suffered from a drifting calibration, it was necessary to make small offsets to match the pictures. In most cases the plot indicated that the pictures were a good fit. In one case the plot was not linear. After extensive experimentation we concluded that a particular image had been incorrectly processed before it reached us. The researchers using the mosaics were alerted as to the high uncertainty of that image.

The mosaic code also needed to accommodate lost data points. The IRAS images are incomplete. The images are dotted with black holes where there is not data. The program needed to avoid corrupting good data adjacent to missing data in the interpolation process. For the sake of scientific accuracy, the program blanked any data points averaged with missing data points. This makes it especially important that the code was modifed to prevent images from getting interpolated repeatedly. Otherwise, very large holes would grow from missing data points as images passed through the mosaic code repeatedly.

In order for the mosaicked images to be have any scientific value, the researchers needed a handle on the noise level. By knowing the noise level, researchers can say with a certain level of confidence what in the data is a trend and what is just random error. In search of random error, it was posible to take advantage of certain aspects of the IRAS data. IRAS circled the earth numerous times, scaning nearly the entire sky three times. Because of this, there are three images of the each region. By subtracting images taken at different times, it is posible to get a picture of the random error in the images before the mosaic program did any processing. The difference images showed calibration changes between scan lines, a small amount of background noise, and a little bit of the historesus affect. Also, asteroids showed up in the difference images. Asteroids changed location

between images while stars remained fixed. Histograms of the difference images show how large the random errors are. As anticipated, the histogram was a normal distribution centered at zero. The asteroids were outliers in the histogram and got labeled as unreliable data points. To make sure that good data was not being removed, unreliable data was highlighted in the images. This allowed asteroids to be seen and made sure they were all that was being labled unreliable. Discounting unreliable data points, the standard deviation of the difference images was minuscule. Knowing this noise level allows researchers using the data to differentiate between trends and random noise and to defend the validity of their observations. Knowing the noise level of the original pictures also allowed the affects of the mosaic program's processingto be seen. As expected, our processing introduced no increase in the level of random noise.

Zodiacal dust removal

The next step in the image processing was removing the influence of zodiacal dust from the needed images. Fortunately the zodiacal dust has certain characteristics that help distinguish it from the galactic dust outside of our solar system. The zodiacal dust spins with the disk shape of the solar system, thus the dust can be recognized as wide bands of higher intensity that stretch along ecliptic lines of longitude. Remove these bands was necessary because the researchers were only concerned with the infrared emitting dust outside of the solar system. In order to make the pictures usable therfore necessary to subtract off zodiacal emission. Zodiacal emission is the emission of the dust within the solar system. Unfortunately it is necessary to look through the zodiacal emission to see outside of the solar system. To make matters more difficult, the region of interest lay on the seam where the end of the satellites orbit met the beginning. This means that the satellite was looking through a different part of the zodiacal dust bands on one side of the picture than on the other. This

necesitated separate processing of the left and right of the image. Because of this time gap and because differentiating the zodiacal dust from galactic dust is difficult, it was necessary to experiment with various removal methods.

One meathod of attack was to subtract a mathematical model of the zodiacal dust. Because these bands have been studied and modeled by other researchers, software already exists that can generate an image of the dust bands when given coordinates and a date. By subtracting this model one should get an image of just the infrared emmitting dust outside of our solar system. Unfortunately the results were extremely inaccurate. The images had gone through a lot of processing before their release and an early model of the bands had already been subtracted. This previous model was simple and only accounted for broad zodiacal emission, it left behind large bands that striped across our images. When the more recent and more accurate model was subtracted, certain regions had been over acounted for and the resulting image was worse.

Another removal method involved fitting polynomials to the zodiacal bands. First it was necessary to rotated the images from equatorial coordinates into ecliptic coordinates. Equatorial coordinates are based on the earth and its rotation. Ecliptic coordinates are based on the rotation of the solar system. By rotating the image into ecliptic coordinates, it becomes easier to isolate intensity offsets caused by zodiacal band because the bands are horizontal and run nicely along rows in the image array. The next step was to take all of the intensity values along the horizontal lines of elements in the array and fit a low order polynomial. Subtracting the polynomial filters out gradual intensity changes and overall offsets along horizontal lines. This method is a form of high pass filter. To prevent the bright stars from skewing the polynomial fitting they were blanked.

Since the researchers needed to see subtle changes in data we needed to find the data's

uncertainty. To find a measure of uncertainty difference images were used again. We used this method of zodiacal removal on multiple images of the same region and subtracted them. Unfortunately the level of random noise had decreased. This implies that unwittingly the data was being smoothed. Unfortunately calculating difference images will not help uncover errors that are being made systematicaly. These errors can only avoid through careful anylisis.

Conclusion

Philips lab now has specialized mosaicking software. This software will combine any number of adjacent FITS images. The software allows the user to choose the type of interpolation and intensity correction that is used. The program also monitors missing data and updates the header of the final image. The user can choose to see plots that analyze how well the images match. Presently mosaics from this software are being used in a study of declining infrared emission near class B star clusters.

Visual Supplement

IMAGE A

The central plate used in the mosaicked images. The star cluster in the upper left is the Pleiades. Note the intensity scale, the regions of high intensity are black. Thus stars appear as black dots.

IMAGE B

The plate just left of the central plate.

IMAGE C

The mosaic of image A and B. In the mosaicking process, image B was warped and had its intensity calibrated to match up with image A.

IMAGE D

The complete mosaic of all eight plates in the desired field of view. The white lines are missing data points. The left portion of the image is darker because it was taken at a different time and through a different part of the zodiacal dust bands. The most prominent zodiacal dust band can be seen as a dark region running diagonally across the picture.

IMAGE E

The model that was fit to Image D. The line separating the different processing halves can be seen clearly.

IMAGE F

The final image after the zodiacal dust bands had been removed. This image is a composite of mosaics from all of the passes the satellite made over this region.

IMAGE A

i275b1h0.fit

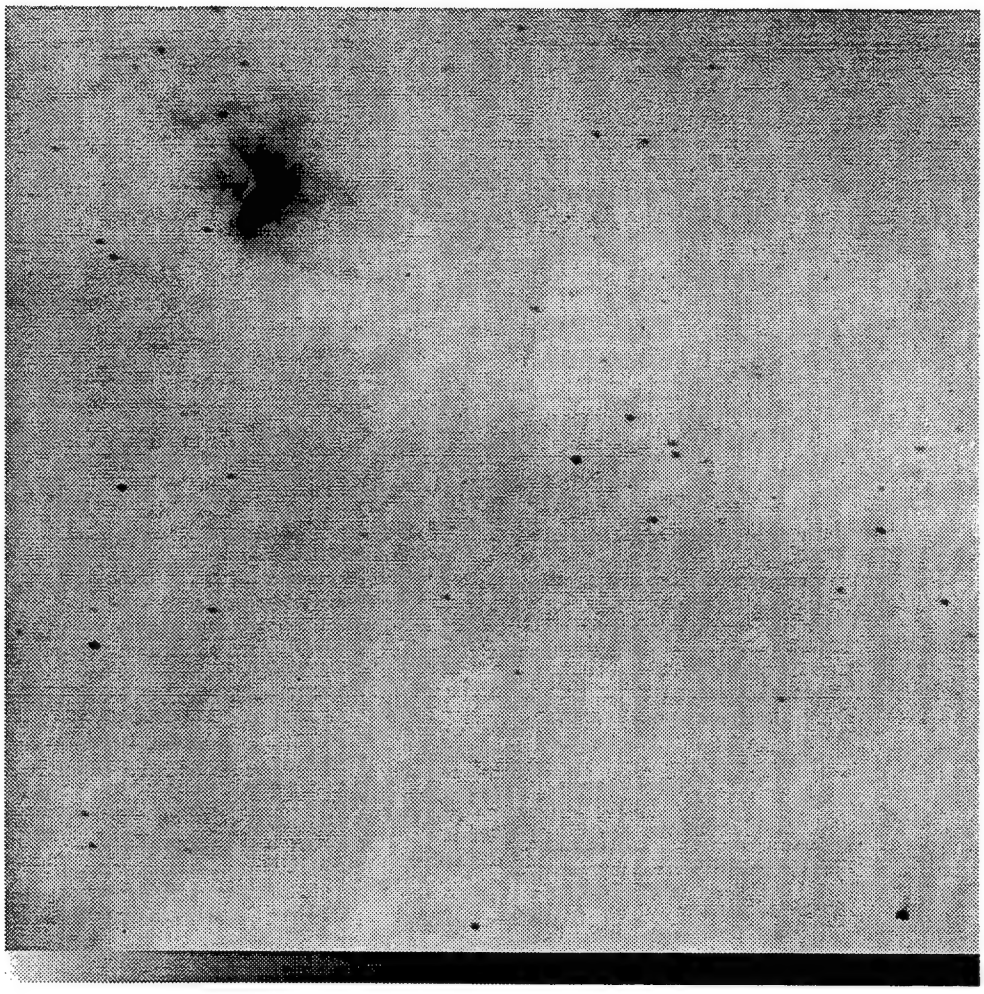

−3.0 MJy/sr 6.0 MJy/sr

12 μm HCON: coadd

IMAGE B

i276b1h0.fit

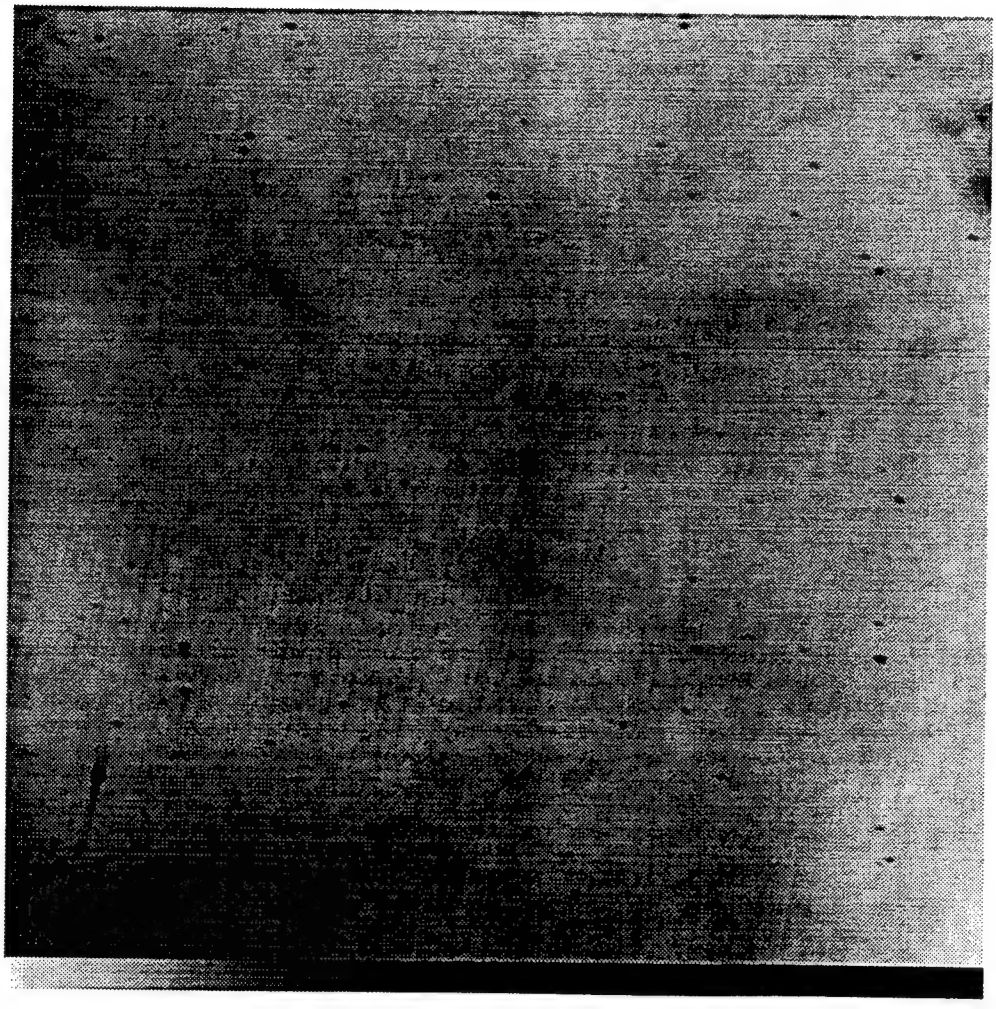

−3.0 MJy/sr

6.0 MJy/sr

12 μm HCON: coadd

IMAGE C

small_mosaic.fit

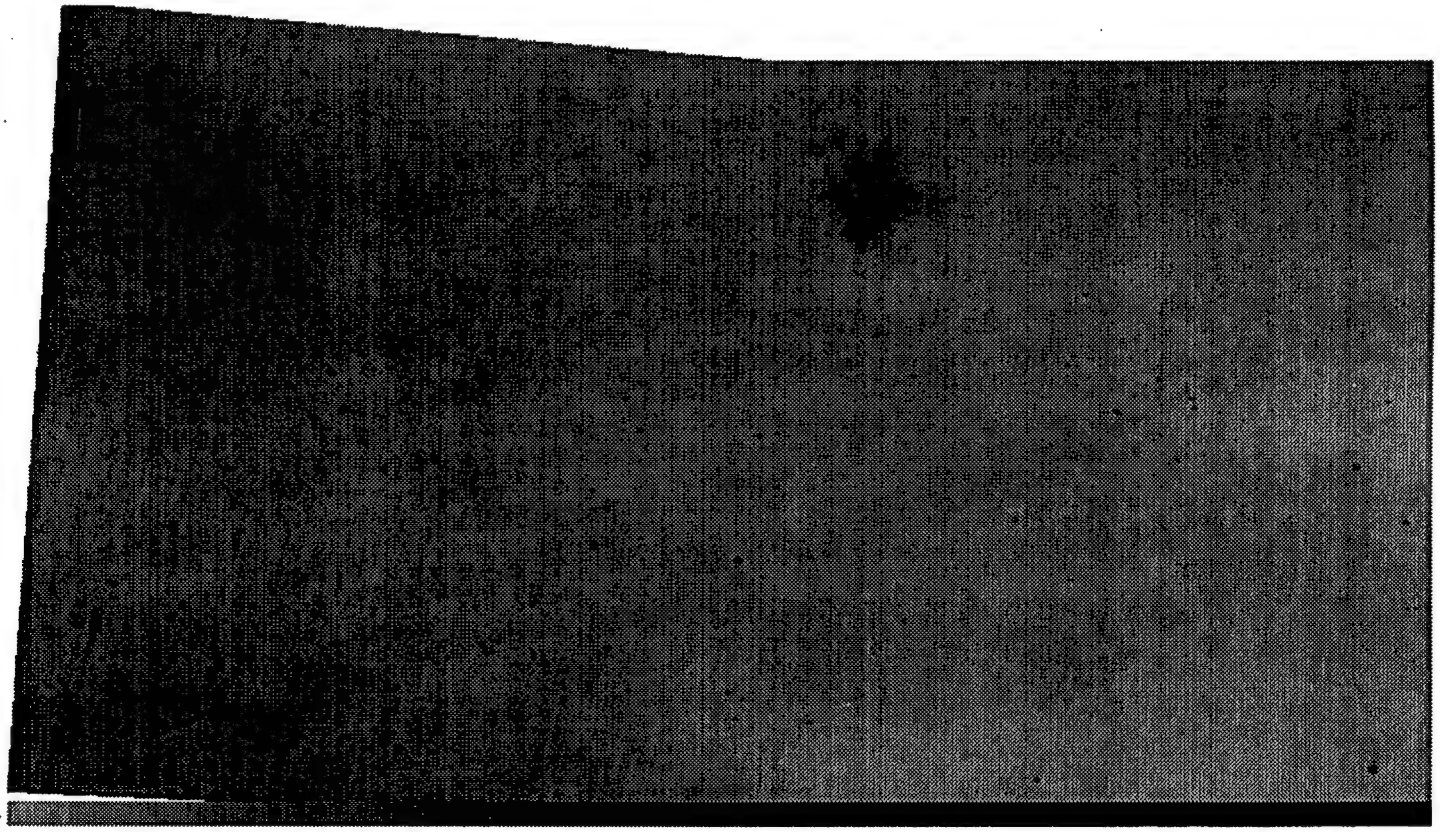

−3.0 MJy/sr

6.0 MJy/sr

IMAGE D

pl.b1h2.crop.fit

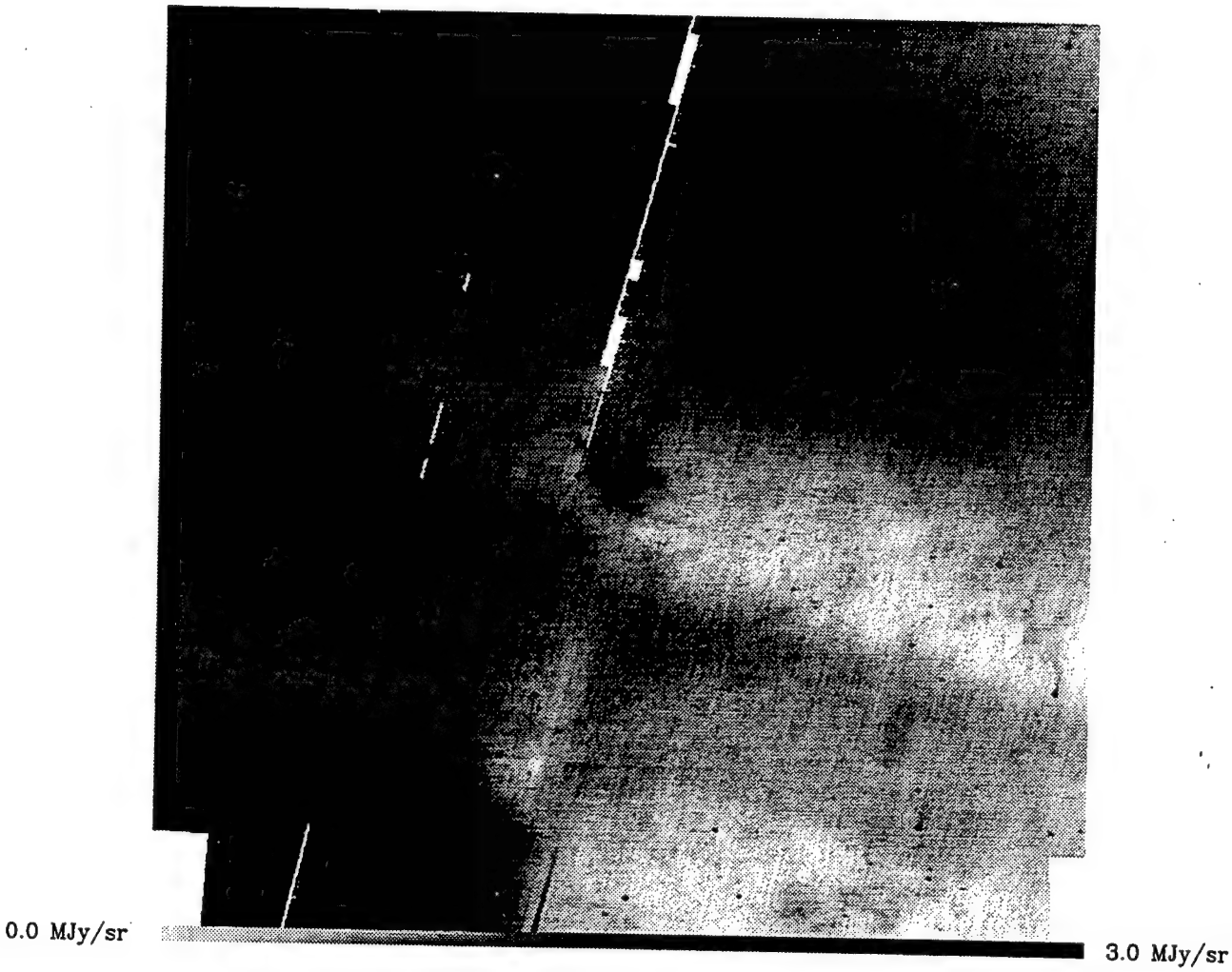

12 μm HCON: 2

IMAGE E

pl.b1h2.crop.fit.zmod

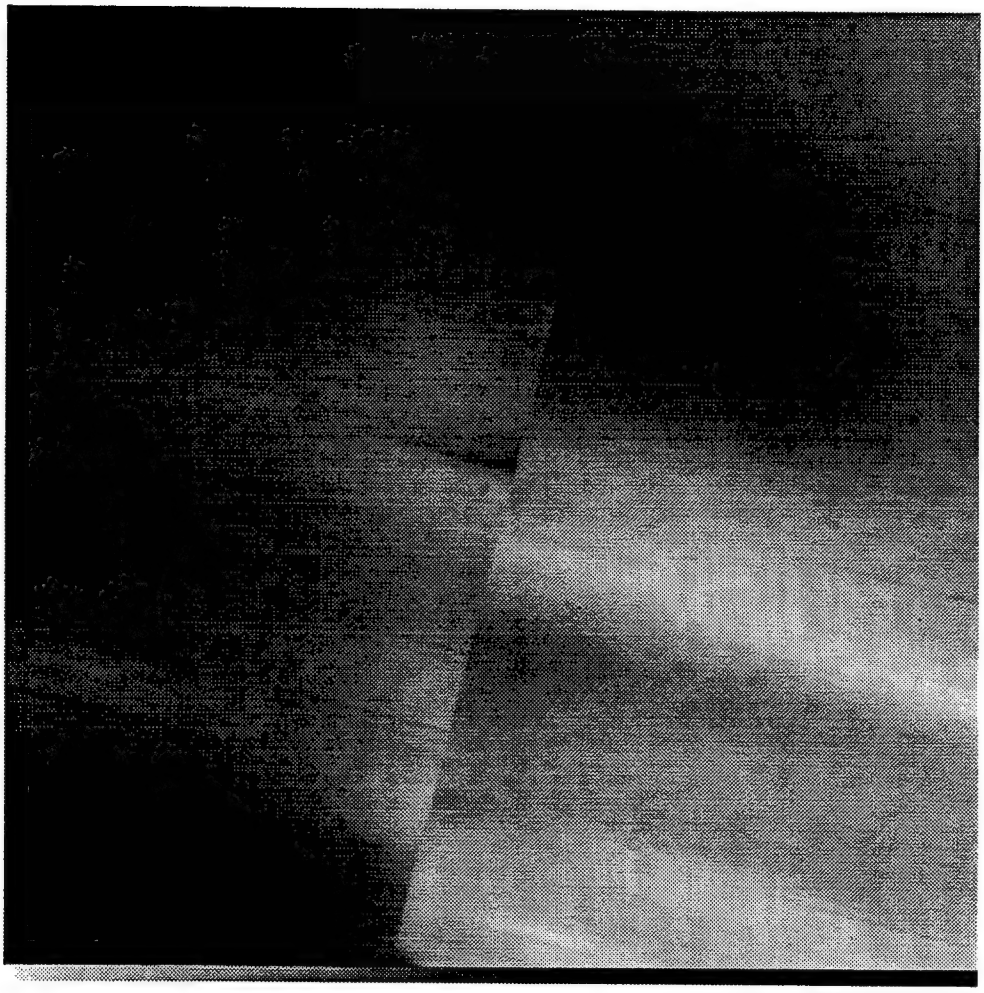

0.0 MJy/sr

3.0 MJy/sr

12 μm HCON: 2

IMAGE F

coadd.b1

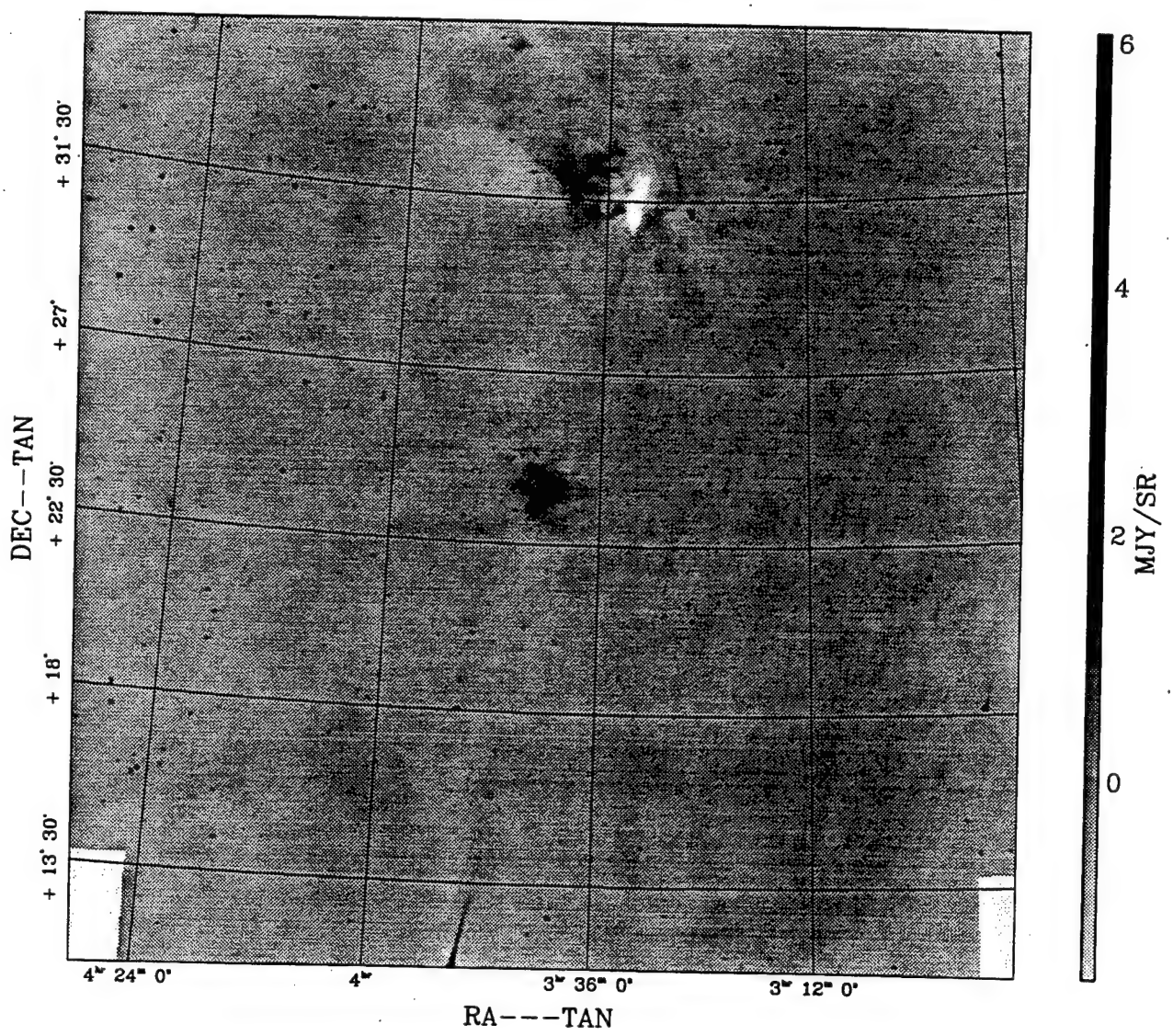

band: 12 μm HCON: coadd

SIMULATING A SPACE ENVIRONMENT

Julie A. Niemeyer

Valley High School
1505 Candelaria
Albuquerque, NM 87107

Final Report for:
High School Apprentice Program
Phillips Laboratory

Sponsored by:
Air Force Office of Scientific Research
Bolling Air Force Base, DC

and

Phillips Laboratory

August 1995

SIMULATING A SPACE ENVIRONMENT

Julie Niemeyer
Valley High School

Abstract

In today's growing technological world there is a greater number of satellites and other space vehicles. This in turn requires testing of the future space vehicle and all components of the vehicle before launch. Thermal Vacuum Chambers simulate the space environment. This simulation of the space environment is one of importance and safety. It also saves money, time and energy that can be lost if a satellite cannot function in the harsh space environment. The thermal vacuum chamber can detect the most of the problems that could occur while the satellite or space vehicle is in orbit.

SIMULATING A SPACE ENVIRONMENT

Julie Niemeyer
Valley High School

With the advancement of technology comes the need for more advanced testing and evaluation of space equipment before the equipment is even put in orbit. This specialized testing is done in three parts: Thermal Vacuum Test, Thermal-Cycling Test, and Thermal Balance Test. These three tests are described in MIL-STD-1540B, all standards mentioned hereafter come refer to this document. This advanced testing can and will detect problems that arise when a vehicle is operating in the harsh space environment.

The thermal vacuum test is a performance test at temperature extremes. This test emphasizes on component and subsystem interaction, and end to end performance of the space vehicle. The temperature extremes are based on the worse case analytic predictions, these temperatures are to be monitored to avoid overstressing the space vehicle. There is a minimum of eight thermal vacuum cycles required for qualification and a minimum of four cycles are required for acceptance. The minimum for acceptance can be reduced to one if space vehicle thermal cycling is performed, performing only one cycle is not recommended but performing four is highly encouraged.

The parameters for the thermal vacuum test qualifications are in paragraph 6.2.7, and the acceptance parameters are in paragraph 7.1.7. Temperature range and extremes are the minimum and maximum predicted for a single component in each equipment area for the acceptance test. The qualification test is the same plus an environmental design margin of 10 deg C. The pressure must be 10^{-4} Torr or less.

There is also an eight hour dwell required before the functional testing is done, to ensure equilibrium is achieved. A shorter time may be used if it is a small satellite and equilibrium can be

proved. During this state of equilibrium there can only be a temperature rate of change can only be less than 3 degrees C per hour. The full function tests are performed at ambient temperature and pressure before and after the thermal vacuum test.

Thermal cycling is an environmental screen that exposes design, workmanship, material, and processing defects. The integrity of mounting cables and connectors are also tested. This test is optional at the spacecraft level. There is a minimum of fifty qualification cycles or 125 percent of the acceptance, and forty acceptance cycles. During the acceptance test the minimum temperature is 50 deg C with qualification at 70 deg C.

The thermal balance test is conducted during the thermal vacuum test. The purpose of this test is to verify thermal analytic models and to test the functional capability of thermal control hardware. The test establishes the ability of thermal control hardware for all phases. It is conducted for one of a kind space craft, the lead vehicle of a series, block change, upperstages, and sortie pallets on the space shuttle. Most but not all phases are tested, only one or two vehicle configurations. The intent of the test is not to drive all components to qualification level testing, but to exercised all internal heat flow paths, and the external solar flux radiative and absorptive surfaces. Only minimal conditions for equipment usage, bus voltage and solar heating are tested. During the test operation large appendages, solar arrays, booms, antennas, are sometimes not part of the test configuration. Deployable antennas are stowed during the test.

Non-operational mission nodes may also require simulation. Transfer-orbit, storage and safe mode are the most important factors to be tested. There must be a dedicated cold phase to verify and characterize the heater operation. Heat loads are divided between an absorbed flux and incident flux. If the heaters are directly affixed heat loss must be understood, and refurbishment is

required if the qualification vehicle is the flight vehicle. The comparisons between the pretest temperature prediction and the corresponding data should be within 3 deg C, though 6 deg C is often used also.

The thermal balance test is successful in correcting major thermal-modeling repairs, the verification of the design and performance of thermal control hardware is also done. The primary and redundant heaters are exercised. These few tests can save money by detecting some of the small and large problems that occur in the space environment to cause the space vehicle to become non-functional. If these problems are solved in the simulated space environment, then there is not the waste in time and money to repair a vehicle that is currently in orbit.

A STUDY OF THE VISCOSITY CHARACTERISTICS OF POLY (VINYL ALCOHOL) (PVA) IN THE SOLVENTS S-HAN 5 AND WATER

Jamie B. Nyholt

Quartz Hill High School
6040 West Ave L
Quartz Hill , Ca 93536

Final Report for:
High school Apprenticeship Program
Phillips Laboratory

Sponsored by:
Air Force Office of Scientifc Research
Bolling Air force Base, DC

and

Phillips Laboratory

August 1995

15-1

A STUDY OF THE VISCOSITY CHARACTERISTICS OF POLY (VINYL ALCOHOL) (PVA) IN THE SOLVENTS S-HAN 5 AND WATER

Jamie B. Nyholt
Quartz Hill High School

Abstract

The behavior of poly (vinyl alcohol) (PVA) in water and S-HAN 5 was investigated. The sol-gel transitions were studied by varying concentrations of PVA in the solvents water and S-HAN 5. The physical state was observed by the meniscus-tilt method. The affect of concentration and molecular weight on a range of poly vinyl alcohols with varying molecular weights in the solvents water and S-HAN 5 was studied. Elvanol HV, Airvol #103 PVA and Airvol #107 PVA were used. These solutions were made by dilutions of the highest concentration of each soution. Viscosity measurements were taken for each solution at varying concentrations at 25^{o}C. These viscosities were used to find the intrinsic viscosity of each solution. The intrinsic viscosities were then plotted against the weight average molecular weights to find the interaction parameter. This parameter shows the interaction between a specific polymer and solvent at a given temperature, in this case 25^{o} C.

A STUDY OF THE VISCOSITY CHARACTERISTICS OF POLY (VINYL ALCOHOL) IN THE SOLVENTS S-HAN 5 AND WATER

Jamie B. Nyholt

Introduction

By obtaining the intrinsic viscosity using samples with known average molecular weights a relationship between concentration and inherent (or reduced) viscosity can be determined. This information allows for the determination of the intrinsic viscosity. The intrinsic viscosity is defined by the equation:

$$[\eta] = \lim_{C \Rightarrow 0} \eta\text{-}\eta s / \eta_s c$$

Using the Stockmayer - Fixman Equation, an interaction parameter, which is a constant for a polymer/solvent/temperature system, can be obtained {1}. This parameter expresses the interaction between polymer and solvent at a specific temperature.{2} The intrinsic viscosity can be found using calculations obtained from viscosity measurements which involve fairly simple equipment and measurements. The intrinsic viscosity which is the capacity of a polymer molecule to enhance the viscosity is said to depend on the size and the shape of the molecules (both solvent and solute molecules). {3} The magnitude of the affect molecular weight has on the intrinsic viscosity of solutions of poly (vinyl alcohols) (PVA) in the solvents water and S-HAN 5 (Stabilized Hydroxyl Ammonium Nitrate) was investigated.

A gel is a semisolid. The mixture is immobilized by solvating a polymer in a solvent, forming a gel. The particles of a viscous solution, a sol, crosslink by forming hydrogen bonds and swelling. When the molecules become larger, they do not flow as easily and the solution becomes thick and viscous. When the molecules become large enough or crosslink to the point they can no longer flow, the solution is said to be a gel. This point of transition from a sol to a gel is the gel point.{4} Solutions of PVA (Elvanol HV) in water were made at 70^{o} C. Dilutions were made to vary concentration. The transitions from a sol to a gel were observed.

Methodology

Sol-Gel Transitions

In order to observe the sol-gel transitions of poly vinyl alcohol in water, solutions of concentrations ranging from 0.3-7% were made. Poly vinyl alcohol (Elvanol HV) was dissolved in water using the apparatus in

Figure 1 at 70^0 C. A 7% solution was made. This solution was diluted to form the lower concentrations. These solutions were placed in tubes which were placed in a controlled temperature water bath (circulator). The bath was set at temperatures ranging from -18-20^0 C. The solutions were allowed to equilibrate for 1 hour. The meniscus tilt method, used by Komatsu, Inoue and Miyasaka was used to identify the solution as a sol or a gel. The tubes were tilted. If the meniscus deformed under its own weight it was still a sol. If the meniscus did not deform it was identified as a gel.{4} These observations are shown in Figure 2.

Viscosity

The same method used for making the solutions in the sol-gel transitions was used to make solutions of Elvanol HV in water, Airvol #103 PVA in water, Airvol #107 PVA in water, Elvanol HV in S-HAN 5, and Airvol #107 PVA in S-HAN 5. A water titration was done on the S-HAN 5 solution to find the amount of water it contained. This amount would be used to calculate a more accurate overall density. These solutions were made at lower concentrations (0.3 - 3 wt.%). Viscosity measurements were made on these solutions using different sized Cannon-Fenske viscometers. Viscosity measurements were also made on the solvents in each tube to obtain an experimental solvent viscosity. The solvent viscosities are shown in Figure 2. The solutions were placed in an appropriate size tube and allowed to equilibrate in a glycol / water bath at 25^0 C for 20 min. The solutions were forced above the top timing line. Then the liquid was allowed to flow and was timed. At least 3 consecutively similar measurements were taken to insure accuracy. These measurements are shown in Table 1. The averages of these viscosity times (in seconds) were multiplied by the calibrated constants to find the kinematic viscosity:

Time (secs) * Viscometer Constant = Kinematic Viscosity (Centistokes)

The product of the kinematic viscosity and the density of the solution produces the absolute viscosity. To find the absolute viscosity the density of the solution was calculated (water was included only with S-HAN 5).

Solution Density =

Amount solute*Solute Density + Amount solvent*Solvent Density + (Amount water*Water Density)

Absolute Viscosity = Kinematic Viscosity * Solution Density

The absolute viscosity is simply referred to as the viscosity. For the relative viscosity (η_r), experimental solvent viscosity values were found. In the water solutions the kinematic viscosity for each tube was used. In the S-HAN 5 solutions an average of the kinematic viscosities was used. Using the viscosity (η)and the solvent viscosity (η_s), η_r and the specific viscosity (η_{sp}) can be found.

$$\eta_r = \eta / \eta_s$$

$$\eta_{sp} = \eta_r - 1$$

With this information the inherent viscosities (η_{inh}) and reduced viscosities (η_{red}) can be determined.

$$\eta_{inh} = \ln (\eta_r) / c$$

$$\eta_{red} = \eta_{sp} / c \quad \{3\}$$

These values were then used to find the intrinsic viscosity by plotting the inherent and the reduced viscosity vs concentration. Theoretically the lines on the graphs should intersect each other at $[\eta]/ M^{1/2} = 0$. Since this did not occur we will improvise and decide where the lines would have intersected. To do this the average of the y intercepts was taken. This point is the intrinsic viscosity. {2} The intrinsic viscosities of PVA solutions are shown in Figures 3 - 5. The intrinsic viscosities of HAN solutions are shown in Figures 7 - 8.

The intrinsic viscosities were then used in the Stockmayer - Fixman Equation :

$$[\eta] = K\theta\, M^{1/2} + BM$$

where B denotes the interaction parameter, M the molecular weight and $K\theta$ a constant. This equation was used in its converted form:

$$[\eta]/M^{1/2} = K\theta + BM^{1/2} \quad \{5\}$$

to determine $K\theta$ and B for the various poly)vinyl alcohols) in water and then in S-HAN 5. These graphs are shown as Figures 6 and 9 respectively.

Results

Sol - Gel Transitions

The points of transition from a sol to a gel were recorded and are shown in Figure 2. These results did not prove efficient for the solutions of lower concentration. This is due to the amount of water present. The

temperatures at which gelation would occur was too low. The water in the solutions froze before a gel could be formed. Some conclusions can be made from the data obtained. It is obvious that the gel points of solutions increase with an increase in concentration. Therefore it can be concluded that the gel point is dependent of concentration. All of the solutions eventually froze. The solution of 7 % concentration slightly froze. When it was placed at room temperature it resumed gel form. It was a rubbery, fairly tough yet viscoelastic material. The 7% and 5% solutions never resumed sol form when placed at room temperature. All other solutions melted at room temperature (approx. 23^{o} C) and resumed the form of a viscous solution.

Viscosity

The viscosity measurements which were made and interpreted into kinematic viscosity show certain immediate results. In looking at the kinematic viscosities in Table 1 it can be confirmed that the kinematic viscosity increases with concentration. This would be expected because the more particles there are to hinder the flow of the solution (the higher the concentration) the more viscous the solution would be. In comparing the kinematic viscosities of the solutions of different molecular weight it can be seen that the kinematic viscosities are higher for solutions of PVA with a higher molecular weight. Similarly it can be observed that the kinematic viscosities of solutions containing HAN are higher. HAN, with a density of 1.68 is more dense than water with a density of 1.00 {6}. With a higher density it would be assumed and is obvious that HAN is more viscous than water and remains this way when combined with PVA. Consequently HAN / PVA solutions are more viscous than Water / PVA solutions. Following this noticeable trend the intrinsic viscosity of HAN / PVA solutions is higher than that of Water / PVA solutions.

In comparing the intrinsic viscosities of the various molecular weights of PVA in the solvents S-HAN 5 and water we see that the HAN solutions have intrinsic viscosities of almost double those of the water solutions. This is consistent with the previous data.

Using this information in the Stockmayer - Fixman Equation the interaction parameter (B) and constant ($K\theta$) can be obtained. This data is shown in Figures 6 and 9. The graph in Figure 9 shows the interaction parameter for PVA / S-HAN 5 solutions to be -.0015048. For PVA / Water solutions this parameter is -.00056709. The interaction parameter for HAN solutions is higher . As the molecular weight increases the solution becomes

more independent of molar mass{3}. The closer the interaction parameter is to 0 the less interaction occurs. Since water has a smaller interaction parameter it is able to dissolve more material because it does not interact with the particles to the extent HAN does.

There are many reasons for slight errors in these results. Different size viscometers were used. Viscosity calculations for the solvents HAN and water produced slightly varying results. The viscosities of the water solutions were very similar to each other (ηab = 0.8575, 0.94017, 0.900965, 1.183 centipoise). A textbook value for viscosity of 0.898 centipoise (cps) was obtained for comparison {7}. These values were very similar. Because of this each individual viscosity value for each viscometer size was used for more precise calculations. The viscosity values for the solvent HAN were also fairly similar. The viscosity values were larger which made a slightly larger viscosity difference than that of water. Viscosity values of 22.5814, 24.1412, 25.875 centistokes were found for HAN. There was no textbook reference for the viscosity of HAN. Due to the slightly larger difference the average value was taken and used as the viscosity of HAN (24.199116 centistokes, or ηab = 40.6545 cps). This difference in solvent viscosity values could account for error.

For HAN / PVA solutions only two different molecular weights were used. This did not allow for much comparison as to the accuracy of the data collected. Another test using Airvol #103 PVA or some other PVA with a different molecular weight would allow for more accurate results. However, these results are comparable. From information provided by Air Products it is given that Airvol #103 PVA has a viscosity range from 3.2 - 4.2 cps. This measurement is given at 20^{0} C for a 4% aqueous solution. Table 1 shows experimental findings of Airvol #103 having an absolute viscosity at 25^{0} C of a 4% aqueous solution of 3.22998 cps. The viscosity given by Air Products for Airvol #107 PVA of a 4% aqueous solution at 20^{0} C is between 5.4 -6.5 cps.{8} Table shows the experimental finding of the absolute viscosity for a 4% aqueous solution at 25^{0} C to be 4.775 cps. These numbers are close to the recommended range. Slight differences can be attributed to temperature difference and errors covered previously.

Conclusion:

The points of sol - gel transitions are dependent of concentration and temperature. Highly concentrated solutions have higher gel points. Solutions with lower concentrations have lower gel points. Problems in obtaining data occurred when the temperature of gelation was lower than the freezing point of water.

From the acquired data it can be concluded that molecular weight does affect the viscosity of solutions. Viscosity is also dependent on temperature and concentration. Intrinsic viscosities vary with molecular weight. An increase in molecular weight creates an increase in viscosity. This is true in comparing PVA / Water solutions of different molecular weights, comparing PVA / HAN solutions of different molecular weights and in comparing water and HAN solutions.

For S-HAN 5 / PVA solutions at 25^{o} C an interaction parameter of -.0015048 was found. For Water / HAN solutions at 25^{o}C an interaction parameter of -.00056709 was found. From this information it can be concluded that water is a better solvent than HAN. Water has a smaller interaction parameter (it is more negative) which means it has more attraction, more solute can be dissolved in it. This parameter also indicates that water does not interact with its solute to the extent HAN does. Water has a higher attraction but has less interaction than HAN which makes water a better solvent.

References

1. R.J.Young and P.A Lovell, Introduction to Polymers. Chapman and Hall, 1981.

2. W. Van Krevelen, Properties of Polymers. Elsevier, 1990.

3. J. Brandrup and E. H. Immergut, Polymer Handbook. John Wiley and Sons, 1989.

4. Komatsu, Insue, Miyasaka, J.Polym. Sci., 24, 303 (1986).

5. Fred W. Billmeyer, Textbook of Polymer Science. Wiley and Sons Inc., 1962.

6. Max S. Peters and Klaus D. Timmerhaus, Plant Design and Economics for Chemical Engineers. McGraw-Hill, Inc., 1991.

7. L.H. Sperling, Introduction to Physical Polymer Science. John Wiley and Sons, 1986.

8. Air Products and Chemicals, Inc., MSDS form. 1995.

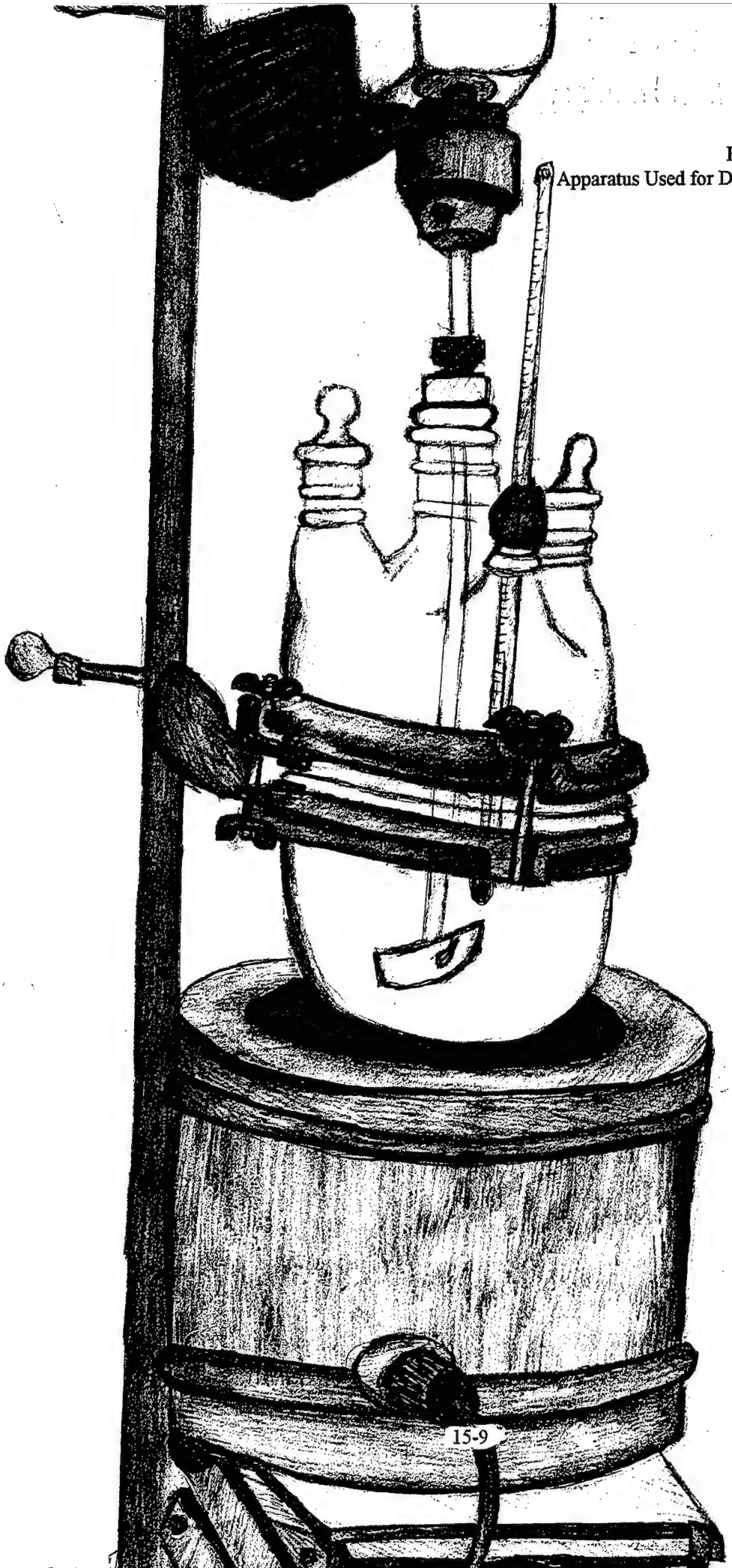

Figure 1
Apparatus Used for Dissolving Solutions

Results

Figure 2

Sol / Gel Transition Behavior of (PVA) in water (H_2O)
Temperature vs. Concentration

Temperature	.3	.5	.7	1	2	3	4	5	6	7
20	s	s	s	s	s	s	s	s	s	s
10	s	s	s	s	s	s	s	s	s	s
9	s	s	s	s	s	s	s	s	s	s
8	s	s	s	s	s	s	s	s	s	s
7	s	s	s	s	s	s	s	s	s	s
6	s	s	s	s	s	s	s	s	s	s
5	s	s	s	s	s	s	s	s	s	s
4	s	s	s	s	s	s	s	s	s	s
3	s	s	s	s	s	s	s	s	s	s
2	s	s	s	s	s	s	s	s	s	s
1	s	s	s	s	s	s	s	s	s	s
0	s	s	s	s	s	s	s	s	s	s
-1	s	s	s	s	s	s	s	s	s	s
-2	s	s	s	s	s	s	s	s	s	s
-3	s	s	s	s	s	s	s	s	G	G
-4	s	s	s	s	s	s	s	s	G	G
-5	s	s	s	s	s	s	s	G	G	G
-6	s	s	s	s	s	s	s	G	G	G
-7	s	s	s	s	s	s	s	G	G	G
-8	s	s	s	s	s	s	s	G	G	G
-9	s	*	s	s	s	s	s	G	*	G
-10	s	*	s	s	s	s	s	G	*	G
-11	s	*	s	s	s	s	s	G	*	G
-12	s	*	s	s	s	s	s	G	*	G
-13	s	*	s	s	*	s	G	G	*	G
-14	s	*	s	s	*	s	G	G	*	G
-15	*	*	s	s	*	s	G	G	*	G
-16	*	*	*	*	*	*	*	G	*	G
-17	*	*	*	*	*	*	*	*	*	G
-18	*	*	*	*	*	*	*	*	*	*

Concentration (wt.%)

s - sol G - gel * - froze / crystallized

Table 1
Viscosity Calculations

Polymer conc. (%)	Time (sec)	Density of Solution	Kinematic Viscosity	Viscosity	Relative Viscosity	Reduced Viscosity	Inherent Viscosity
			PVA / WATER				
0.003	474.7	1.0032995	1.229	1.233055086	1.311523539	103.84118	90.39648939
0.005	608.3	1.0038325	1.575	1.581036188	1.681649263	136.32985	103.9550032
0.007	731.3	1.0043655	1.894	1.902268257	2.023323715	146.1891	100.6773661
0.01	39	1.005165	2.703	2.716960995	3.015612144	201.56121	110.3802842
0.02	133	1.00783	9.2176	9.289773808	10.31091531	465.54577	116.6601536
0.03	336.67	1.010495	79.656	80.49198972	68.04056612	2234.6855	140.6701363
0.04	399.67	1.01316	94.562	95.80643592	80.98599824	1999.65	109.856907
			AIRVOL#103				
0.003	211.333	1.0032995	0.97255	0.975758929	1.137911287	45.970429	43.06479254
0.005	234.333	1.0038325	1.0784	1.082532968	1.262429117	52.485823	46.60754716
0.007	246	1.0043655	1.132092	1.137034148	1.325987344	46.569621	40.30819248
0.01	244.333	1.005165	1.2442	1.250626293	1.458456318	45.845632	37.73785602
0.02	25	1.00783	1.7326	1.746166258	1.93810665	46.905333	33.08557715
0.03	33	1.010495	2.287065	2.311067747	2.565102692	52.17009	31.39995046
0.04	46	1.01316	3.18803	3.229984475	3.585027692	64.625692	31.91915496
			Airvol #107				
0.003	223.333	1.0032995	1.02778	1.03117116	1.202531965	67.510655	61.47643496
0.005	251	1.0038325	1.155102	1.159528928	1.352220325	70.444065	60.34958528
0.007	261	1.0043655	1.201122	1.206365498	1.406840231	58.120033	48.76374553
0.01	305.333	1.005165	1.405142	1.412399558	1.647113188	64.711319	49.90241724
0.02	31	1.00783	2.148455	2.165277403	2.403286923	70.164346	43.84186758
0.03	46	1.010495	3.18803	3.221488375	3.575597692	85.853256	42.47107829
0.04	68	1.01316	4.71274	4.774759658	5.299606154	107.49015	41.69081268

Table 1 (cont.)
Viscosity Calculations

			PVA / HAN				
0.00504	543.667	1.68895606	37.679	63.63817538	2.629785338	323.37011	191.845679
0.00839	183	1.68757921	43.2978	73.06846712	3.019482917	240.70118	131.7146123
0.01174	280.333	1.68620236	66.327	111.8407439	4.621709324	308.49313	130.3888092
0.01676	421.333	1.68413914	99.687	167.8867784	6.937756868	354.28144	115.5715098
0.03344	60	1.67728366	338.724	568.1362304	23.47767389	672.17924	94.37948332
0.05003	156	1.67046517	880.6824	1471.149275	60.7938045	1195.159	82.10049738
			PVA#107/HAN				
0.00825	455	1.68763675	31.5338	53.21759975	2.199165244	145.35336	95.52458836
0.01375	167	1.68537625	39.5122	66.59292347	2.751887411	127.40999	73.62087328
0.01925	207.333	1.68311575	49.05499	82.56522629	3.411927199	125.29492	63.75466455
0.02749	10	1.67972911	56.4535	94.82658731	3.918615947	106.1701	49.68128472
0.054889	22	1.668468121	124.1977	207.2199032	8.563159765	137.79008	39.12385457

Table 2 - Solvent Viscosities

VISCOSITY MEASUREMENTS / CALCULATIONS FOR KINEMATIC VISCOSITY

S-HAN 5 SOLUTIONS

Elvanol HV:				Airvol #107 PVA:			
Concentration (wt. %)	Average Time (secs)	Viscometer Constant	Kinematic Visc. (Centistokes)	Concentration (wt. %)	Average Time (secs)	Viscometer Constant	Kinematic Visc. (Centistokes)
0.3	543.667	0.069305	37.67884144	0.3	455	0.069305	31.533775
0.5	183	0.2366	43.2978	0.5	167	0.2366	39.5122
0.7	280.333	0.2366	66.3267878	0.7	207.333	0.2366	49.0549878
1	421.333	0.2366	99.6873878	1	10	5.6454	56.454
2	60	5.6454	338.724	2	22	5.6454	124.1988
3	156	5.6454	880.6824				

WATER SOLUTIONS

Elvanol HV:				Airvol #103 PVA:			
Concentration (wt. %)	Average Time (secs)	Viscometer Constant	Kinematic Visc. (Centistokes)	Concentration (wt. %)	Average Time (secs)	Viscometer Constant	Kinematic Visc. (Centistokes)
0.3	474.7	0.00259	1.229473	0.3	211.333	0.004602	0.972554466
0.5	608.3	0.00259	1.575497	0.5	234.333	0.004602	1.07840046
0.7	731.3	0.00259	1.894067	0.7	246	0.004602	1.132092
1	39	0.069305	2.702895	1	244.333	0.004602	1.124420466
2				2	25	0.069305	1.732625
3				3	33	0.069305	2.287065
				4	46	0.069305	3.18803

Airvol #107 PVA:			
Concentration (wt. %)	Average Time (secs)	Viscometer Constant	Kinematic Visc. (Centistokes)
0.3	223.333	0.004602	1.027778466
0.5	251	0.004602	1.155102
0.7	261	0.004602	1.201122
1	305.333	0.004602	1.405142466
2	31	0.069305	2.148455
3	46	0.069305	3.18803
4	68	0.069305	4.71274

Figure 3

DETERMINATION OF INTRINSIC VISCOSITY [n]
AIRVOL #103 PVA-mol. wt. 18 000 / WATER
[n] = 45.093

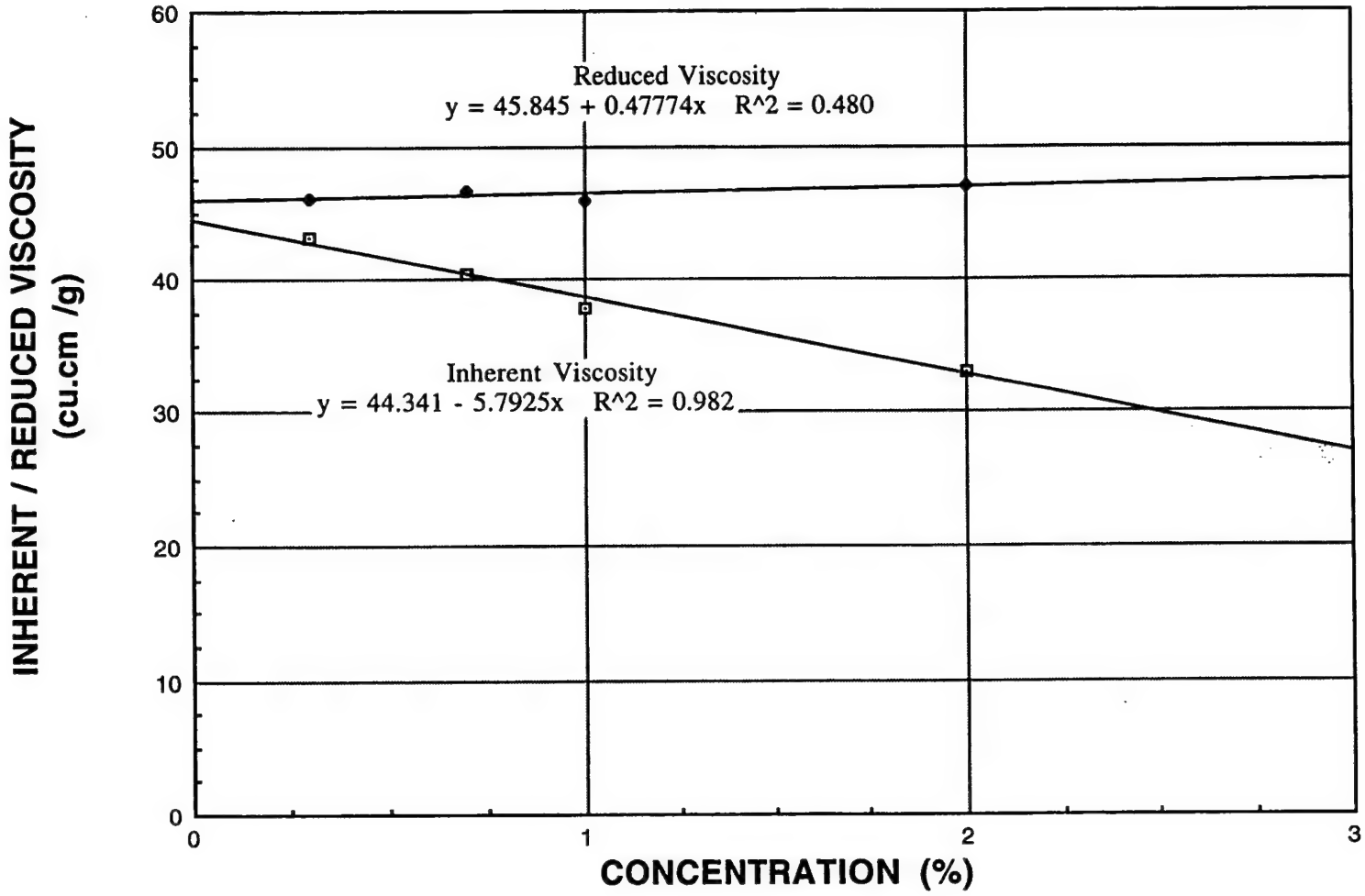

Figure 4

DETERMINATION OF INTRINSIC VISCOSITY [n]
AIRVOL #107 PVA- mol. wt. 21 000 / WATER
[n] = 48.9965

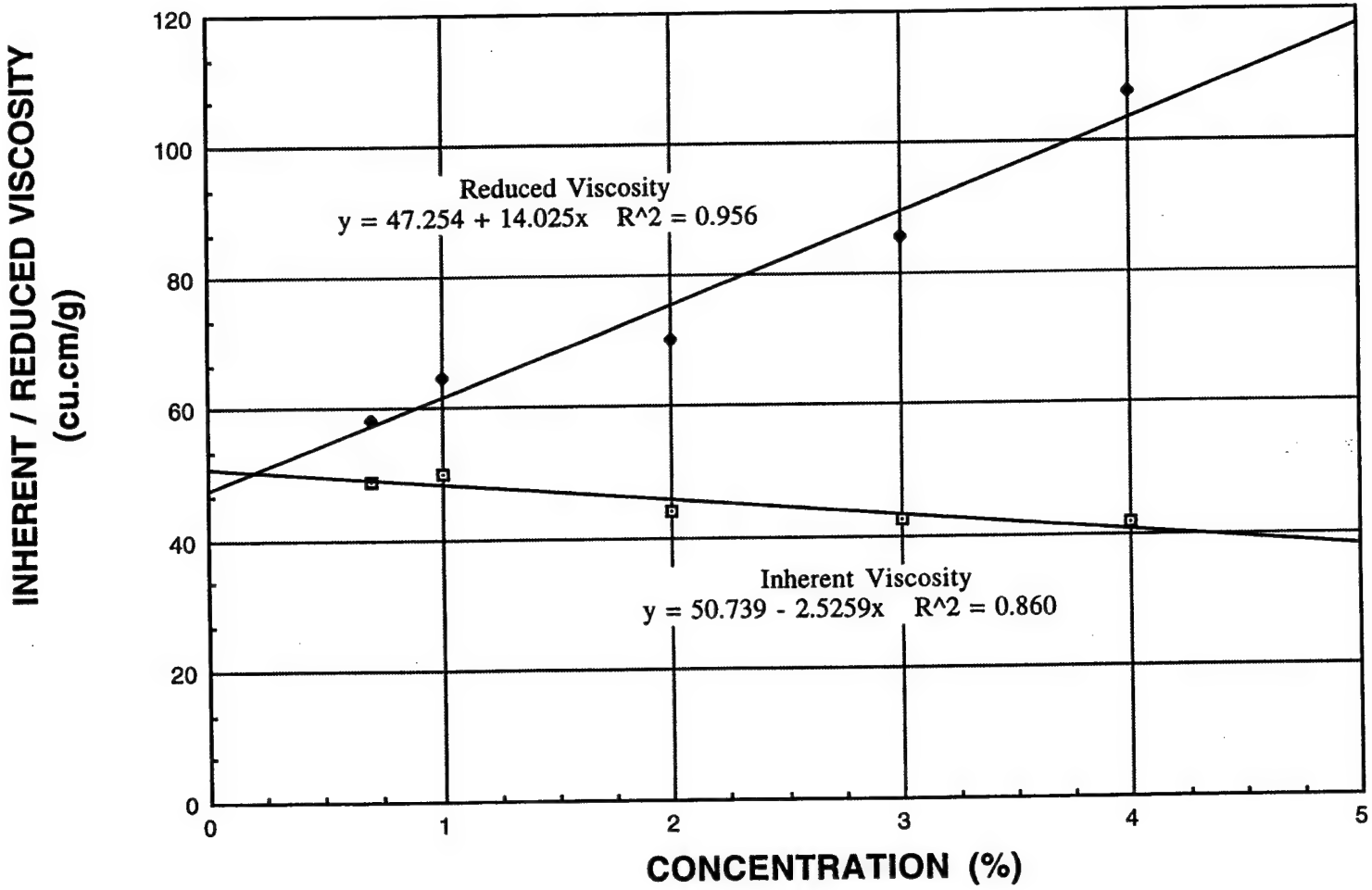

Figure 5

DETERMINATION OF INTRINSIC VISCOSITY [n]
PVA (ELVANOL HV)-mol. wt. 176 000 / WATER
[n] = 74.715

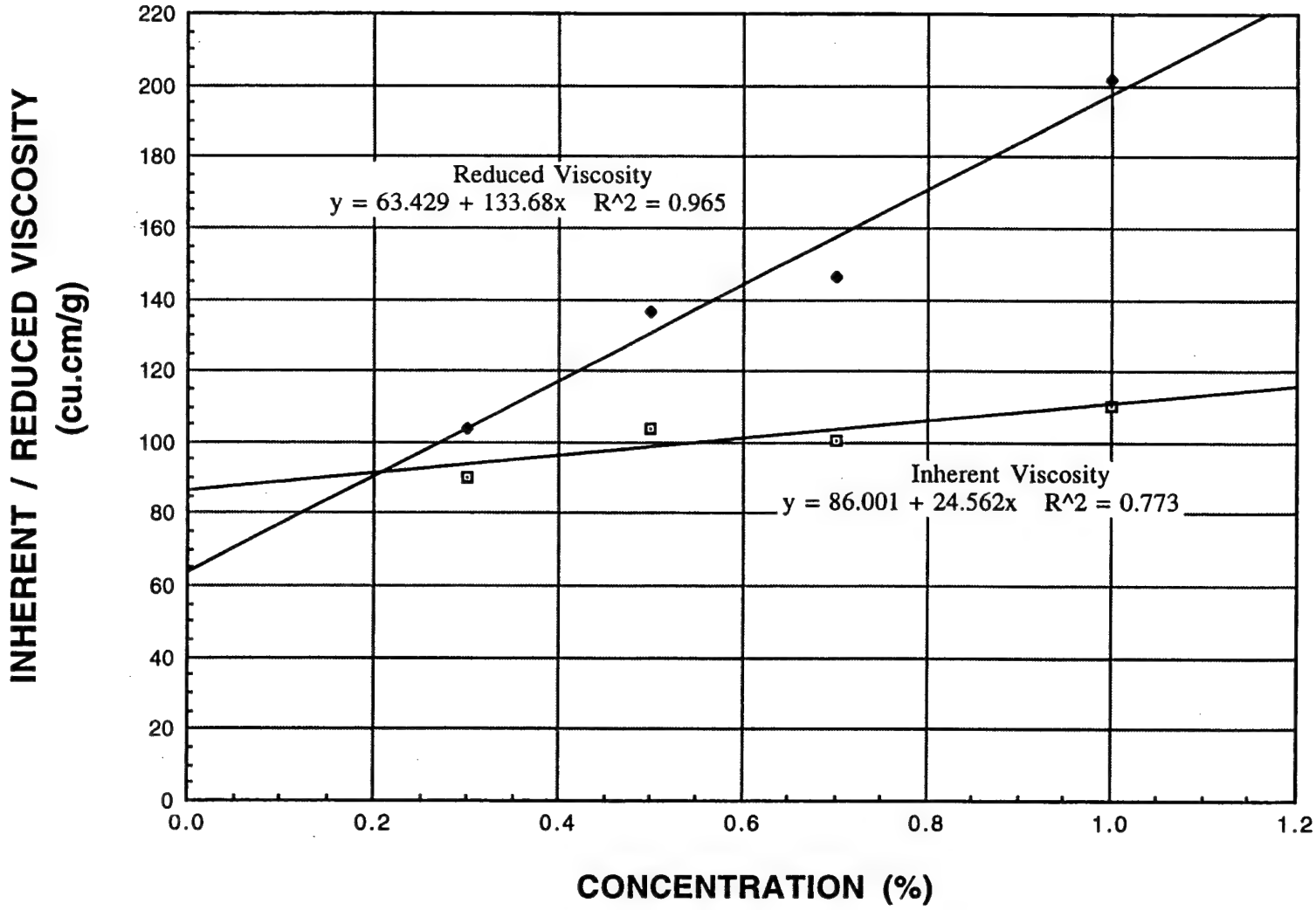

Figure 6

DETERMINING INTERACTION PARAMETER USING STOCKMAYER - FIXMAN EQUATION: [n] = K M^1/2 + BM FOR PVA / WATER SOLUTIONS

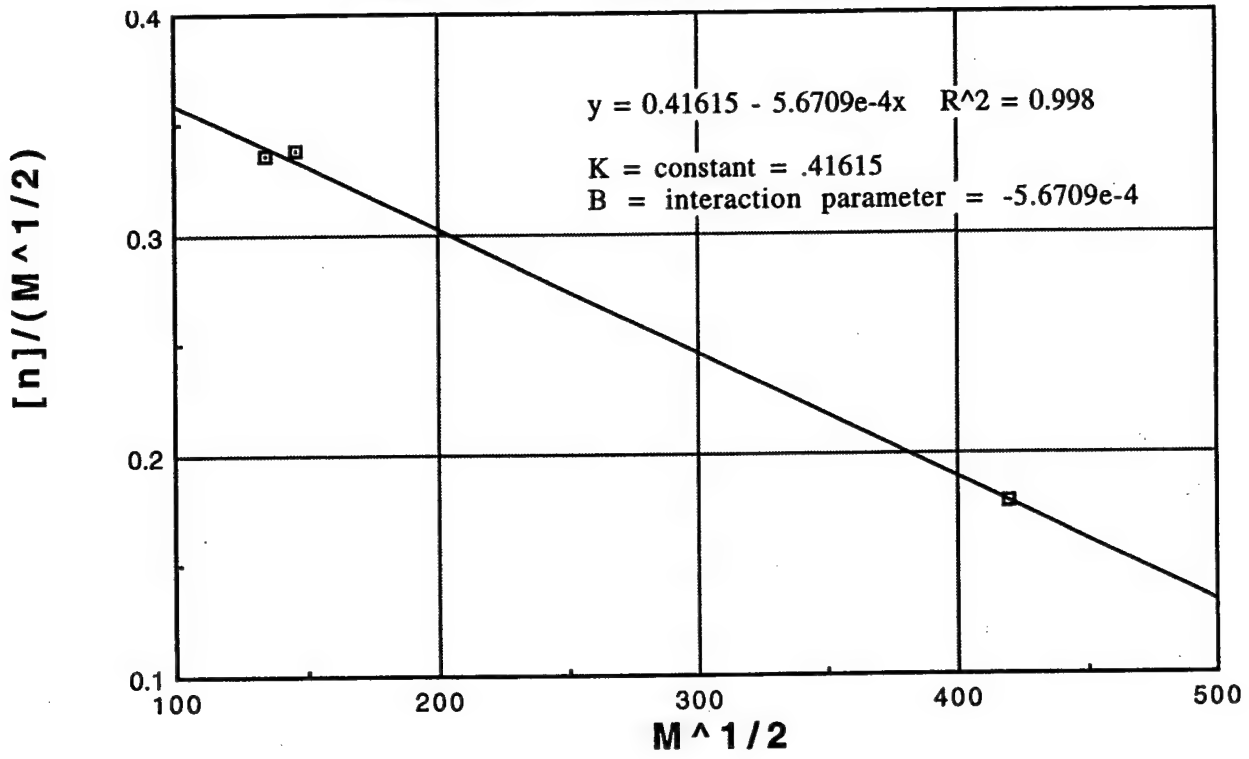

Figure 7

DETERMINATION OF INTRINSIC VISCOSITY [n]
AIRVOL #107 PVA-mol. wt. 21 000 / S-HAN 5
[n] = 110.00

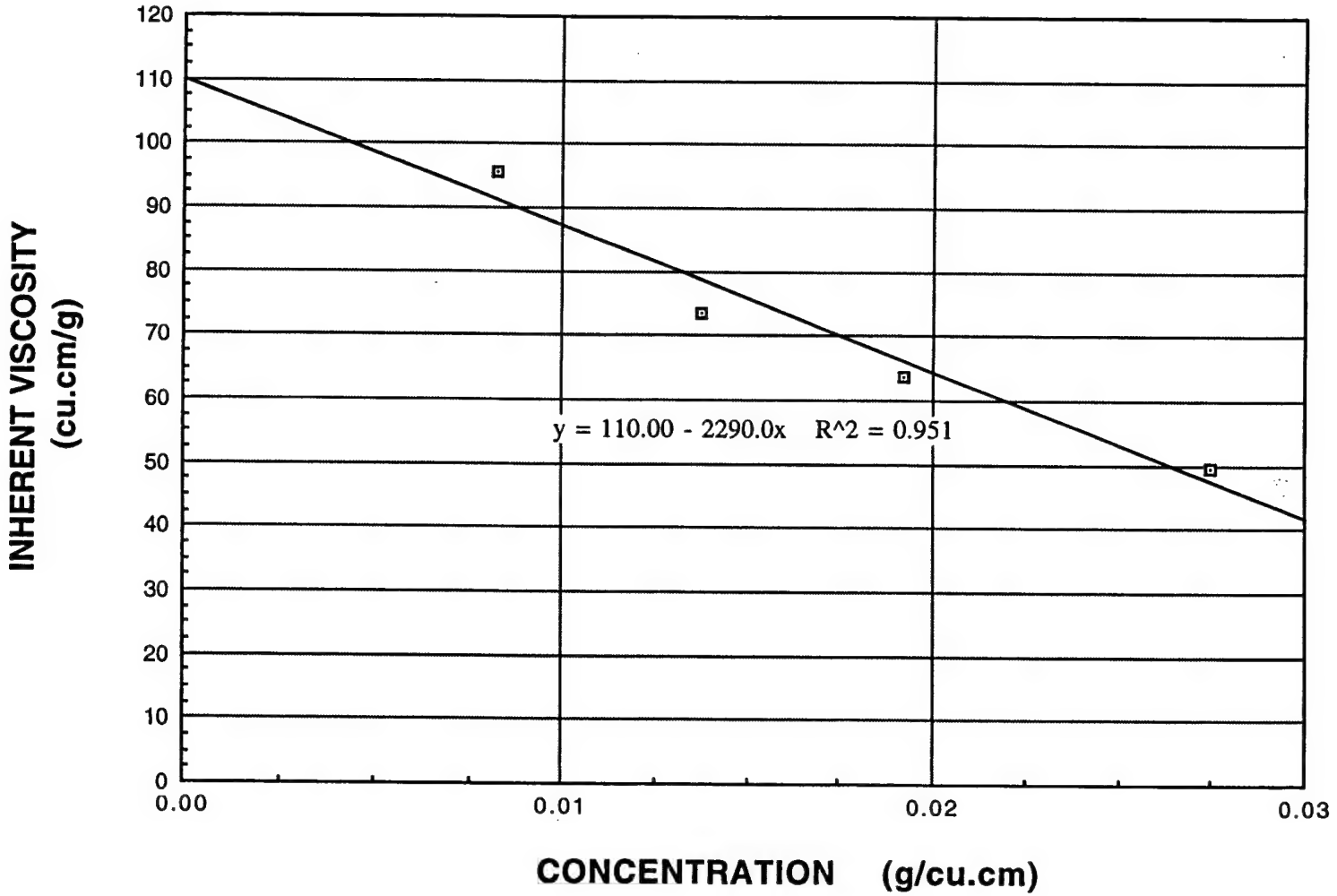

Figure 8

DETERMINATION OF INTRINSIC VISCOSITY [n]
PVA (Elvanol HV)-mol. wt. 176 000 / S-HAN 5
[n] = 145.09

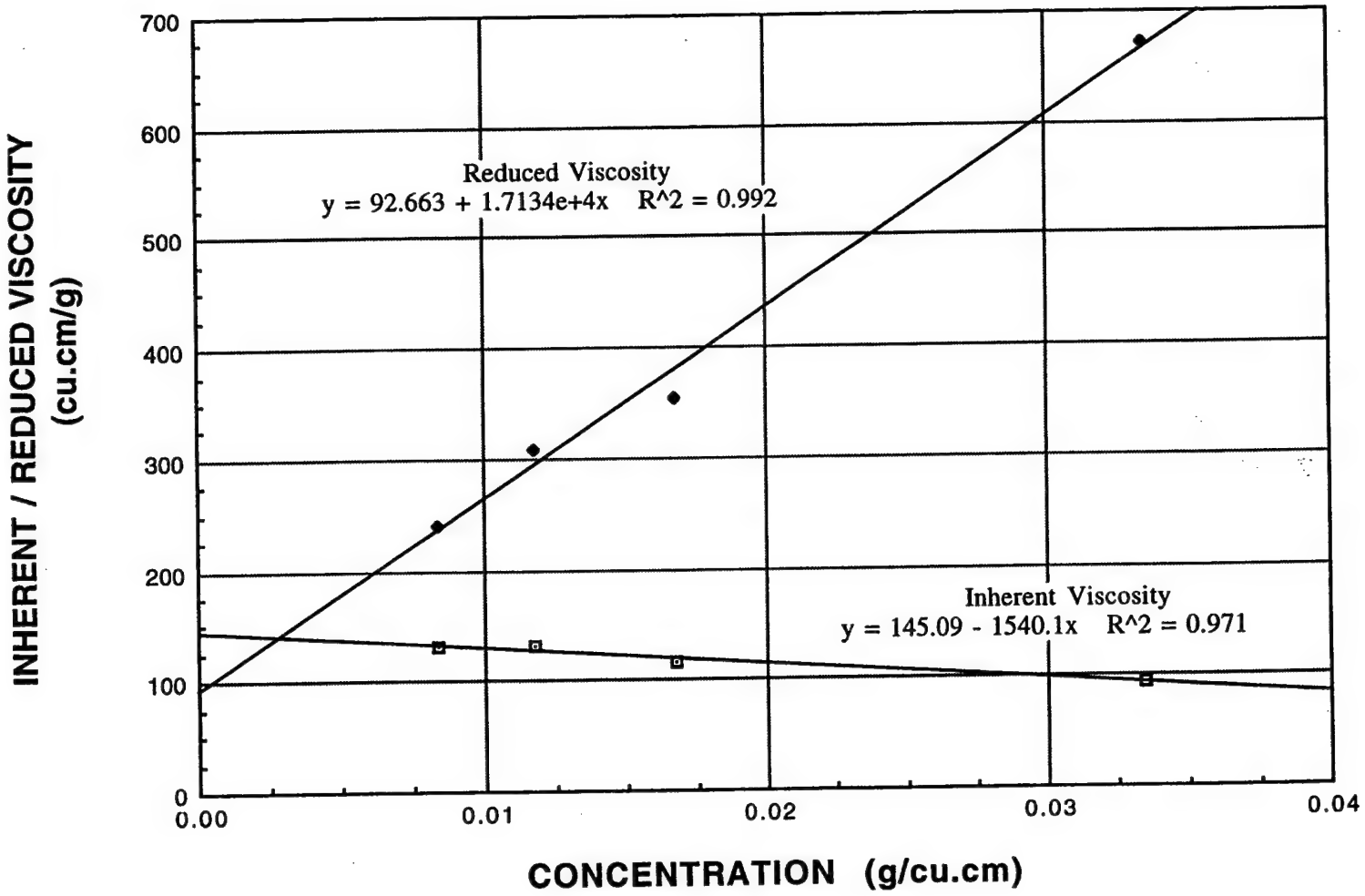

Figure 9

DETERMINING INTERACTION PARAMETER USING STOCKMAYER - FIXMAN EQUATION: [n] = K M^1/2 +BM FOR PVA / S-HAN 5 SOLUTIONS

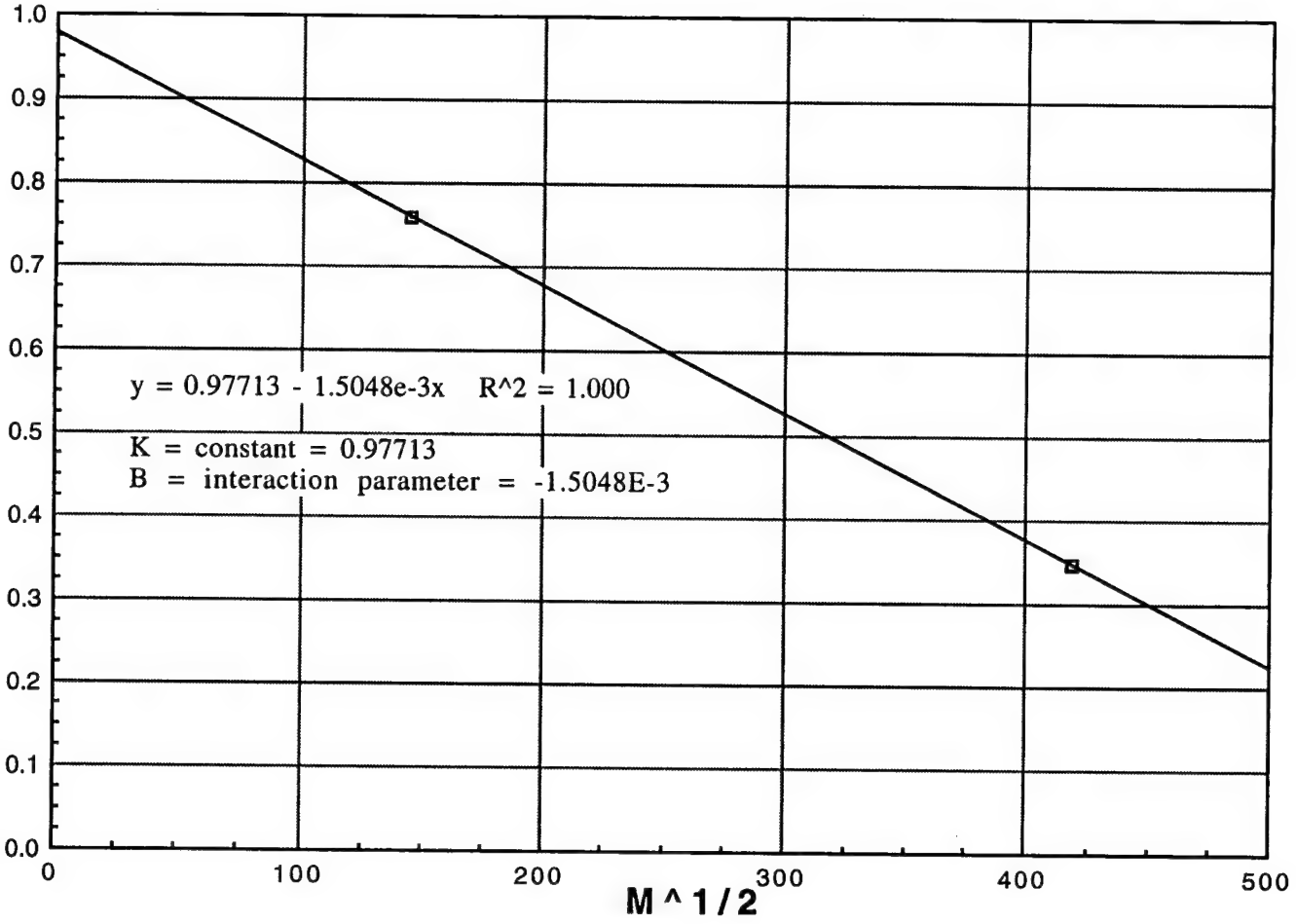

IMPLEMENTATION OF DIAGNOSTIC SOFTWARE FOR PHOTOLUMINESCENCE STUDIES

Lewis P. Orchard

Sandia Preparatory School
532 Osuna NE
Albuquerque, NM 87113

Final Report for:
High School Apprentice Program
Phillips Laboratory

Sponsored by:
Air Force Office of Scientific Research
Bolling Air Force Base, DC

and

Phillips Laboratory

August 1995

IMPLEMENTATION OF DIAGNOSTIC SOFTWARE FOR PHOTOLUMINESCENCE STUDIES

Lewis P. Orchard
Sandia Preparatory School

Abstract

When working with large arrays of data it is necessary to create an automated collection process. My project was to develop a computer data collection program to interface a computer with a digitizer and a spectrometer. This program displays relative intensity verses spectral Wavelength. The data collection software manages to interface with the spectrometer and a digitizer through the IEEE 488 bus.

My Program applies to: the study of wavelength emissions from an Indium Gallium Arsenic semiconductor emitter. To study the wavelengths we fired a twenty watt Yag CW laser onto the sample and recorded the data using a spectrometer. Viewing the emissions over it's spectrum allowed for an understanding of the emitter. It was predetermined that the emitter did not work to its theoretical potential and it was our task to explain this phenomenon.

Introduction-

The study of semiconductor lasers is a blossoming field throughout the scientific community. There are innumerable commercial uses of the semiconductor lasers. The semiconductor laser has already proved itself in the market place as the keystone in many popular new technologies. Some of the more common uses include; laser pointer's, CD player's, and a myriad of medical devices. In the future we can expect semiconductor lasers to operate many new technologies ranging from new communication technology to detectors for gas leaks.

New emitters are under constant development. Studying semiconductor lasers will allow us to both improve laser efficiency and increase power. This will allow developers to envision the full range of technologies that can be created from the increasing understanding of semiconductor lasers.

Our project was to optically pump an Indium Gallium Arsenic semiconductor emitter. By optically pumping the laser we hoped the emissions would explain why the emitter was not performing up to its theoretical potential.

To do this we needed to generate a software package that could manipulate thousands of data points and control the experiment. To complete this I had to control a digitizer, a plotter, a shutter, and a spectrometer. The data recorded through the IEEE 488 bus helped begin to shine light on the problem.

Methodology-

To excite the emitter we optically pumped the semiconductor

emitter. To do this we fired a 20 watt CW yag laser onto the emitter. We were then able to view the wavelength spectrum through a spectrometer. The next big obstacle was obtaining and manipulating the data from the spectrometer on a computer. It also became neccessary to control the experment with a computer. My primary responsibility was to write the program that would both control the experiment and digitize the data.

Discussion of the problem-

My job was to prepare a program designed to run the experiment. This program allowed the scientists to run the experiment without constantly manipulating the equipment while getting more results over a shorter period of time.

The program began by preparing the digitizer to act as a hub between the spectrometer and the computer. Second it would open and close the shutter to take a data and a background set of data points. The program analyzed the difference of the two sets of data points and plotted the results on the screen. You could then manipulate the data, plot the data, or save the data for later manipulation or examination.

Shortly after the creation of the basic program it became evident that the program was going to need to be expanded. Innumerable conflicts appeared in the data caused by the limitations of the equipment that needed to be accounted for.

It quickly became evident that the range of electromagnetic emissions was greater than the total number of Angstroms the spectrometer was capable of viewing on the same frame (102A). So it became necessary to have the program move the spectrometer across the

spectrum. By scanning the spectrometer the program was able to view a predetermined set of Angstroms and by concatenation of the arrays we were able to view the excess of data points created by stepping through the program.

After examining the data it became evident that the spectrometer's detector array did not evaluate the light with the same sensitive across the array. In order to avoid bad data we stepped the spectrometer a fifth of the total 102A. By only stepping in fifths (20.4 A) we were able to average each fifth together after viewing it from five different points on the array. After averaging the sets of data together most of the resolution problems were cleared up.

Results-

The program was able to generate graphs in order to analyze the photoluminescence given by the laser emitter. The graphs allowed us to determine the locations of the photoluminescence peaks across the spectrum. In example A and B you see a single peak given off from the Yag laser. This was used as a diagnostic tool to test the program. Example A displays a spectral window of 204A. In example B you see the concatenation of eleven different steps totaling 1122A across. The Yag laser demonstrates a single mode laser emitting over a narrow spectrum window; all the power is being deposited in a central spike. Example C demonstrates the actual data given off by the emitter across eleven steps 1122A across. In Example C you see the spread of power across the spectrum.

Conclusions-

Throughout the internship my key responsibility was to generate the software to run the experiment and manipulate the data. I managed to complete this project while generating a number of features for reading in and the manipulation of data; including scaling capabilities, plotting, and exporting of data. This software is unique in that it interfaces with a Tektonics digitizer, and a Spex spectrometer, using the IEEE 488 bus.

APPENDIX A

GRAPHS

EXAMPLE A

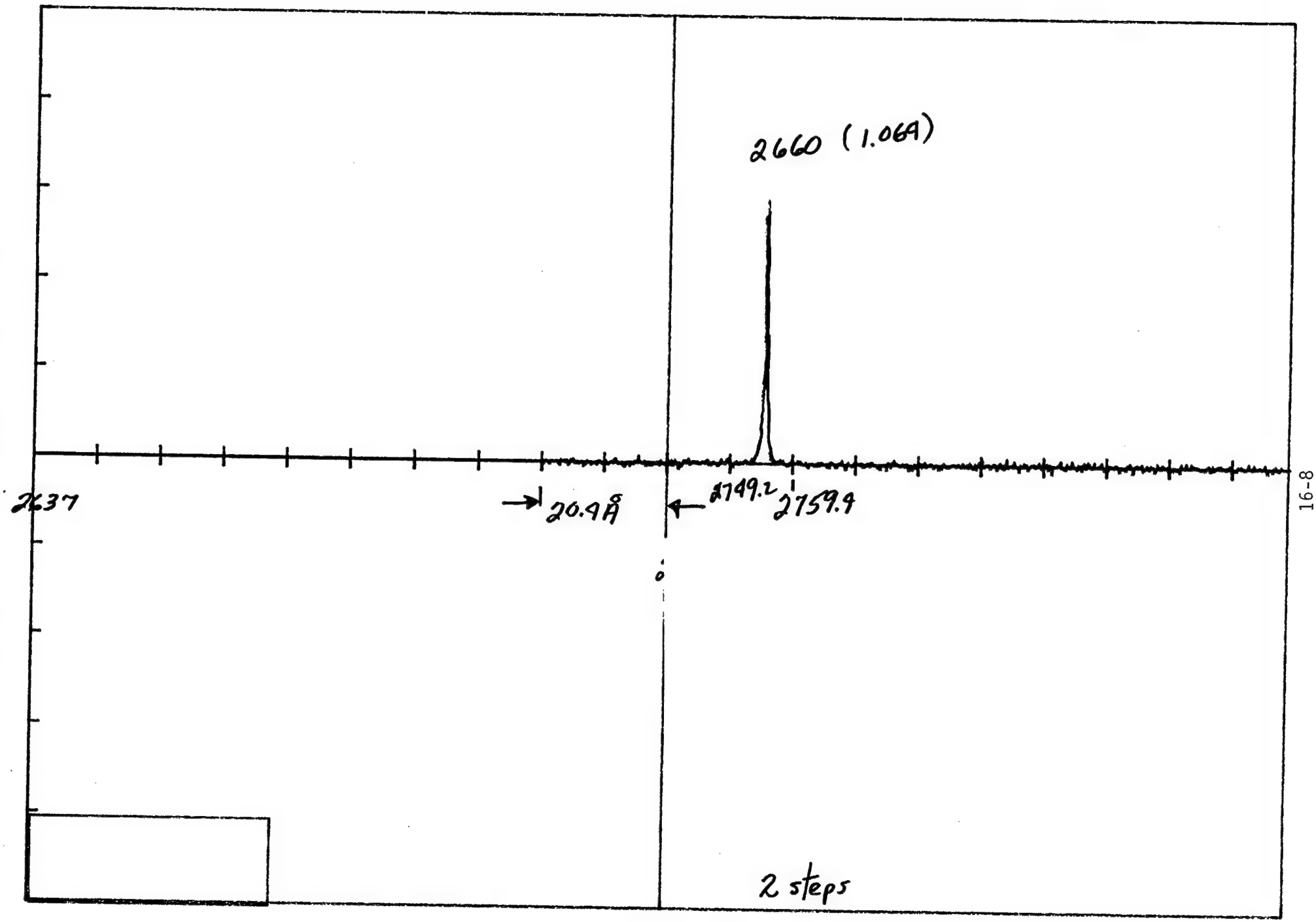

EXAMPLE B

2.0

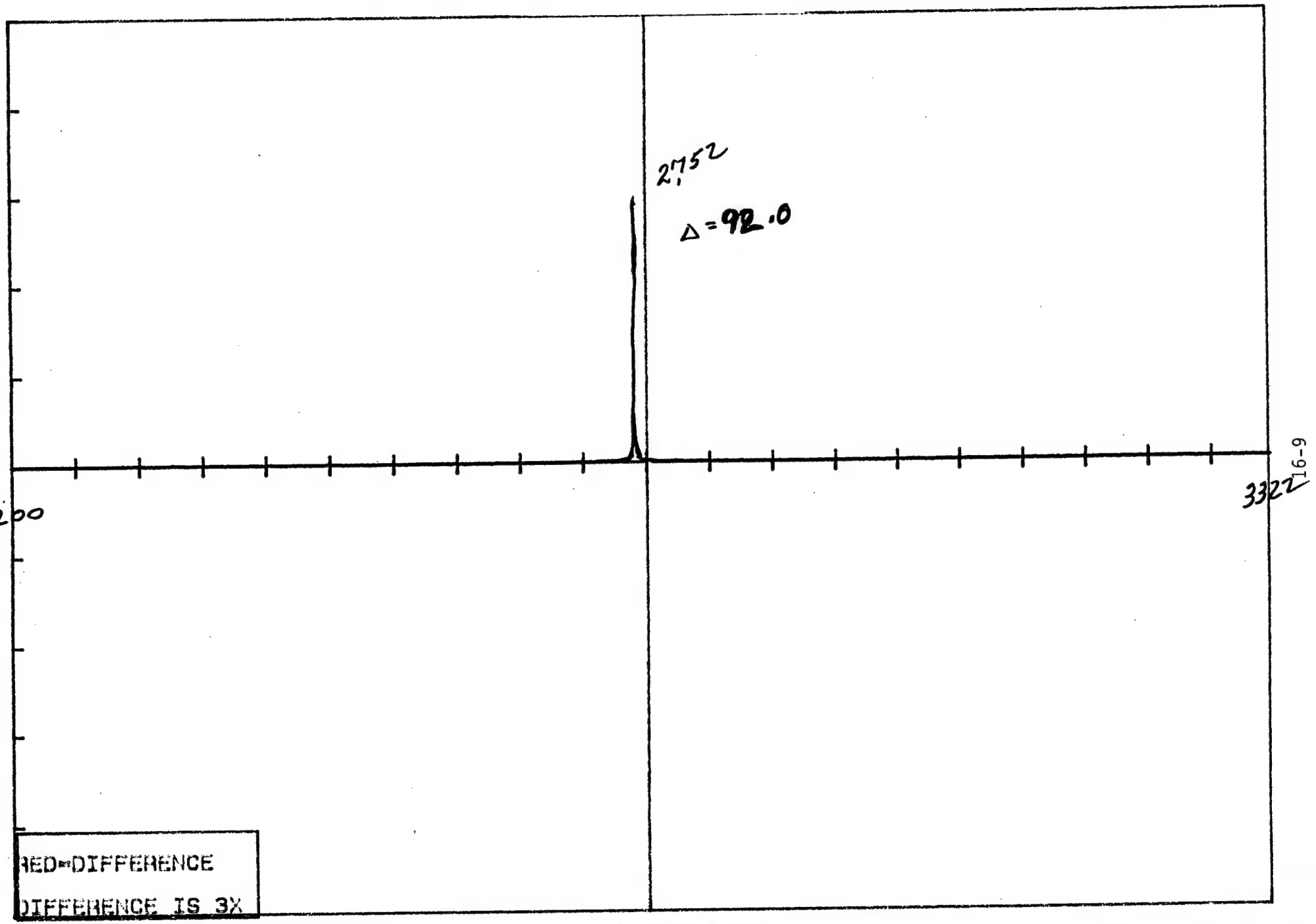

EXAMPLE C

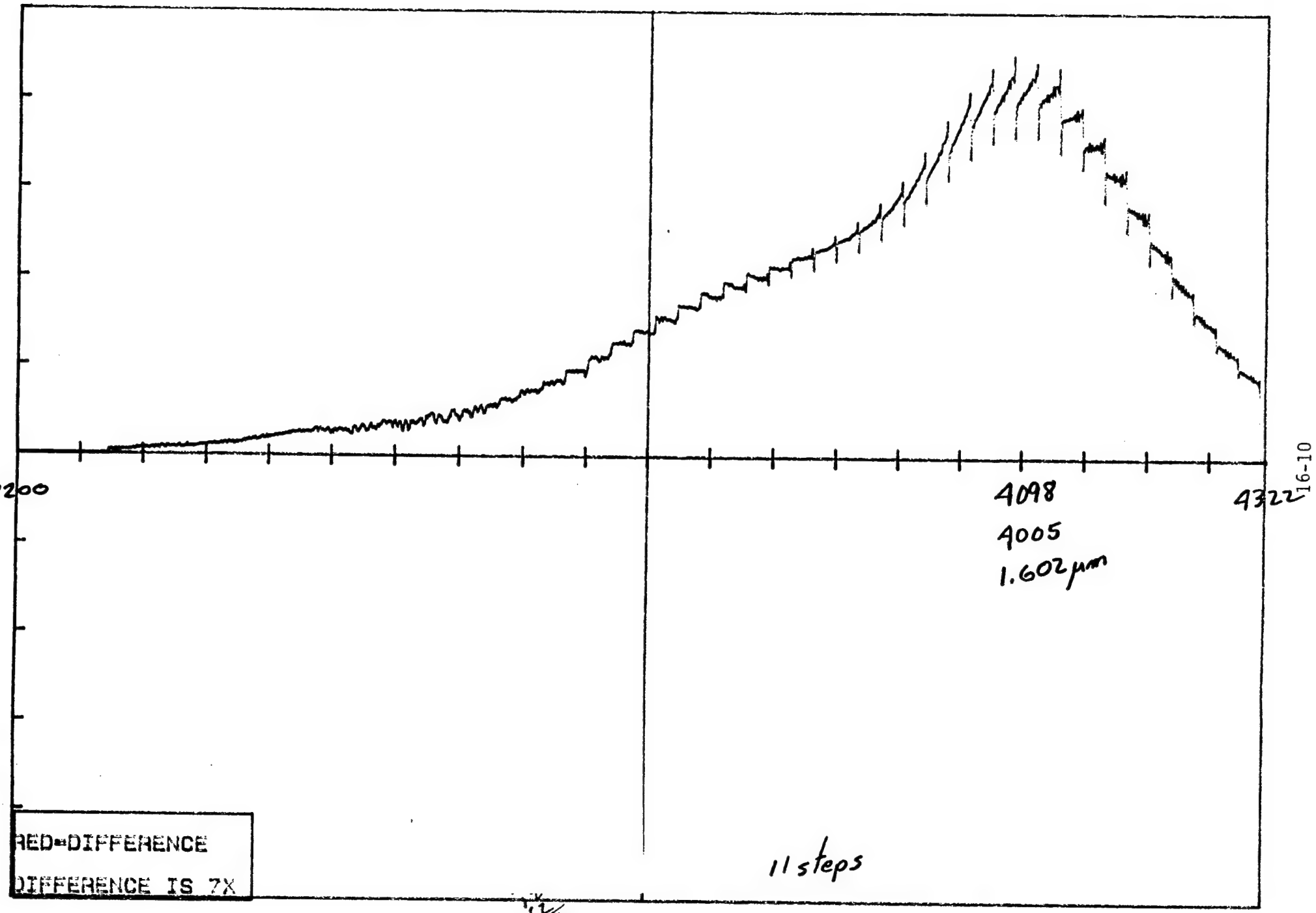

16-10

APPENDIX B

CODE

```
10 CLEAR SCREEN
20 CLEAR 724 !Clears buffer 724 of the digitiser
30 ASSIGN @Tek TO 724;EOL CHR$(13) END !renames port 724 as @Tek
40 ASSIGN @Tek1 TO 724  !renames port 724 as @Tek1 one digit
50 !
60 REM ****COMANDS TO SEE IF THE DIGITISER IS OUT THEIR****
70 !
80 OUTPUT @Tek;"ID?;"  !command to see if the digitiser is out there
90 ENTER @Tek;C$
100 PRINT "DEVICE ID: ";C$
110!
120 REM ********END OF DIGITISER OUT THEIR*****************
130 Ars=995
140 Count6=1
150 Viewsz=102
160!
170 B=SPOLL(724)!statice of buffer 724
180 PRINT "polling status: ";B!output of statice of buffer 724
190 INPUT "Do you want grating(y/n)",Grat$
200 IF Grat$="n" THEN GOTO 480
210 IF Grat$="N" THEN GOTO 480
220 REM ********************INPUT OF GRADING
INFORMATION************************
230!
240 INPUT "Enter total number of A to view",Grating1
250 Step=Grating1/Viewsz
260 PRINT Step
270 Grading=250
280 Gloop=4
290 Stepp=Grading*.02*Gloop
300 PRINT
310 Steps=Grating1/Viewsz
320 Check=Steps-CINT(Steps)
330 Steps=CINT(Steps)
340 IF Check<0 THEN
350 END IF
360 IF Check>0 THEN
370 Steps=Steps+1
380 END IF
390 Step1=(Steps*Viewsz)-Grating1
400 PRINT Step1
410 PRINT "Total number of steps to be taken:";Steps*5
420 INPUT "Enter current spectrometer settings (ang): ",Oldspect
430 Finalspect=Oldspect+Viewsz*Steps
440 Currentspect=Oldspect
450 !
460 REM ********************END OF GRATING************************
470 !
480 REM ************DETERMINING THE DIGITISER SETTINGS**************
490 !
500 PRINT "The follow questions concern the digitisers settings"
510 !!~~~~~~~~~~~~~~~~~~~~~~~~~~~~~~~~~~~~~~~~!!
520 INPUT "Please input the trigger source?  (1 for CH1, 2 for EXT)",Trig
```

```
530 IF Trig=1 THEN
540 PRINT "channel 1 selected"
550 OUTPUT @Tek1;"TSR CH1;" ! telling the digitiser that it needs to use and internal trigger
560 ELSE
570 PRINT "external trigger selected"
580 OUTPUT @Tek1;"TSR EXT;" ! Requesting the digitiser to use an external timer
590 END IF
600 !!~~~~~~~~~~~~~~~~~~~~~~~~~~~~~~~~~~~~~~~~~~~~~~!!
610 INPUT "Please select sample clock? (1 for internal, 2 for external)",Clk
620 IF Clk=1 THEN
630 PRINT "Internal clock selected"
640 OUTPUT @Tek1;"SFA 20000;" !output neccessary for the internal clock
650 ELSE
660 PRINT "External clock selcected"
670 OUTPUT @Tek1;"SFA EXT;" !output neccessary for the external clock
680 END IF
690 !!~~~~~~~~~~~~~~~~~~~~~~~~~~~~~~~~~~~~~~~~~~~~~~!!
700 IF Grat$="y" THEN
710 INPUT "Enter the total # of points to average",Avg
720 IF 2005*Steps/Avg>32767 THEN
730 PRINT "ERROR: Your array size is to large please increase the total # of points to average"
740 GOTO 710
750 END IF
760 ALLOCATE Combined(1:2005*Steps/Avg)
770 END IF
780 IF Grat$="Y" THEN
790 INPUT "Enter the total # of points to average",Avg
800 IF 2005*Steps/Avg>32767 THEN
810 PRINT "ERROR: Your array size is to large please increase the total # of points to average"
820 GOTO 790
830 END IF
840 ALLOCATE Combined(1:2005*Steps/Avg)
850 END IF
860 PRINT "AQUIRING CHANNEL 1 ONLY"
870 OUTPUT 724;"VMO CH1;" ! Aquiring channel 1 command to digitiser
880 INPUT "Input the Voltage Range (.1V to 50V; 1,2,5 sequence): ",Vrange
890 OUTPUT @Tek1;"IR1 ";Vrange;";" !outputing the voltage range
900 INPUT "Enter the DC offset(-99 to 99):",Offset
910 OUTPUT @Tek1;"OF1 ";Offset;";" !output of the DC offset
920 INPUT "# of times to loop throught the experiment",Loop
930 OUTPUT 724;"CP1 DC;" !setting ch1 output to DC
940 OUTPUT 724;"TCP DC;" !setting trigger to DC
950 OUTPUT 724;"TLV +50;" !dettermines trigger level
960 OUTPUT 724;"RMO POS;" !sets the record mode to posttigger
970 OUTPUT 724;"TSL POS;" !sets slope to positive
980 !
990 REM ****************ARRAY DECLARATIONS*********************
1000 Count11=1
1010!
1020 ALLOCATE Temp(1:2005)!Temorary data storage
1030 ALLOCATE Specstd(1:2005)!data taken with the laser on
1040 ALLOCATE Background(1:2005)!data taken without the laser on
1050 ALLOCATE Answer(1:2005)!the deffernce between Specstd-Background
```

```
1060 ALLOCATE Answer2(1:2005)!average of answers
1070 ALLOCATE Fith1(199)
1080 ALLOCATE Cfith1(199)
1090 ALLOCATE Fith2(199)
1100 ALLOCATE Cfith2(199)
1110 ALLOCATE Fith3(199)
1120 ALLOCATE Cfith3(199)
1130 ALLOCATE Fith4(199)
1140 ALLOCATE Cfith4(199)
1150 ALLOCATE Fith5(199)
1160 ALLOCATE Cfith5(199)
1170 ALLOCATE Ccomfith(199)
1180!
1190 REM ************************************************
1200!
1210 REM ***************MAIN LOOP STARTS HERE*************************
1220!
1230 FOR Count=1 TO Loop
1240 IF Grat$="n" THEN GOTO 1270
1250 IF Grat$="N" THEN GOTO 1270
1260 FOR Count5=1 TO Steps*5
1270 CLEAR 724
1280 OUTPUT 724;"RES;"
1290 !
1300 !
1310 REM ************INPUT OF BACKGROUND*********************
1320 OUTPUT 724;"TMO SGL;"
1330 OUTPUT @Tek1;"ARM MAN;"
1340 OUTPUT @Tek1;"ARM MAN;"
1350 PRINT "Recieving Data"
1360 OUTPUT @Tek;"READ CH1, 15,2004"
1370 ENTER @Tek USING "#,1A";Var1$
1380 ENTER @Tek USING "#,B";Dcount1
1390 ENTER @Tek USING "#,B";Dcount2
1400 ENTER @Tek USING "%,B";Temp(*)
1410 FOR N=1 TO Ars
1420 M=N*2
1430 Background(N)=((Temp(M-1)*256+Temp(M))-512)*Vrange/512 !minupulation of back
1440 NEXT N
1450 REM ************************************************
1460 WAIT 1/2
1470 CLEAR 724
1480 OUTPUT 724;"RES;"
1490 OUTPUT 724;"TMO SGL;"
1500 OUTW &H213,&HFF ! Opening the Shutter
1510 BEEP
1520 WAIT 1/4
1530 BEEP
1540 REM ***************Data with the laser**************
1550 PRINT "Receiving signal 2 NOW"
1560 OUTPUT @Tek1;"ARM MAN;"
1570 OUTPUT @Tek1;"ARM MAN;"
1580 OUTPUT @Tek;"READ CH1, 15,2004"
```

```
1590 ENTER @Tek USING "#,1A";Var1$
1600 ENTER @Tek USING "#,B";Dcount1
1610 ENTER @Tek USING "#,B";Dcount2
1620 ENTER @Tek USING "%,B";Temp(*)
1630 FOR N=1 TO Ars
1640 M=N*2
1650 Specstd(N)=((Temp(M-1)*256+Temp(M))-512)*Vrange/512 ! Minipulation of background
1660 NEXT N
1670 REM ************************************************
1680 !
1690 !
1700 REM **********SUBTRACTING THE BACKGROUND FROM THE DATA***********
1710 FOR N=1 TO Ars
1720 Answer(N)=Specstd(N)-Background(N)
1730 NEXT N
1740 REM ************************************************************
1750 !
1760 Count10=1
1770 Count12=1
1780 REPEAT
1790 IF Count10<200 THEN Fith1(Count12)=Answer(Count10)
1800 IF 199<Count10 AND Count10<399 THEN Fith2(Count12)=Answer(Count10)
1810 IF 398<Count10 AND Count10<598 THEN Fith3(Count12)=Answer(Count10)
1820 IF 597<Count10 AND Count10<797 THEN Fith4(Count12)=Answer(Count10)
1830 IF 796<Count10 AND Count10<996 THEN Fith5(Count12)=Answer(Count10)
1840 IF Count12=199 THEN Count12=0
1850 Count10=Count10+1
1860 Count12=Count12+1
1870 UNTIL Count10=996
1880 IF Count11=6 THEN Count11=1
1890 SELECT Count11
1900 CASE 1
1910 FOR N=1 TO 199
1920 Ccomfith(N)=Cfith5(N)/5
1930 Cfith1(N)=Cfith1(N)+Fith1(N)
1940 Cfith2(N)=Cfith2(N)+Fith2(N)
1950 Cfith3(N)=Cfith3(N)+Fith3(N)
1960 Cfith4(N)=Cfith4(N)+Fith4(N)
1970 Cfith5(N)=Fith5(N)
1980 NEXT N
1990 CASE 2
2000 FOR N=1 TO 199
2010 Ccomfith(N)=Cfith1(N)/5
2020 Cfith2(N)=Cfith2(N)+Fith1(N)
2030 Cfith3(N)=Cfith3(N)+Fith2(N)
2040 Cfith4(N)=Cfith4(N)+Fith3(N)
2050 Cfith5(N)=Cfith5(N)+Fith4(N)
2060 Cfith1(N)=Fith5(N)
2070 NEXT N
2080 CASE 3
2090 FOR N=1 TO 199
2100 Ccomfith(N)=Cfith2(N)/5
2110 Cfith3(N)=Cfith3(N)+Fith1(N)
```

```
2120 Cfith4(N)=Cfith4(N)+Fith2(N)
2130 Cfith5(N)=Cfith5(N)+Fith3(N)
2140 Cfith1(N)=Cfith1(N)+Fith4(N)
2150 Cfith2(N)=Fith5(N)
2160 NEXT N
2170 CASE 4
2180 FOR N=1 TO 199
2190 Ccomfith(N)=Cfith3(N)/5
2200 Cfith4(N)=Cfith4(N)+Fith1(N)
2210 Cfith5(N)=Cfith5(N)+Fith2(N)
2220 Cfith1(N)=Cfith1(N)+Fith3(N)
2230 Cfith2(N)=Cfith2(N)+Fith4(N)
2240 Cfith3(N)=Fith5(N)
2250 NEXT N
2260 CASE 5
2270 FOR N=1 TO 199
2280 Ccomfith(N)=Cfith4(N)/5
2290 Cfith5(N)=Cfith5(N)+Fith1(N)
2300 Cfith1(N)=Cfith1(N)+Fith2(N)
2310 Cfith2(N)=Cfith2(N)+Fith3(N)
2320 Cfith3(N)=Cfith3(N)+Fith4(N)
2330 Cfith4(N)=Fith5(N)
2340 NEXT N
2350 END SELECT
2550 REM ************************************************
2560 FOR N=1 TO Ars
2570 Answer2(N)=Answer(N)+Answer2(N)
2580 NEXT N
2590 REM ************************************************
2600 OUTW &H213,&H80 !close shutter
2610 IF Grat$="y" OR Grat$="Y" THEN
2620 Comp=1
2625 Times=1
2630 Avg1=0
2640 REPEAT
2650 Avg1=Avg1+Ccomfith(Comp)
2660 Comp=Comp+1
2670 UNTIL Comp=Avg*Times
2680 Combined(Count6)=Avg1/Avg
2690 Count6=Count6+1
2700 IF Comp>(Ars*Steps/Avg)-Step1 THEN GOTO 2820
2710 IF Comp+Avg>199 THEN GOTO 2820
2720 IF Comp<199 THEN
2730 Times=Times+1
2740 Avg1=0
2750 GOTO 2640
2760 END IF
2770 END IF
2780 REM FOR N=1 TO Ars
2790 REM Answer2(N)=0
2800 REM Answer(N)=0
2810 REM NEXT N
2820 IF Grat$="n" THEN GOTO 2930
```

```
2830 IF Grat$="N" THEN GOTO 2930
2840 REM ******************MOVING GRADING*********************
2850 FOR Mv=1 TO Gloop
2860 OUTPUT 11 USING "#,B";Grading
2870 NEXT Mv
2880 OUTPUT 11 USING "#,B";20
2890 CALL Pollspect
2900 Currentspect=Currentspect+20.4
2910 PRINT "Wavelength(ang): ",Oldspect,Currentspect,"[";Finalspect;"]"
2920 REM ****************************************************
2930 IF Grat$="n" THEN GOTO 2970
2940 IF Grat$="N" THEN GOTO 2970
2950 Count11=Count11+1
2960 NEXT Count5
2970 NEXT Count
2980 REM ****************** END MAIN LOOP *************************
2990 !
3000 !
3010 FOR N=1 TO 796/Avg
3020 Combined(N)=0
3030 NEXT N
3040 REM ****************** LOOP TO DETERMINE THE AVERAGE*********************
3050 FOR Count2=1 TO Ars
3060 Answer2(Count2)=Answer2(Count2)/Loop
3070 NEXT Count2
3080 REM ******************************************************************
3090 !
3100 !
3110 REM ******************PLOTING TO SCREEN AND TO PLOTTER******************
3120 Scale=1
3130 CLEAR SCREEN
3140 WINDOW 0,995,-Vrange,Vrange
3150 PEN 7
3160 FRAME
3170 AXES 50,1
3180 GRID 500,600
3190 PEN 2
3200 IF Grat$="Y" THEN Grat$="y"
3210 IF Grat$="y" THEN
3220 PLOT 1,Combined(1)*Scale,-2
3230 FOR Count3=1 TO Ars*Steps/Avg
3240 PLOT Count3,Combined(Count3)*Scale,1
3250 NEXT Count3
3260 PEN 7
3270 IF Plot$="Y" THEN Plot$="y"
3280 IF Plot$="y" THEN
3290 OUTPUT 705;"IN;PA100,1000;"
3300 OUTPUT 705;"EA2000,300;"
3310 PEN 2
3320 OUTPUT 705;"IN;PA100,700;"
3330 OUTPUT 705;"SI;LBRED=DIFFERENCE",CHR$(3)
3340 OUTPUT 705;"PA100,350;"
3350 OUTPUT 705;"SI;LBDIFFERENCE IS";Scale;"X",CHR$(3)
```

```
3360 OUTPUT 705;"PG 1"
3370 END IF
3380 ELSE
3390 PLOT 1,Answer2(1)*Scale,-2
3400 FOR Count3=1 TO 995
3410 PLOT Count3,Answer2(Count3)*Scale,1
3420 NEXT Count3
3430 PEN 1
3440 PLOT 1,Background(1),-2
3450 FOR Count4=1 TO 995
3460 PLOT Count4,Background(Count4),1
3470 NEXT Count4
3480 PEN 6
3490 PLOT 1,Specstd(1),-2
3500 FOR Count5=1 TO 995
3510 PLOT Count5,Specstd(Count5),1
3520 NEXT Count5
3530 IF Plot$="y" THEN
3540 PEN 7
3550 OUTPUT 705;"IN;PA100,1000;"
3560 OUTPUT 705;"EA2000,300;"
3570 PEN 2
3580 OUTPUT 705;"IN;PA100,700;"
3590 OUTPUT 705;"SI;LBRED=DIFFERENCE",CHR$(3)
3600 OUTPUT 705;"PA100,850;"
3610 PEN 1
3620 OUTPUT 705;"SI;LBGREEN=BACKGROUND",CHR$(3)
3630 OUTPUT 705;"PA100,550;"
3640 PEN 6
3650 OUTPUT 705;"SI;LBPURPLE=SIGNAL",CHR$(3)
3660 OUTPUT 705;"PA100,350;"
3670 PEN 2
3680 OUTPUT 705;"SI;LBDIFFERENCE IS";Scale;"X",CHR$(3)
3690 OUTPUT 705;"PG 1"
3700 END IF
3710 IF Plot$="Y" THEN
3720 PEN 7
3730 OUTPUT 705;"IN;PA100,1000;"
3740 OUTPUT 705;"EA2000,300;"
3750 PEN 2
3760 OUTPUT 705;"IN;PA100,700;"
3770 OUTPUT 705;"SI;LBRED=DIFFERENCE",CHR$(3)
3780 OUTPUT 705;"PA100,850;"
3790 PEN 1
3800 OUTPUT 705;"SI;LBGREEN=BACKGROUND",CHR$(3)
3810 OUTPUT 705;"PA100,550;"
3820 PEN 6
3830 OUTPUT 705;"SI;LBPURPLE=SIGNAL",CHR$(3)
3840 OUTPUT 705;"PA100,350;"
3850 PEN 2
3860 OUTPUT 705;"SI;LBDIFFERENCE IS";Scale;"X",CHR$(3)
3870 OUTPUT 705;"PG 1"
3880 END IF
```

```
3890 PEN 0
3900 END IF
3910 PLOTTER IS CRT,"INTERNAL";COLOR MAP
3920 REM ************************************************************
3930 INPUT "Do you want to rescale the Differnce(y/n)",Regraph$
3940 IF Regraph$="y" THEN
3950 INPUT "What scale would you like to see the Diffence",Scale
3960 Plot$="n"
3970 GOTO 3130
3980 END IF
3990 IF Regraph$="Y" THEN
4000 INPUT "What scale would you like to see the Diffence",Scale
4010 Plot$="n"
4020 GOTO 3130
4030 END IF
4040 INPUT "Do you want to plot this graph?(y/n)",Plot$
4050 IF Plot$="y" THEN
4060 PLOTTER IS 705,"HPGL"
4070 GOTO 3140
4080 END IF
4090 IF Plot$="Y" THEN
4100 PLOTTER IS 705,"HPGL"
4110 GOTO 3140
4120 END IF
4130 REM ************************SAVE**************************
4140 INPUT "SAVE?(y/n)",Save$
4150 IF Save$="n" THEN GOTO 4300
4160 IF Save$="N" THEN GOTO 4300
4170 INPUT "Enter Filename:",Filename$
4180 CREATE "C:\"&Filename$,995
4190 ASSIGN @File TO "C:\"&Filename$;FORMAT ON
4200 IF Grat$="y" THEN
4210 FOR Count4=1 TO Ars*Steps/Avg
4220 OUTPUT @File;Count4;",";Combined(Count4)
4230 NEXT Count4
4240 ELSE
4250 FOR Count4=1 TO 995
4260 OUTPUT @File;Count4;",";Answer2(Count4)
4270 NEXT Count4
4280 END IF
4290 REM ************************************************************
4300 CLEAR SCREEN
4310 CLEAR 705
4320 CLEAR 724
4330 OUTPUT 724;"RES;"
4340 PRINT "PROGRAM COMPLETE"
4350 END
4360 REM ***************SUBROUTINE CHECKS/grading ******
4370 SUB Pollspect
4380 Bittest=BIT(STATUS(11,11),4)
4390 IF Bittest=0 THEN 4380
4400 SUBEND
4410 REM ************************************************
```

Brooke Palmquist report not available at time of publication.

EXPERIMENTAL TESTING FOR THE LINEAR RANGE OF A MECHANICAL SHAKER

Michael P. Schoenfeld

New Mexico Military Institute
10 West College Blvd.
Roswell, NM 88201-5173

Final Report for:
High School Apprenticeship Program
Phillips Laboratory

Sponsored by:
Air Force Office of Scientific Research
Bolling Air Force Base, Washington DC

and

Phillips Laboratory

August 1995

EXPERIMENTAL TESTING FOR THE LINEAR RANGE OF A MECHANICAL SHAKER

Michael P. Schoenfeld
New Mexico Military Institute

Abstract

Testing of a mechanical shaker was conducted to determine its linear range of operation. A sine wave was chosen as the test signal since, for a given constant amplitude harmonic input, the output of any linear system would also be harmonic with just an amplitude and a phase change. A spectrum analyzer was used to generate the source signal as well as analyze the output signal from the shaker. The degree of fidelity of the shaker's output sine signal determined its linear range. Test-runs included a wide range of frequencies to determine if the linearity of the shaker was frequency dependent. Experimental results indicate that the shaker's lower linear limit is roughly 5.0 lbf with negligible dependence on signal frequency.

EXPERIMENTAL TESTING FOR THE LINEAR RANGE OF A MECHANICAL SHAKER

Michael P. Schoenfeld

INTRODUCTION

The Phillips Laboratory's Precision Structures and Controls Division is currently conducting a test of a vibration isolation and suppression system to be used on a space platform. One of the test components in this experiment is a mechanical shaker which will be used to generate the excitation force. It is extremely important to determine the linear, operational range of this shaker in order to gain confidence in the actual characteristic of the force being transferred to the test article. If the shaker were to be operated outside this range, any input signal to the shaker would not necessarily be faithfully produced by the shaker, thereby, yielding misleading results. Therefore, preliminary testing of the mechanical shaker was conducted to characterize its fidelity. The upper limit for the shaker was already specified by the manufacturer. The goal of this experiment is to determine the lower limit.

METHODOLGY

Experimental set-up for testing of the shaker can be found on page 18-4 in Figure 1.

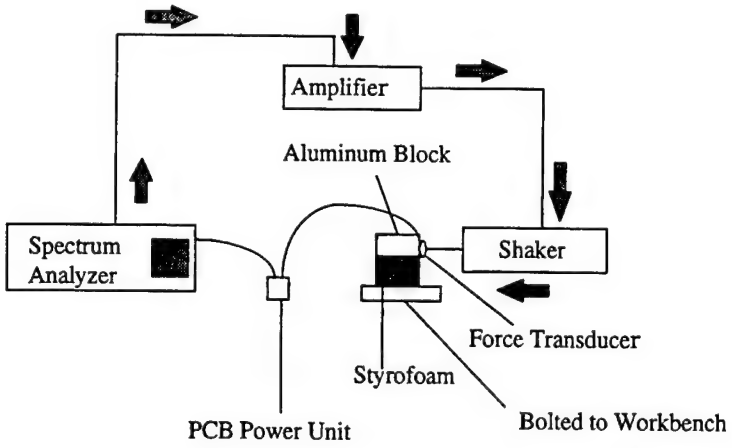

Figure 1: Test Set-Up

An HP 35665A Dynamic Signal Analyzer (spectrum analyzer) provided the sine wave signal source. Since the output voltage from the spectrum analyzer is a low-power signal, an APS power amplifier was required to drive an APS Electro-Seis Shaker. Measurement of the shaker's output force was accomplished via a PCB Model 208A3 force transducer that was attached to the end of the shaker's stinger. A makeshift structure, composed of a piece of Styrofoam glued between two Aluminum blocks and attached to a workbench, provided the necessary resistance for load measuring from the force transducer. The signal from the force transducer is transmitted to a PCB Power Unit for amplification and fed into the spectrum analyzer where it is analyzed for signal quality. No scientific procedure was used in gauging the quality of the shaker's output signal since a precise determination of the shaker's lower linear limit was not necessary. Rather, only an estimation of this limit is required. Thus, engineering judgement was considered adequate in determining the acceptable level of resolution of the output signal's harmonic characteristics.

RESULTS

The test matrix, to include the experimental results, is presented below in Table 1.

Frequency (Hz)	Input Signal (mVpk)	Output Signal (mVpk)	Force (lbf)
1	30	11.25	1.04
5	27	11.25	1.04
10	20	10.12	0.93
20	20	12.75	1.18
50	150	14.62	1.35
70	165	16.13	1.49
100	155	19.12	1.77
150	175	19.12	1.77
180	180	19.49	1.80
200	170	19.12	1.76

Table 1: Test Matrix

The first column indicates the ten different frequency values at which the shaker was tested. These values were chosen as a representative sample of the frequency spectrum which the vibration isolation system will be tested at. As can be seen from the matrix, a total of ten test runs were conducted. The second column contains the value of the peak voltage level of the source signal as generated by the spectrum analyzer. These values represent the amplitudes of the source sine wave. The third column shows the voltage level of the incoming signal into the spectrum analyzer as received from the force transducer. These values represent the amplitudes of the sine wave as produced by the shaker. The last column contains the minimum, mechanical force level of the shaker before unacceptable degradation of signal quality occurs.

Calculation of the shaker's force level was achieved by knowing the sensitivity of the load cell. Every load cell is calibrated such that it will produce an electrical signal with a specified voltage level for a given mechanical force load. The sensitivity of the particular force transducer used in the test is 10.84 mv/lbf, giving

the results seen in the last column. It can be seen that the minimum force level of the shaker is approximately 1.4 lbf and is fairly frequency independent with a standard deviation of only 0.35 lbf. This deviation is negligible since the lower linear range can be safely established at 5.0 lbf to account for experimental errors and electrical component noise. In other words, for force levels less than 5.0 lbf, the shaker can not be confidently relied upon to faithfully reproduce its input signal.

CONCLUSION

The APS-Electro Seis Shaker can effectively be operated as low as 5.0 lbf before distortion of the input signal reaches an unacceptable level. This operational limit has been shown to be independent of the frequency of the source signal. However, this conclusion only applies to the circumstances of the experiment, mainly for a frequency range of 1- 200 Hz. If much higher excitation frequencies are expected for the test article, then the shaker should be retested at these new values to ensure data variation does not become significant.

THE USE OF Labview* FOR HEAT-SENSITIVE DATA ACQUISITION

Seth B. Schuyler

Sandia Prepatory School
532 Osuna Road N.E.
Albuquerque, NM 87110

Final Report for:
High School Apprentice Program
Phillips Laboratory

Sponsored by:
Air Force Office of Scientific Research
Bolling Air Force Base, DC

and

Phillips Laboratory

August 1995

THE USE OF Labview® FOR HEAT-SENSITIVE DATA ACQUISITION

Seth B. Schuyler
Sandia Prepatory School

Abstract

Labview has been recently been introduced into the lab with very positive results. It saves time and increases the output of each individual researcher, all with a minimal cost.

THE USE OF Labview® FOR HEAT-SENSITIVE DATA ACQUISITION

Seth B. Schuyler

Introduction

The acquisition of data is time consuming, and it takes even longer to get data for a heat sensitive device. Any instrument built to be used in space must be tested, and sense they will be working in extreme cold, they must be tested in extreme cold. The processes to cool these instruments, and test them, occupy several man-hours, but with Labview many of those man-hours can be replaced with computer-cycles.

Problem

To begin the cooling process, a small volume must be insulated from the atmosphere, currently accomplished with a vacuum chamber which is a small part of a tool named a cryogenic Dewer. Then with liquid Nitrogen, a small plate which has the part to be tested mounted to it, is cooled to 77 degrees Kelvin. Once the part has reached 77 K, the liquid Nitrogen is replaced by liquid Helium. The liquid Helium brings the part down to 4 degrees Kelvin. Then the part is cold enough to test.

Once the part has reached 4 degrees Kelvin, (see Cooling Process for details) it has to be monitored to make sure that the temperature is stable. When the temperature is confirmed stable then a signal is passed through the part. The signal could be an infrared-laser pulse, a pulse from an infrared black-body, or a series of voltages. Then the parts response must be recorded. The response could be incorrect because of electro-magnetic noise, so a series of signals are sent, and their respective responses recorded. Then the average of these responses must be taken. After all this, the goal temperature is changed and the testing process begins again. For some real critical parts the Dewer may be cooled again for more data.

Methodology

The cooling process can not be helped, but the testing process can be programmed and put under a computer's control. Text based compilers do run faster than Labview, but are much more confusing. Because several experiments are only run once, the time it would take to write a text based program would far exceed the time saved. Labview is a visually based programming language. It is more complex which means it takes more computing

cycles, so it runs much slower, but it saves time in programming. Because Labview runs faster than the experiment, it still maintains its value for experiments that will be repeated. The computer can run the experiment faster than a human, and can run multiple experiments, plus the entire time the computer is running the experiment, or experiments, it leaves the researchers hands free.
The computer can run constantly and consistently, which makes it a better worker than most humans.

Results

Labview quickly and efficiently gathers data.

Conclusion

Labview pays for its self in a very short time, and quickly becomes profitable.

References

Labview is a product of National Instruments.

TEMPERATURE-DEPENDENT REFLECTANCE MEASUREMENTS

Damian F. Sieja

Sandia High School
7801 Candelaria Rd. NE
Albuquerque, N.M.
87109
(Graduate)

Final Report for:
High School Apprenticeship Program
Phillips Laboratory

Sponsored by:
Air Force Office of Scientific Research
Bolling Air Force Base, DC

and

Phillips Laboratory

August 1995

TEMPERATURE-DEPENDENT REFLECTANCE MEASUREMENTS

Damian F. Sieja

Introduction

Estimates of laser-material coupling are needed for system definition and effectiveness studies to evaluate the potential of laser weapon concepts. Current prediction algorithms incorporate room-temperature reflectance measurements data to determine the vulnerability of the targets of interest. To increase the accuracy of these vulnerability predictions, temperature-dependent reflectance measurements are needed because previous laser experiments indicate that reflectance properties are temperature dependent.

This test will generate temperature-dependent reflectance measurements at several wavelengths on test coupon as the material is heated up to 600°C. These measurements will be performed at the Laser Effects Test Facility (LETF).
The Lasers Effects Branch will use the test results to generate an accurate reflectance measurements data base of materials. So, in addition to supporting the space arena, these measurements will also improve the potential application of the Airborne Laser (ABL), and Ground-Based Laser (GBL) weapon concepts for the Theater Missile Defense.

Methodology

Temperature-dependent reflectance measurements were taken. Reflectance of the test samples were measured at several wavelengths through a temperature range from room temperature to 600°C. The reflectance measurements were performed in the reflectance lab using the integrating hemispheres and a Data Acquisition System (DAS). The targets were small coupons, approximately 4 cm^2 by 1.5mm thick, of various materials. The physical properties of the test articles (i.e. size, weight, composition, etc.) were recorded for each material, as well as the condition of the test articles. The DAS instrumentation system was used for recording temperature, reflected energy from the detector, reflectance input beam power from the power head and meter, and time at a sample rate of about .1 Hz.

The configuration of the reflectance lab includes:

A. Heated stage with power supply

B. Optical detectors

C. Beam conditioning optics (focusing lenses)

D. Lasers/wavelengths used:

   a. 1.3 um Nd:YAG laser

   b. 1.06 um Nd:YAG laser

E. Integrating hemisphere- The hemisphere contains a gold metallic reflectance coating of reflectance > 95% above 1000 nm, thus this type of sphere is best for near IR to far IR range. Light energy entering the hemisphere from the sample coupon is reflected from the walls, distributing the energy uniformly around the interior. A detector, placed at a point as equally offset from the hemisphere's

focal point as the coupon, sees an output. The specular reflection of a sample may be removed by placing a light trap at the specular reflection port, thus enabling separate measurements of diffuse and specular reflectance. The integrating hemispheres and meters are periodically calibrated.

F. Reflectance standards are available for wavelengths up to 2.0 microns

G. Thermocouples (type K TCs)- Placed on the test article to measure the temperature of the sample.

H. Photographic support.

Results

The reflected energy on the detector had to be chopped at .1 Hz to discriminate the reflected laser energy from ambient or black body emissions. This sample rate caused the data to jump from highs to lows (Fig. 1). The difference signal (the part of the total signal caused by the reflected laser energy) can be manually determined by subtracting the high (B points) from their corresponding low (A points). The resultant data can then be plotted over temperature data (Figs. 2 and 3) to show the material's absorbency at a room to 600° C temperature.

Conclusions

The dynamic reflectance data provides insight on surface deteration of various materials and paints. As a database, it will need constant updating and many more material samples and wavelengths will need to be tested. To make future tests run smoother and with increased overall accuracy several steps should be taken. First, Spherical aberration caused a portion of the reflected light to

miss the detector because it was slightly offset from the hemisphere's focal point. To reduce spherical aberration, an elliptical reflector (2 focal points) should be used instead of the hemispherical one. Second, a higher response rate detector and a higher chop rate on the laser should be used. Not only will this increase the amount of data sampled, but it would allow for instant filtering of the data (rather than a manual, post-test separation) by putting a bandpass filter on the output of the detector. Last, the temperature should be taken to the samples melting point, seeing as a real world target might not be destroyed unless it is melted.

Figure 1

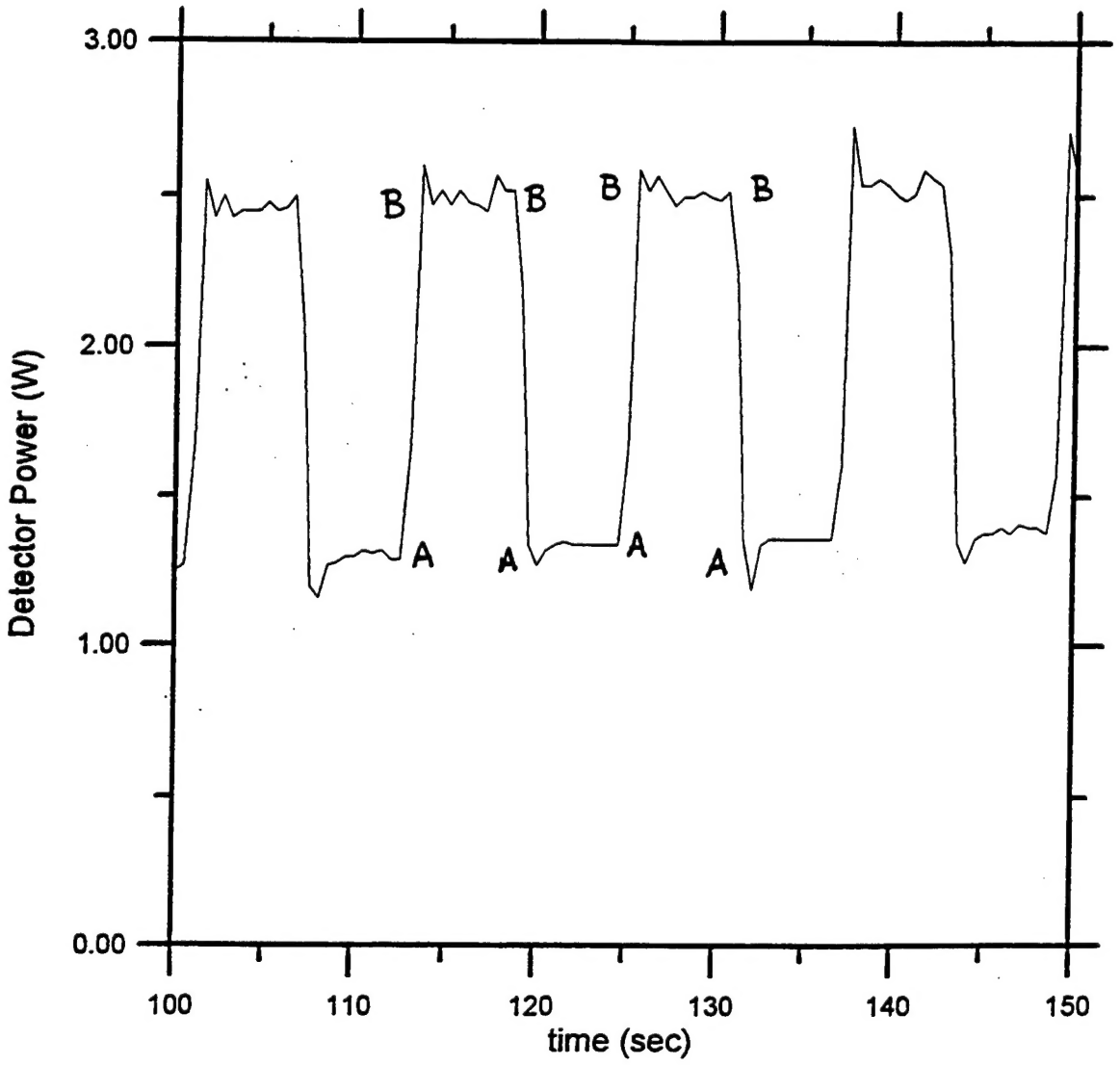
3.00
2.00
1.00
0.00
Detector Power (W)
B
B
B
B
A
A
A
A
100
110
120
130
140
150
time (sec)

Figure 2

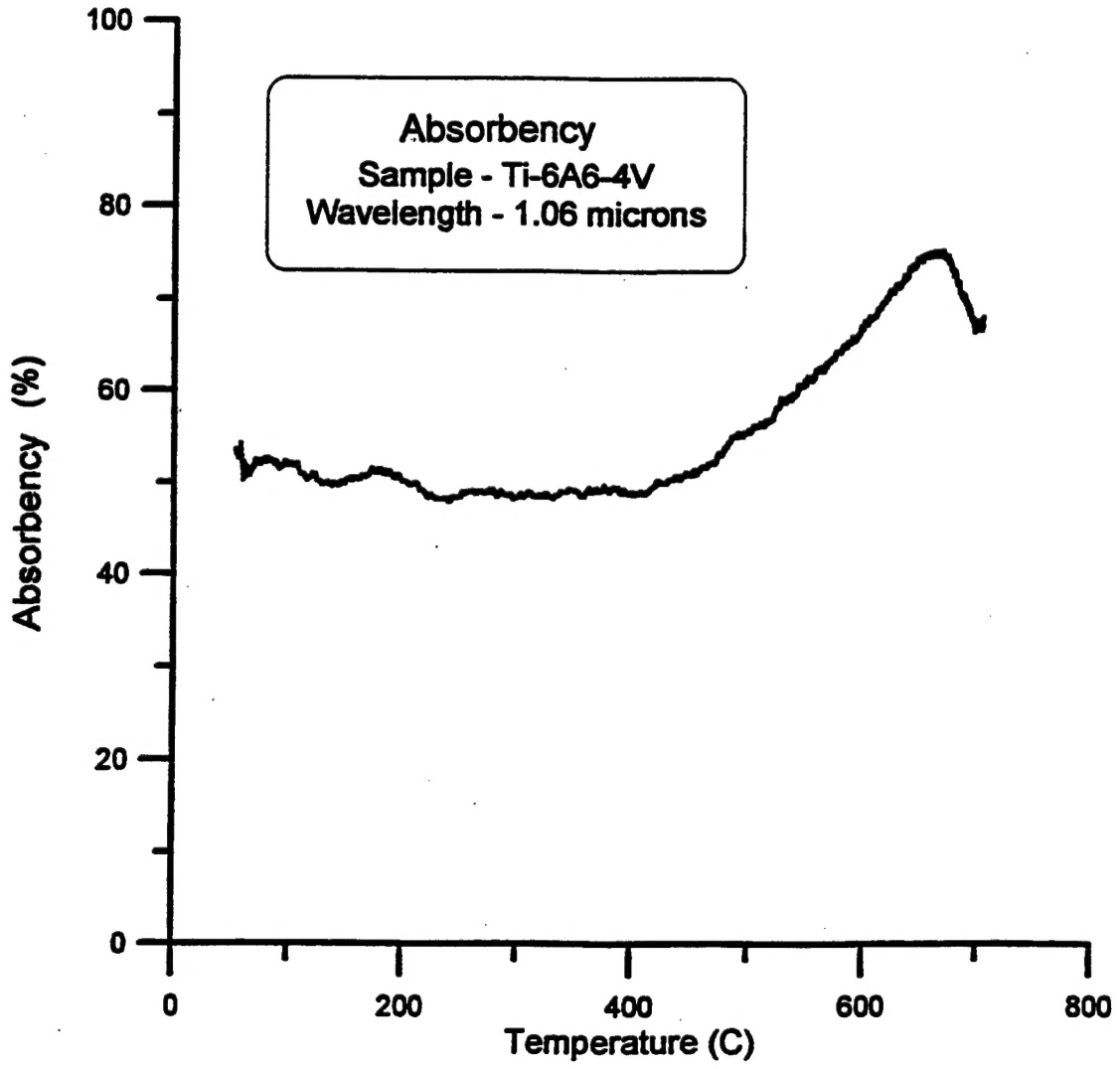
Absorbency
Sample - Ti-6A6-4V
Wavelength - 1.06 microns
Absorbency (%)
100
80
60
40
20
0
0
200
400
600
800
Temperature (C)

Figure 3

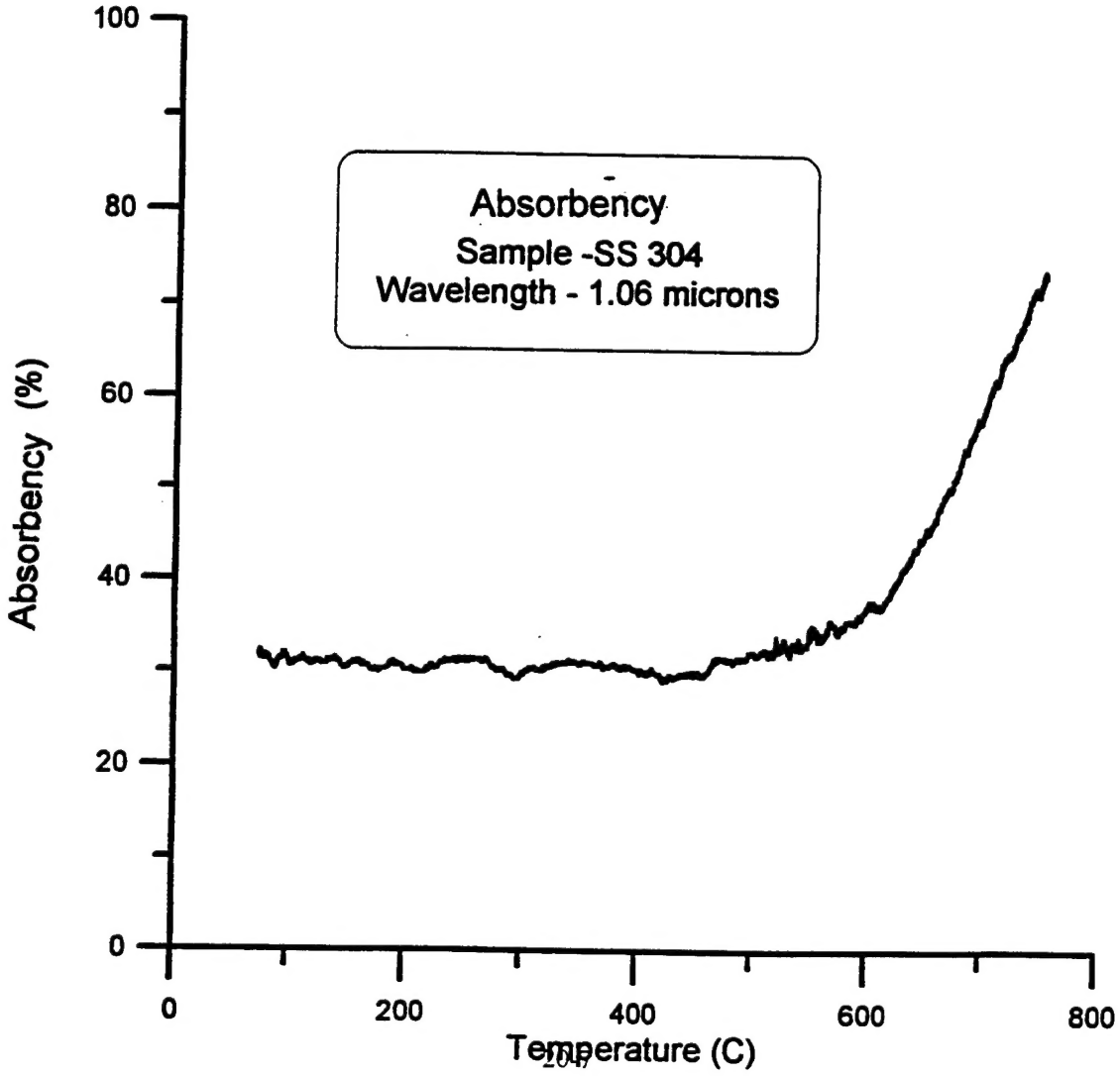
Absorbency
Sample -SS 304
Wavelength - 1.06 microns
Absorbency (%)
100
80
60
40
20
0
0
200
400
600
800
Temperature (C)